ÉCOLE DOCTORALE SANTE, SCIENCES BIOLOGIQUES ET CHIMIE DU VIVANT

Laboratoire Orléanais/Laboratoire Etranger

THÈSE EN COTUTELLE INTERNATIONALEprésentée par :

Anna Tejchman

soutenue le : 06 Avril 2017

pour obtenir le grade de :

Docteur de l'Université d'Orléans
et de l'Institut d'Immunologie et Thérapie Expérimentale de l'Académie Polonaise des Sciences

Discipline : Biologie

L'influence de l'hypoxie sur l'expression de podoplanine dans les fibroblastes associés au cancer (CAF) et son rôle dans la progression du cancer du sein

THÈSE dirigée par :

Mme Claudine Kieda	Professeur, Centre de Biophysique Moléculaire, CNRS
Mr Maciej Ugorski	Professeur,Institut d'Immunologie et Thérapie Expérimentale,PAN

RAPPORTEURS :

Mme Alicja Jozkowicz	Professeur, Université Jagellon
Mr Dariusz Rakus	Professeur, Université de Wroclaw
Mr André Mazur	Professeur, Centre de recherche Auvergne Rhône-Alpes, INRA

JURY (indiquez tous les membres du jury – y compris directeur(s) thèse et rapporteurs) :

Mr Egbert Piasecki	Professeur, Institut d'Immunologie et Thérapie Expérimentale, PAN
Mme Claudine Kieda	Professeur, Centre de Biophysique Moléculaire, CNRS
Mr Maciej Ugorski	Professeur, Institut d'Immunologie et Thérapie Expérimentale
Mme Alicja Jozkowicz	Professeur, Université Jagellon
Mr Dariusz Rakus	Professeur, Université de Wroclaw
Mr André Mazur	Professeur, Centre de recherche Auvergne Rhône-Alpes
Mme Catherine Grillon	Chargée de Recherche,Centre de Biophysique Moléculaire, CNRS

Konradowi i Marysi

The thesis has been prepared in the frame of co-tutorial PhD studies, carried onby the Institute of Immunology and Experimental Therapy, Polish Academy of Sciences in Wrocław, Poland and the University of Orleans in France, as a fulfilment for the double diploma.

The work was supported by French National league against cancer (CK); CNRS PAN agreement IITD/CBM (CK); Polish-French grant "MiRTango"; Polish national research centre NCN N°N-N401-570340

I acknowledge that during the work on my thesis I have been a scholarship fellow:

- **Ministry of Polish education and research**
- **French Ministry of Foreign affairs**

The results presented in the thesis are a part of original research paper, which is accepted for publication in Oncotarget:

Anna Tejchman, Nathalie Lamerant-Fayel, Jean-Claude Jacquinet, Aleksandra Bielawska-Pohl, Katarzyna MLeczko-Sanecka, Catherine Grillon, Salem Chouaib, Maciej Ugorski, Claudine KiedaTumor hypoxia modulates podoplanin/CCL21 interactions in CCR7+ NKcells recruitment and CCR7+ tumor cells mobilization

Moreover, I am a co-author of the following research papers:

Original articles:

1. Jarosław Suchanski, **Anna Tejchman**, Maciej Zacharski, Aleksandra Piotrowska, Jedrzej Grzegrzolka, Janusz Rys, Piotr Dziegiel, Claudine Kieda and Maciej Ugorski Podoplanin increases the migration of human fibroblasts and affects the angiogenesis of endothelial cells. The possible role of cancer-associated fibroblasts in breast cancer progression (under revision)

2. Nanbakhsh A, Pochon C, Amsellem S, Pittari G, **Tejchman** A, Bourhis JH, Chouaib S. J Immunother. 2014 Jun;37(5):278-82. doi: 10.1097/CJI.0000000000000039.PMID: 24810639 Enhanced cytotoxic activity of ex vivo-differentiated human natural killer cells in the presence of HOXB4.

Review papers:

1. Collet G, El Hafny-Rahbi B, Nadim M, **Tejchman A**, Klimkiewicz K, Kieda C. Contemp Oncol (Pozn). 2015;19(1A):A39-43. doi: 10.5114/wo.2014.47130. Review.PMID: 25691820 Hypoxia-shaped vascular niche for cancer stem cells.

Acknowledgements

Firstly, I would like to express my gratefulness to my supervisors Prof. dr hab. Maciej Ugorski and Prof. Claudine Kieda for their precious scientific advice, guidance and great support.

Moreover, I am grateful to Prof. dr hab. Alicja Józkowicz from Jagiellonian University in Kraków, Poland and Prof. Dr hab. Dariusz Rakus from University of Wrocław for reviewing the thesis.

Furthermore, I am immensely grateful to all my colleagues and friends from the Institute of Immunology and Experimental Therapy, for their help, support in scientific work and precious advices.

Especially I would like to acknowledge dr Alicja Kmiecik, dr Aleksandra Bielawska-Pohl, dr Agnieszka Krawczenko, dr Maria Paprocka, lek. Wet. Marek Chadalski, dr Jarosław Suchański, dr Maciej Zacharski, dr Tomasz Owczarek and other colleagues.

Moreover, I would like to express my gratefulness to Prof. Claudine Kieda's

research group (CBM, CNRS, Orleans, France), who greatly supported me not only in scientific work, but also in everyday life during my stayin Orleans. Especially I would like to acknowledge dr Catherine Grillon, Fabienne Fasani, dr Giovanni Busco, Shalina Hassanaly and the other colleagues.

Furthermore, I would like to acknowledge David Gosset from the Cytometry Platform of CBM UPR4301, CNRS Orleans, France for his technical assistance with flurorescence microscopy and flow cytometry.

I would like to acknowledge Prof. Dr hab. Piotr Dzięgiel, Dr Bartosz Puła and Aleksandra Jethon-Jabłońska from Medical University in Wrocław for providing samples of breast cancer resections from patients and IHC staining.

Especially I would like to thank my parents dr Waldemar Tejchman and Małgorzata Tejchman who always believed in me and supported me all along my life.

Table of contents

1. List of abbreviations:

3'UTR:3'-untranslated region
ACTB: actin βgene
AKT: kinase B protein
ANGPT1: angiopoietin-1
ANGPT2: angiopoietin-2
ATP: adenosine triphosphate
BSA: bovine serum albumin
CAF: carcinoma/cancer-associated fibroblast
CBP: CREB Binding Protein
CDC42: cell division cycle 42
cDNA: complementary deoxyribonucleic acid
CMV: cytomegalovirus
CSC: cancer stem-like cell
CSF1: colony-stimulating factor 1
Ct: cycle threshold
DCs: dendritic cells
DMEM: Dulbecco's modified Eagle's medium
DNA Pol II: DNA polymerase II
DNA: Deoxyribonucleic acid
EC: Endothelial cells
ECM: extracellular matrix
EDTA: ethylene diamine tetraacetic acid
EGF: epidermal growth factor
FACS: fluorescence-activated cell sorter
FBS: fetal bovine serum
FGF: fibroblast growth factor
Gal: galactose
GalNAc: N- acetylgalactosamine
GFP: green fluorescent protein
HEK293: human embryonic kidney 293T cell
HIF: hypoxia inducible factor
HRE: hypoxia response element
IC: isotypic control
ICAM: intercellular cell adhesion molecule
IgG: immunoglobulin G
ILx: interleukin x
IRES: internal ribosome entry site
KDa: kilo Dalton
LOX : lysyl oxydase
miRNA: micro RNA
MMP: matrix metalloproteinase

mRNA: messenger ribonucleic acid
MSC: mesenchymal stem cell
mTOR: mammalian target of rapamycin
OptiMEM: opti-minimum essential medium
PBSc: complete phosphate buffer saline
PCR: polymerase chain reaction
PDPN: podoplanin
PE: phycoerythrin
PECAM: platelet endothelial cell adhesion molecule
PEI: polyethyleneimine
PFA: paraformaldehyde
PHD: prolyl hydroxylase
PI3 kinase: phosphoinositide 3 kinase
PIP2: phosphatidylinositol 4,5-bisphosphate
PlGF: placenta growth factor
PMSF: phenylmethylsulfonyl fluoride
PO_2: dioxygenpartial pressure
pVHL protein : von Hippel Lindau protein
qPCR: quantitative polymerase chain reaction
RACK1: receptor for activated C-kinase 1
RBX1: Ring-Box 1
RT-PCR: reverse transcriptase polymerase chain reaction
SDF1-α: stromal cell-derived factor α (=CXCL12)
SDS-PAGE: polyacrylamide gel electrophoresis under denaturing conditions
SEM: standard error of the mean
siRNA: small interfering ribonucleic acid
TGF-beta: tansforming growth factor-beta
TNFα: tumor necrosis factor α
Tris – Tris (hydroxymethyl) aminomethane
TRITC: tetra methyl rhodamine iso thio cyanate
UTR: untranslated region
UV: ultraviolet
VCAM: vascular cell adhesion molecule
VE-Cadherin: vascular endothelial-cadherin
VEGF: vascular endothelial growth factor
vWf: von Willebrand factor
WHO: World Health Organization
ΔCp: difference in Cp (crossing points)
ΔIF: difference in intensity of fluorescence

2. ABSTRACT

Tumor is a pathologic tissue including, in addition to cancer cells, a modified extracellular matrix, endothelial cells, blood and lymphatic vessels, immune and inflammatory cells as well as activated fibroblasts called cancer-associated fibroblasts (CAFs). Tumor microenvironment plays an important role in both tumor development and metastasis. However, the knowledge about individual components of the microenvironment is very limited. Podoplanin (PDPN), mucin-type transmembrane glycoprotein is expressed in tumor cells and CAFs, depending on the tumor type. Podoplanin induces platelet aggregation, which promotes metastasis. In vivo, its role in metastasis promotion has been demonstrated for breast cancer cells into lymph nodes. Here we show that it modulates the activity of the CCL21/CCR7 chemokine/receptor axis in a hypoxia-dependent manner. In the present model, breast cancer MDA-MB-231 cells express CCR7 surface receptor for CCL21 which is a potent chemoattractant able to bind to podoplanin. The role of CCL21/CCR7 axis in the adhesion of MDA-MB-231 breast cancer cells was reduced by hypoxia, as in the tumor environment. Cancer progression is strongly affected by the tumour stroma in which CAFs are characterized by distinct gene expression and properties from normal fibroblasts. They promote tumour growth, recruitment of endothelial progenitor cells and angiogenesis via secretion of stromal cell-derived factor-1. In breast cancer up to 80% of fibroblasts display the CAF phenotype. Here a podoplanin expressing model of CAFs made it possible to demonstrate the involvement of CCL21/CCR7 axis in the tumor cell-to-CAF recognition through podoplanin binding of CCL21. Podoplanin was induced by hypoxia and its overexpression undergoes reduction of adhesion, making it an anti-adhesion molecule in the tumor, in the absence of CCL21. Little is still known about podoplanin influence on cancer cells. In this view, microRNA, which control gene expression at post-transcriptional level are good candidates. MiR-21 is a key regulator of the oncogenic process, through its downstream target proteins among which the tumor suppressor phosphatase and tensin homologue deleted on chromosome ten, PTEN. We analysed the effect of miR-21, but also oncogenic and hypoxia dependent miRs: miR-210 and miR-29b, on podoplanin expression in fibroblasts in conditions mimicking the intra tumor microenvironment, i.e. in hypoxia. This points to crucial differences as compared to normoxia. Moreover we uncover the effect of podoplanin on angiogenesis by endothelial cells colocalizing with CAFs expressing podoplanin and expression of most prominent proangiogenic factors. Podoplanin on CAFs has a direct impact on pseudo-tube formation into aberrant vascular network. It also increased migration of fibroblasts and endothelial cells in normoxia but this effect is annihilated by hypoxia while it does not impact breast cancer cells motility.

3. STRESZCZENIE

Guz stanowi rodzaj patologicznej tkanki, zbudowanej z komórek rakowych, zmodyfikowanej macierzy zewnątrzkomórkowej, komórek śródbłonka, naczyń krwionośnych i limfatycznych, komórek odpornościowych, jak również aktywowanych fibroblastów zwanych fibroblastami towarzyszącymi nowotworom (*ang. Cancer-associated fibroblasts, CAFs)*. Mikrośrodowisko guza odgrywa ważną rolę zarówno w rozwoju nowotworu jak i przerzutowaniu. Jednakże wiedza o poszczególnych składnikach mikrośrodowiska jest bardzo ograniczona. Podoplanina (PDPN) jest transbłonową glikoproteiną typu mucyny i ulega ekspresji w komórkach rakowych i CAFs, w zależności od rodzaju nowotworu. Podoplanina indukuje agregację płytekkrwi, co ułatwia tworzenie przerzutów. In vivo, wykazano jej rolę w promowaniu przerzutów komórek rakowych piersi do węzłów chłonnych. W niniejszej pracy przedstawiono, że podoplanina moduluje aktywność osi CCL21/chemokina CCR7/receptor, w sposób zależny od hipoksji. W przyjętym modelu,komórki raka sutka MDA-MB-231 wykazują ekspresję receptora powierzchniowego CCR7 dla CCL21, która jest silnym chemoatraktantem zdolnym do wiązania podoplaniny. Wpływ osi CCL21/CCR7 na adhezję komórek raka sutka MDA-MB-231 zmniejsza się w warunkach hipoksji, tak jak w środowisku guza. Rozwój raka jestzależny od podścieliska guza, w którym CAFs charakteryzują się zmienioną ekspresją genów i właściwościami odrębnymi od normalnych fibroblastów. Wspierają one rozwój nowotworu, rekrutacjękomórek progenitorowych śródbłonkai angiogenezę poprzez wydzielanie czynnika SDF-1 (*ang. Stromal derived factor-1)*. W przypadku raka piersi do 80% fibroblastów wykazuje fenotyp CAF. W niniejszej pracy utworzenie modelu CAF z nadekspresją podoplaniny pozwoliło wykazać udział osi CCL21/CCR7 w rozpoznaniu komórki nowotworowej przez CAF poprzez wiązanie CCL21 dopodoplaniny. Wzrost ekspresji podoplaniny osiągnięto w warunkach hipoksji, a jej nadekspresja prowadziła do redukcji adhezji, co czyni ją cząsteczką antyandhezyjną przy braku CCL21. Wciąż niewiele wiadomo o wpływie podoplaniny na komórki nowotworowe. Z tego punktu widzenia, dobrymi kandydatami do badania regulacji genów mających wpływ na proces nowotworzenia jak i na ekspresję podoplniny są mikroRNA, które regulują ekspresję genów na poziomie post-transkrypcyjnym. MiR-21 jest kluczowym regulatorem procesunowotworzenia i działa poprzez degradację docelowych mRNA białek takich jak PTEN (*ang. Tumor suppressor phosphatase and tensin homologue deleted on chromosome ten*). Analizowano wpływ miR-21, ale także miRNA zależne od hipoksji i onko-miRy: miR-210 i miR-29b, na ekspresję podoplaniny w fibroblastach w warunkach naśladującychmikrośrodowisko guza, czyli w hipoksji. Wyniki wykazały kluczowe różnice w porównaniu do normoksji. Ponadto wykazano wpływ podoplaniny na angiogenezę poprzez kolokalizację komórek endotelialnych z CAF ekspresjonującymi podoplaninę i ekspresję najważniejszych czynników proangiogennych. Podoplanina ekspresjonowana przez CAFma bezpośredni

wpływ na tworzeniepatologicznej sieci naczyniowej oraz zwiększoną migrację fibroblastów i komórek śródbłonka w warunkach normoksji, czego nie obserwuje się w hipoksji. Podoplanina nie ma wpływu na ruchliwość komórek nowotworowych.

4. RÉSUMÉ

Le site tumoral est un tissus pathologique qui comprend, outre les cellules cancéreuses, une matrice extra cellulaire modifiée, des cellules endothéliales, vaisseaux sanguins et lymphatique et des cellules immunes et inflammatoires, ainsi que les fibroblastes activés appelés fibroblastes associés au cancer (CAFs). Le microenvironnement tumoral joue un rôle important au développement et la métastase des tumeurs. La connaissance des composants individuels du microenvironnement demeure très limitée. La podoplanine (PDPN), glycoprotéine transmembranaire de type mucine, est exprimée dans les cellules cancéreuses et les CAFs, selon le type tumoral. La podoplanine induit l'agrégation des plaquettes, promouvant les métastases. In vivo, son rôle dans la promotion des métastases a été démontré dans le carcinome mammaire envahissant les ganglions lymphatiques. Nous démontrons ici qu'elle module l'activité de l'interaction chimiokine/récepteur de l'axe CCL21/CCR7 d'une manière dépendante de l'hypoxie. Dans le présent modèle, les cellules de carcinoma mammaire MDA-MB-231 expriment en surface CCR7, le récepteur de CCL21, un fort chimioattractant qui se lie à la podoplanine. Le rôle de CCL21/CCR7 dans l'adhésion des cellules de carcinome MDA-MB-231 est réduit par l'hypoxie qui mime le microenvironnement de la tumeur. La progression cancéreuse est fortement contrôlée par le stroma tumoral où les CAFs se caractérisent par une expression génique et des propriétés particulières par rapport aux fibroblastes normaux. Ils promeuvent la croissance tumorale, le recrutement des précurseurs endothéliaux et l'angiogenèse par la sécrétion du facteur-1 dérivé des cellules stromales. Dans le cas du carcinome mammaire, 80% des fibroblastes ont un phénotype CAF. Ici un modèle de CAFs exprimant la podoplanine a permis de démontrer l'implication de l'axe CCL21/CCR7 dans la reconnaissance entre cellules tumorales et CAFs via la liaison de CCL21 par la podoplanine. Cette dernière est induite par l'hypoxie, sa surexpression entraîne un réduction de l'adhésion, faisant de la podoplanine une molécule anti-adhésive dans la tumeur, en l'absence de CCL21. L'influence de la podoplanine sur les cellules cancéreuses est mal connue. Les microARN qui contrôlent l'expression des gènes au niveaupost-transcriptionel sont ainsi des candidats de choix. Ainsi, MiR-21 est un régulateur oncogène fondamental, par son action sur les protéines cibles parmi lesquelles la PTEN, suppresseur de tumeur : « phosphatase and tensin homologue deleted on chromosome ten ». Nous avons analysé l'effet de miR-21, ainsi que de miR-210 and miR-29b qui sont des miRs oncogènes et dépendant de l'hypoxie, sur l'expression de la podoplanine dans les fibroblastes en conditions mimant le microenvironnement intratumoral. Ceci a mis en évidence les différences biologiques cruciales dues à l'hypoxie comparativement à la normoxie. Nous montrons en outre, l'effet de la podoplanine sur l'angiogenèse par les cellules endothéliales en colocalisation avec les CAFs exprimant la podoplanine et l'expression des facteurs proangiogéniques. La popoplanine exprimée par les CAFs a une action directe sur la formation des pseudo-tubes résultant en un réseau vasculaire chaotique. Elle accroît aussi la migration des fibroblastes et des

cellules endothéliales en normoxie. Cet effet est annihilé par l'hypoxie, tandis qu'aucun effet n'est observé sur la motilité des cellules de carcinome mammaire.

5. INTRODUCTION

Invasive breast cancer, which represents a group of malignant epithelial tumors witha high tendency to metastasize to distant organs, is the most common carcinoma in women[1]. The geographicareas of high risk are the highly developed countries except Japan and China, where incidence rates are still low[1]. Tumor formation or carcinogenesis, including breast cancer, is a complex multifactorial process involving three main stages: initiation, promotion and progression[2]. At the stage of initiation, a normal cell acquiresnew non-standard features that provides it with a selective advantage over neighbouring cells. This is exemplified by the uncontrolled proliferation resulting in an imbalance between cell division and cell death, which favours the appearance of mutations in the promotion stage, thus cell transformation in the primary tumor. As a result of subsequent changes in the course of tumor progression, the cells become malignant as they invade adjacent tissue and form metastases by colonizing tissues distinct from the one where cells originated[2]. Metastasis cascade comprises sequential steps such as the local invasion, penetration into the lumen of the blood vessel (intravasation), circulationin the bloodstream, adhesion to endothelium of target organ vessels, migration of the cancer cells from vascular system (extravasation) to the target organ parenchyma, cellular phenotypic adaptations to microenvironment selection forcesand colonization of distant organs in the form of macrometastases[2].

5.1. TUMOR MICROENVIRONMENT

5.1.1. Stages of tumor formation

Early studies on carcinogenesis revealed that formation of tumor requires at least two signals, so called “initiator” represented usually by strong mutagen, and “tumor promoter” represented by agents that cause aberrant repair, fibrosis[3] and woundingwhich may serve as a highly effective promoting stimulus[4][5][3].This was firstly evidenced by Berenblum who showed that benzo(a)pyrene applied with croton oil on mouse skin induces larger numbers of tumors than benzo(a)pyrene alone[6]. Nowadays carcinogenesis is recognized asa multi-step process which requires more than two hitsbut is classicallydivided into three main steps: initiation, promotion and progression[7].

Initiation, which is considered as a first step of carcinogens, is a sequence of irreversible changes in somatic cell caused by spontaneous mutation or exposure to carcinogen[7]. Activation of more than one

oncogene, DNA sequence responsible for transformation, is required for neoplastic transformation. However, a single point mutation may be sufficient to induce initiation as shown for Ha-ras proto-oncogene converted into a functional oncogene[7].

Promotion is the process where initiated cell undergo further proliferation.Neoplastic transformation requires repeated exposures to promoting stimuli and it depends on tumor microenvironment which acts as a source of factors e.g. phorbol esters, cytokines, lipid metabolites that may temporarily change the patterns of specific gene expression. These changes lead to separation of the intercellular communications and increases cellular growth potential[7].

Progression is a process during which tumor grows in size. Growth favours further mutations and creates heterogeneous populations[7].

5.1.2. History of tumor microenvironment

Tumors, includingbreastcancer, are not only composed of cancer cells but also stromal cells such as fibroblasts, immune cells, endothelial cells and the extracellular matrix proteins (ECM)[8][9] (**Fig. 1**).

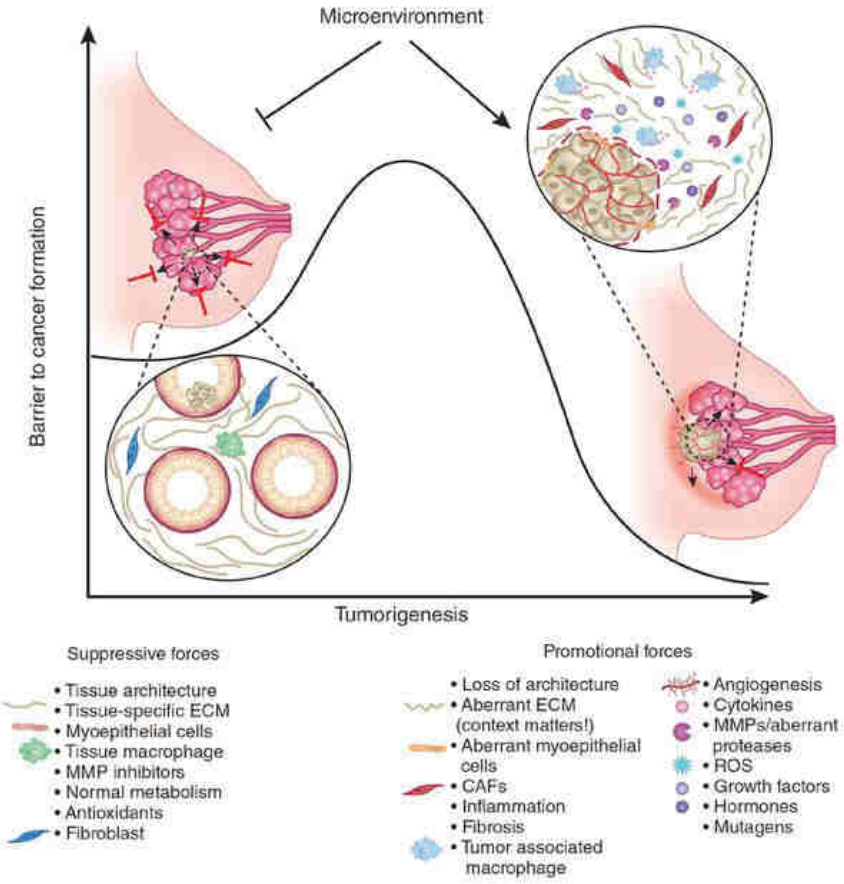

Figure 1. Comparison of normal breast tissue andmicroenvironment of breast cancerous tumor.Bissel and Hines (2011), doi: 10.1038/nm.2328

This particular composition is reminiscent of granuloma tissue formed during wound healing. Tumor is sometimes referred to as a "wound that never heals"[10]. The importance of the tumor microenvironment in cancer progression has been known for many years. Known "seed and soil" hypothesis, proposed by English surgeon Stephen Paget in 1889, describes the cancer cells as seeds[11], which need proper microenvironment to progress similarly as "seedsneedthe right conditions to germinate".Over the past 127 years, a lot of research has shown that the microenvironment,on the one hand, may promote tumor progression and, on the other hand, may have an inhibitory effect on tumor growth or even reverse the process of carcinogenesis through the normalization of microenvironment[6][12][13][3]. For example, the skin microenvironment suppresses the initiated damages caused by chemical carcinogens, acting as a

mutation suppressor and tumor suppressor[6][12].It is known that healthy reaction of controlling the tumor growth is broken when hypoxia and angiogenic switch occur.

5.1.3. Stages of cancer niche formation

Development of cancer from initiation to progression occurs in parallel to changes in tumor microenvironment and creation of tumor niche[14]**(Fig.2)**. First step of this process is a cancer niche setting, involving interactions between initiated cell and host cells that facilitate malignant behaviour and survival[14]. The niche develops bythesecretion of cytokines and chemokines such as interleukin-6 (IL-6), interleukin-8 (IL-8), granulocyte-macrophage colony-stimulating factor (GM-CSF), induction of oncogene(s), inflammation caused by chemical promoters orby physiological conditions[14]**(Fig.2)**.

Niche expansion is characterized by therecruitment of immune cells, mesenchymal stem cells (MSC) and fibroblasts what leads to reprogramming of the stroma[14]**(Fig.2)**.

Progression of cancer requires the maturation of cancer niche whichoccurs by theactivation or modification of the properties of cells in the niche. Mainly observed is the conversion of normal fibroblasts into cancer associated fibroblasts (CAFs),the angiogenic switch, the secretion of transforming growth factor β (TGF-β), stromal derived factor-1 (SDF-1) and exosomes[14]. Exosomes are a key mean for thetransfer of regulatory/activating molecules between cells as for the potent regulators non-coding RNAs called microRNAs which play an important part in the activation of CAFs[14]**(Fig.2)**.

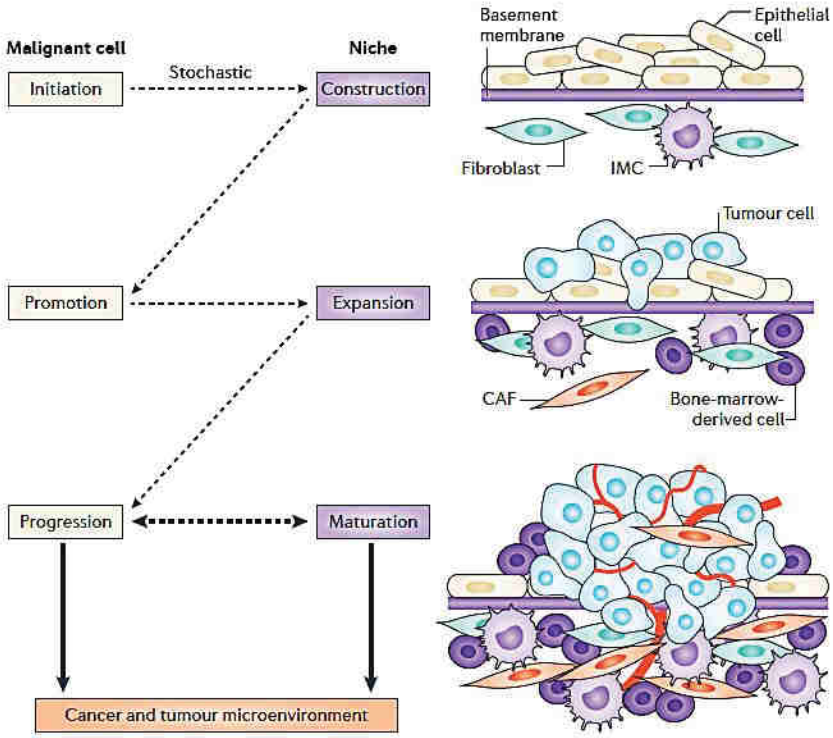

Figure 2. Schematic representation of parallel evolution of initiated cell and cancer niche. The process of cancer niche development involves: niche construction, expansion and maturation which are associated with interactions between initiated cell and host cells leading to angiogenic switch,recruitment of immune cells, mesenchymal stem cells (MSC), fibroblasts, secretion of cytokines, chemokines and growth factors.CAF, cancer-associated fibroblast; IMC, immature myeloid cell. Barcellos-Hoff, Lyden and Wang (2013), doi:10.1038/nrc3536

5.2.FIBROBLASTS IN CANCER

Fibroblasts accompany cancer cells at all stages of cancer progression. Fibroblasts from tumour of patients with malignant melanoma, breast cancer, familial adenomatous polyposis, Wilms tumors or retinoblastoma are characterized by an abnormal phenotype and an increased proliferation rate together with a reducedserum requirementfor proliferation[15].They secrete increased amounts of ECM components mainly collagen type I, tenascin C, extra domain A of fibronectin (EDA-fibronectin)and secreted protein acidic and rich in cysteine (SPARC)**(Fig.3)**. This phenomenon, among others facilitates angiogenesis[16].Fibroblasts produce high amounts of VEGF-A, which increases the microvascular permeability thus causes the diffusionof plasma proteins[16][17]. Those proteins such as fibrins attract more fibroblasts, inflammatory and endothelial cells[16].

5.2.1. Markers of activated fibroblasts

During the development of ductal breast carcinomas, the basement membrane is degraded and the activated stroma which contains immune cells, myofibroblasts and newly formed capillaries comes in direct contact with tumor cells[18]. Activated fibroblasts in tumor stroma are called peri-tumoral fibroblasts, reactive stromal fibroblasts, myofibroblasts, cancer-associated fibroblasts (CAFs) or tumour-associated fibroblasts[19][20]. These fibroblasts are characterized as "activated" based on the expression of markers suchas α-SMA and fibroblast specific protein (FSP)**(Fig.3)**. Stromal fibroblasts of solid tumors overexpress platelet-derived growth factor (PDGF) receptors-β and fibroblast activation protein (FAP)[21]. In breast carcinomas about 80% of stromal fibroblasts acquire anactivated phenotype[22].

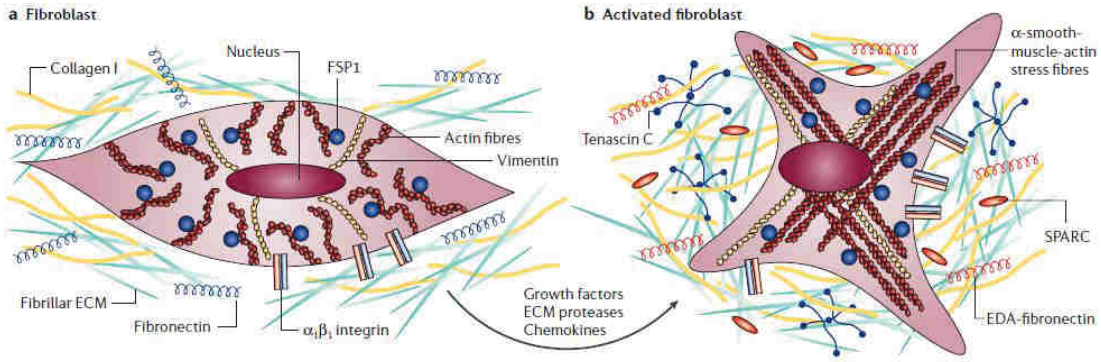

Figure 3. Normal and activated fibroblasts. ECM of normal fibroblasts consists of fibronectin and collagen type I and they interact with microenvironment via integrins such as $\alpha_1\beta_1$ integrin. (**a**) Normal fibroblasts are characterized by their fusiform morphology and expression of vimentin. (**b**) When fibroblasts become activated, they proliferate and secrete increased amounts of ECM mainly collagen type I, tenascin C, EDA-fibronectin and secreted protein acidic and rich in cysteine (SPARC). Activation of fibroblasts may be mediated by growth factors such as TGFβ, chemokines asmonocyte chemotactic protein 1(MCP1), andECM-degrading proteases. Kalluri and Zeisberg(2006),doi:10.1038/nrc1877

5.2.2. Origins of activated fibroblasts (CAFs)

Fibroblasts are heterogeneous and CAFs may derive from different tissues[23] and cells **(Fig. 4)**.Nowadays, they are classified as resident, mesenchymal stem cell (MSC)-derived or mutational[21]. However, the exact origin of CAFs is not fully explained. Resident CAFs are derived from local fibroblasts activated by cancer-derived growth factors as TGF-β, PDGF and bFGF in the process called mesenchymal to

mesenchymal transition (MMT)**(Fig.4)**.This process is accompanied by the expression of genes which are specific for CAFs, such as collagens, αSMA,MMP1, MMP3, etc. [24][25][21]. Another source of CAFs isprovided by thebone marrow–derived MSCs, which may differentiate into muscle, adipocytes, osteocytes and chondrocytes in physiological and pathological processes[26][21]**(Fig.4)**. At injury site, in conditions of neoplasia, of tissue repair and inflammation MSCs achieve homing and engraftment[27]. At the tumor site MSCs are recruited in a manner similar to inflammatory cells during tissue repair. This is due to cytokines and growth factors secreted by cancer cells and stromal cells, as PDGF, VEGF, HGF, EGF, bFGF, and CCL2[28]. MSCs have been shown to differentiate into CAFs and pericytes andto localize in the tumor mass[21].This process was accompanied by theexpression of markers associated with aggressiveness such as α-SMA, FAP, tenascin-c and thrombospondin-1[29][21]. Epithelial cells may become fibroblasts and acquire mesenchymal characteristics through an epithelial to mesenchymal transition (EMT)[30]**(Fig.4)**. EMT is a process in which epithelial cells are transformed to motile mesenchymal cells and occurs mainly during embryogenesis[31]. EMT is connected with cancer progression[31]. Epithelial cells trans-differentiate into activated myofibroblasts through exposition to oxidative stress-drivenmatrix metalloproteinases (MMP), which causes DNA oxidation and subsequent mutations. Altogether these effects may result in the process of EMT[32]. EMT allows cancer cells to acquire mesenchymal cell phenotypeproviding another source of CAFs[30]**(Fig.4)**. Moreover, proliferating endothelial cells can turn into CAFs in aprocess similar to EMT, named endothelial to mesenchymal transition (EndMT) via stimulation by TGF-β**(Fig.4)**. During this process proliferating endothelial cells loose endothelial markers such as CD31 and start to express mesenchymal markers like fibroblast specific protein-1 (FSP-1) and SMA[33].

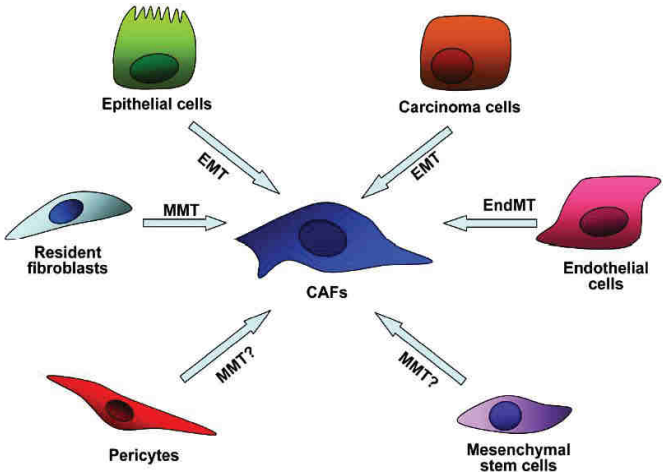

Figure 4. Proposedorigins ofCAFs.Resident fibroblasts and probably mesenchymal stem cells and pericytes may turn into CAFs in a process called mesenchymal to mesenchymal transition (MMT).Epithelial and cancer cells may turn into fibroblasts in a process called epithelial to mesenchymal transition (EMT). Endothelial to mesenchymal transition process (EndMT) occurs when CAFs originate from endothelial cells. Cirri and Chiarugi (2011), Am J Cancer Res 2011;1(4):482-497.

5.2.3. Activation of fibroblasts

In the tumor, quiescent fibroblasts acquirean activated phenotype, namely they proliferate more and produce more ECM constituents, during tissue fibrosis, wounding and inflammation[34]. Numerous factors lead to fibroblastactivation. Decipheringthe molecular mechanisms that lead to activation of fibroblasts, also referred to as myofibroblasts, it was shownthat a conditioned medium collected from cancer cell cultures and TGF-β may cause activation of stromal fibroblasts[35][36] to become myofibroblasts. These myofibroblasts express VEGF-A and other angiogenic factors, which promote angiogenesis[36]. Fibroblasts may also be activated by platelet derived growth factor(PDGF), epidermal growth factor (EGF),fibroblast growth factor 2 (FGF2), bone morphogenic proteins (BMPs) and sonic hedgehog (SHH) [37][34]. Fibroblasts occupy a key position in the process of malignant transformation. Moreover, myofibroblasts proliferation causes fibrosis and increases the risk of cancer[38][39].

5.2.4. Contribution of CAFs in cancer formation

To demonstrate the involvement of fibroblasts in the initiation of cancer, mouse models with genetically altered fibroblasts were designed[16]. Human breast epithelial cells have been shown to form ducts in the stroma of mouse mammary gland and the surrounding murine fibroblasts activated by TGFβ and hepatocyte growth factor initiate growth of breast tumor within the normal murine epithelium[40]**(Fig. 5)**. Studies comparing CAFs isolated from the primary tumour site and normal fibroblasts were conducted to decipher the linksbetween growth factors and CAFs[41][42].CAFs present altered expression of growth factorssuch as keratinocyte growth factor, transforming growth factor-β1, insulin-like growth factors I and II, hepatocyte growth factor/epithelial scatter factor, and platelet-derived growth factor[43]. Prostate epithelial cells transformed with simian virus 40 (SV40) were transplantedinto mice in combination with normal fibroblasts or CAFs. It was found that CAFs co-transplantation led to lesions resembling prostatic intraepithelial neoplasia[41].Massive tumor growth in mice was observed when CAFs were used with immortalized epithelial cells but not normal fibroblasts[41]. It has been shown that CAFs secrete stromal-derived factor-1 (SDF-1), what enhances invasiveness of pancreatic cancer cells[44]. In addition, by secretingCXCL14, pancreatic cancer cells increase growth and migration of fibroblasts, which in turn, increases their activity [42][45]. CAFs recruit pro-angiogenic macrophages through overexpression of SDF-1, IL-6 and IL-1β under the transcriptional control of cyclooxygenase 2 (COX-2) and nuclear factor-κB (NF-κB). This shows the link between inflammatory mediators and CAFs in breast adenocarcinoma[46]. It has to

be noticed that hypoxia affects CAFs and leads to activation of hypoxia-inducible factor-1 (HIF-1), which activatesthesecretion of SDF-1[47]. CAFs secrete also enzymes which degrade ECM and enable tumor angiogenesis and invasion,they cleave cell adhesion molecules, helping EMT and increasingthe cell motility, cleaving pro-inflammatory cytokines, growth factors and their receptors namely metalloproteinases (MMPs) and plasminogen activators[48][49]. Moreover, EMT by which CAFs contribute to metastatic and invasive processes is involved in the induction of cancer stem cells phenotypethrough overexpression of Snail or Twist transcription factors as was shown for breast and prostate cancers[50][51]. These data suggest that CAFs participate tothe initiation and promotion of carcinogenesis in epithelial cells, whereas normal fibroblasts are responsible for maintaining epithelial homeostasis **(Fig. 5)**.

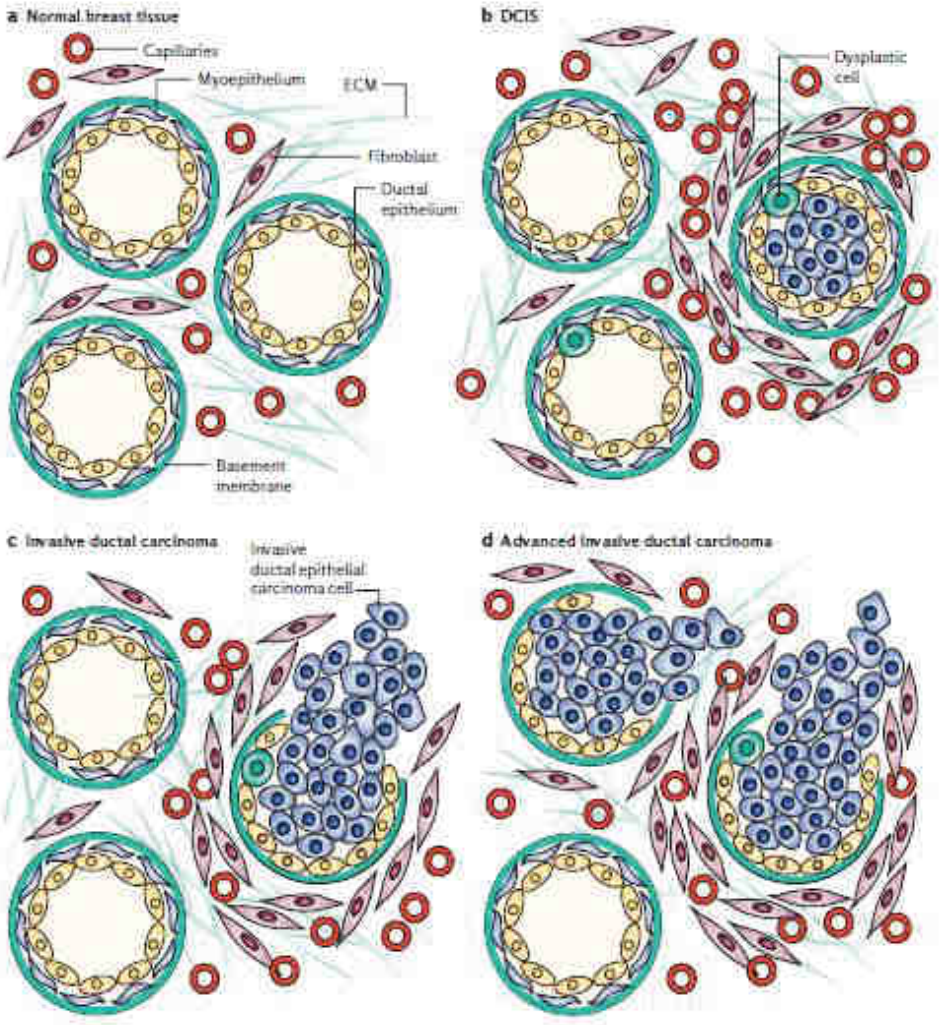

Figure 5. Interactions in tumor stroma during progression of mammary ductal carcinoma**. (a)**Thenormal breast myoepithelial cells and ductal epithelium are separated by a basement membrane from the surrounding connective tissue. **(b)** In ductal carcinoma in situ (DCIS), fibroblasts accumulate and lead to the deposition of fibrillar ECM. (**c)** Invasive ductal carcinomas contain inflammatory infiltrate, myofibroblasts and newly formed capillaries. Moreover, the basement membrane is broken. (**d)** During advanced breast carcinoma cancer cells invade the altered stroma.Kalluri and Zeisberg (2006),doi:10.1038/nrc1877.

CAFs contribute totumorprogression not only through secreted cytokines, growth factors and enzymes**(Fig. 6)**, but also by specific communications with cancer cells, however, this type of interaction remains unclear[16].

There are studies showing that CAFs induce invasiveness in non-invasive cancer cells through increasing cancer cell proliferation and angiogenesis[42]. The interaction between cancer cells and fibroblasts lead to a fibrotic state. This is associated with tumor progressiondue to accumulation of collagen type I and III,degradation of collagen type IV, increasing matrix deposition and stiffening the 3D matrix[52][53][54].

Fibroblasts secretelysyl oxidase (LOX). During the early stages of breast carcinogenesis,LOX catalyses collagen cross-linking; in a later stage LOX is expressed in cancer cellsand its expression isinduced by hypoxic environment[55].

Fibronectin, another key player in tumor ECM is secreted by CAFs and plays a vital role in cell adhesion. Fibronectin is found in the intercellular spaces and on the cell surface. The soluble form is present in high concentrations (300 μg/mL) and serves as a ligand for several members of integrin receptor family[56]. Fibronectinis involved in cell adhesion but also participates in the processes of migration, differentiation and growth[56]. In tumors fibronectin is associated with MMP secretion and higher metastatic potential. Moreover fibronectin up-regulation by inflammatory factors as: NF-κB, CXCL-3, IL-8, TNF-α, COX-2 and Toll-like receptor (TLR) 2 stimulates cancer cell growth[57]. Inaddition, tumoral fibroblasts express high amounts of hyaluronan, which plays a key role in the recruitment of tumor-associated macrophages, CAFs and endothelial cells[58].

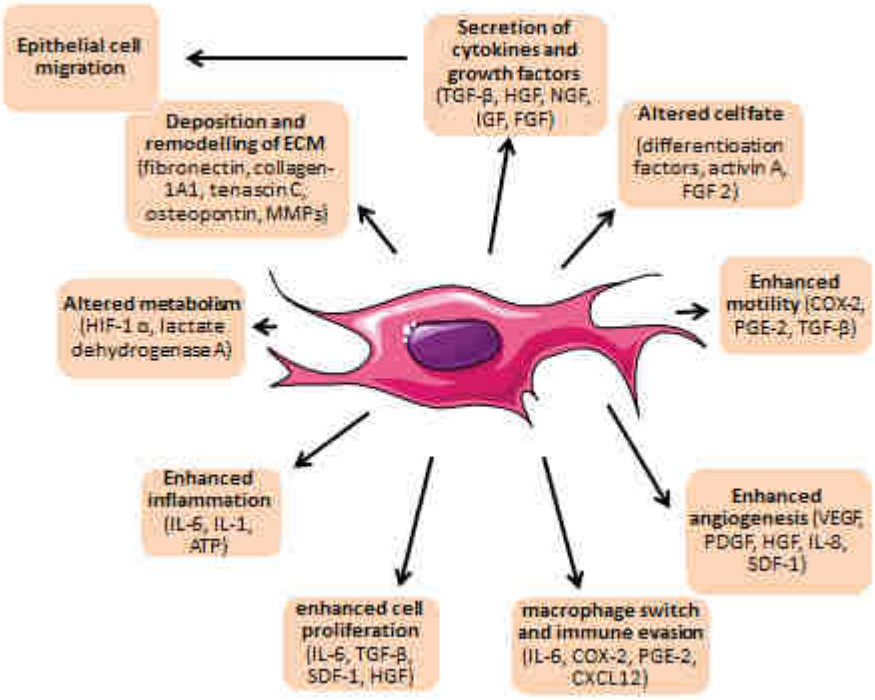

Figure 6. Factors secreted by activated fibroblasts and their involvement in mechanisms leading to tumor progression. Adapted fromGascard andTlsty(2016), doi:10.1101/gad.279737.116

As it was mentioned before, CAFs lead to angiogenesis through thesecretion of increased amounts of ECM components, angiogenic factors and enzymes as well as therecruitment of ECs. Angiogenesis is the main cause modifying the tumor microenvironment.

5.3.ANGIOGENESIS

Blood vessels develop by two processes during embryogenesis. Vasculogenesisoccurs when vessels are created from progenitor cells. Angiogenesis is a process of sprouting new capillaries from existing ones[59]. Angiogenesis occurs in adults during ovulation, implantation, menstruation and pregnancy. Avascular tumours,namelysmall andoccult lesions of 1–2 mm in diameter, stay dormant bykeepinga balance between proliferation and apoptosis[60]. This initial phase of tumor growth, without blood vessels, occurs during cancer development before the tumor starts to develop its blood supply to continue to grow[61]**(Fig. 7)**.During this pre-vascular phase, the tumorremains in a benign state[61]. Typically, without access to oxygen and nutrients, tumor cannot grow more than 2 mm in diameter [62].However, signals for quiescent vasculature to be activated and undergocapillarysprouting, participate to the “angiogenic switch”. This state favours the expression ofpro-angiogenic genesin response to hypoxiawhich occurs within thetumor (**see**

section 5.4.)as a consequence of increased tumor mass.Suchenvironmental stimuli, cause the expression by tumor and stromal cells of moleculeswhich, as the vascular endothelial growth factor A (VEGF-A)[61], promote angiogenesis i.e. formation of new blood vessels *via* extension or remodelling of existing blood vessels[61]. Initiation of angiogenesis is one of the critical steps in tumor development and metastasis[61]**(Fig. 7)**.

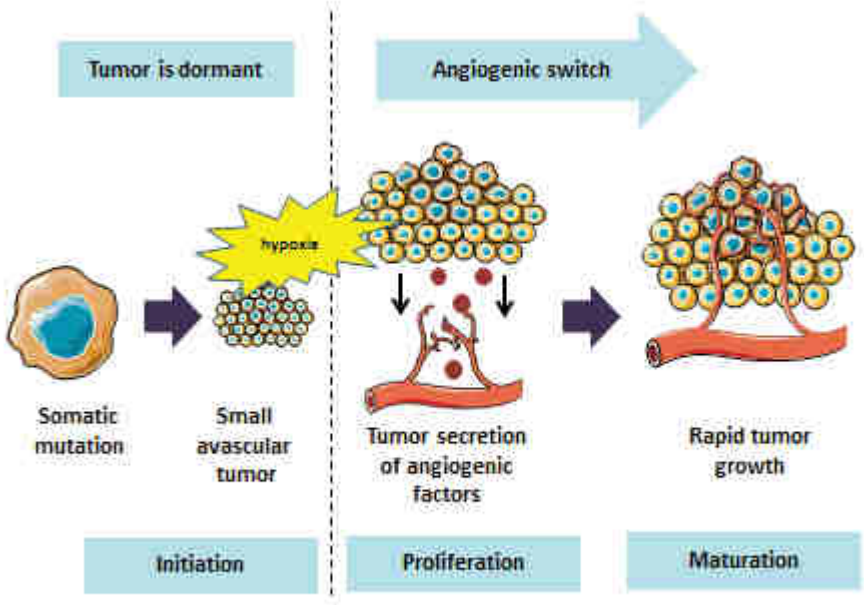

Figure 7. Stages of angiogenesis.AdaptedfromBergers and Benjamin (2003), doi:10.1038/nrc1093

5.3.1. Tumor angiogenesis and normalisation

Although angiogenesis is necessary for tumor development,tumor angiogenesis is very chaotic, theformed vessels are abnormaland theirfunction is impaired. This random distribution of vessels does not permit an efficient blood flow in some regions and while it is excessive inothers[63][64]. Moreover, extravasation of fluids and proteins into the extracellular compartment occurs due to the poor perivascularcell coverage and to dissociation of EC junctions[65]. Such aberrant vascular network, directlyaffects the development of the tumor, through increasing of tumor growth and metastatic potential and helping the tumor cellsescape from the control of host's immune system[66].Therefore, anti-angiogenic therapies were developed in orderto prevent tumor neovascularization by starvation and death of tumorcells[67]. Nevertheless this strategy was not efficient because although vessel destruction causes necrosis and deepens hypoxia, potently killing the bulk of tumor, this hypoxic state triggers resistance in

part of tumor cells and leads to tumor regrowth[68].Increased tumor hypoxia leads to selection of aggressive cancer stem-like cells,highly resistant to drugs[69].Consequently as anti-angiogenic therapies has not fulfilledexpectations, normalization of the vasculature became a promising approach[69][68].It has been shown that fibroblast-specificloss of HIF-1αreduces vascular density and leadsto vessel normalization[70]. This indicates the CAFs contribution to the hypoxic microenvironment of the tumor.

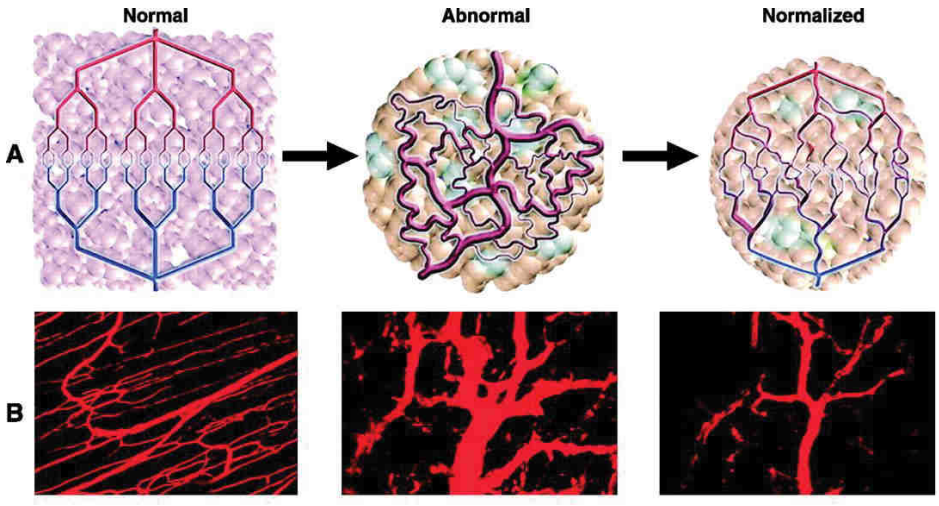

Figure 8.Normalization of tumor vasculature.Hypothesized effects of tumor vessel normalization. Tumor vasculature is structurally and functionally abnormal and antiangiogenic therapies are designed to improve its structure and function. However, continued or aggressive antiangiogenictreatments lead to the formation of a vasculature that is resistant to further treatment and causes impaired delivery of drugs or oxygen.**(A)** Schematic representation.**(B)** Images of vessels.Goel et al. (2012), doi: 10.1101/cshperspect.a006486.

Hypoxia leads tothesecretion of paracrine factors such asTGF-β and PDGF by cancer cells what enables the transformation of precursor cells into CAFs[70]. Nevertheless the direct effect of hypoxia on CAFs remains to be more documented[70].

5.4.HYPOXIA

Tumor angiogenesis is initiated by hypoxia which means a low oxygen tension[62] as compared to physioxia which is the normal tissue pO_2 value.Hypoxic microenvironment, which is observed in many solid cancers, dramatically changes gene expression profiles of cancer cells[71]. Hypoxia-inducible factor-1 (HIF-1) plays key roles in adaptive responses of cells under hypoxic conditions through its

transcriptionalactivity[62][71]. The HIF-1 protein is a heterodimer, composed of a constitutively expressed subunit named HIF-1βand an oxygen regulated subunit named HIF-1α[62]. The expression of HIF-1αis predominantly regulated at posttranslational level[71]. Under oxygen-sufficient conditions, prolyl residues 402 and 564 in the N-terminal domain of HIF-1αprotein are hydroxylated by the action of prolyl hydroxylases (PHDs) in an oxygen-dependent manner[71]. Once hydroxylated, von HippelLindau protein (pVHL) binds HIF-α.This enables the binding of E3 ubiquitin ligase. The complex which includes pVHL, ubiquitin-conjugating enzyme (E2),Cul2, Ring-Box 1 (RBX1),Elongin-B and Elongin-C boundto HIF-1αleads, together with an ubiquitin-activating enzyme (E1), toproteasomal degradation of the HIF-1αprotein[71].On the contrary, because enzymatic activities of PHDs are reducedin hypoxic conditions, the HIF-1αproteinbindsto HIF-1β subunit andcofactors as CREB Binding Protein (CBP)/p300 and the DNA polymerase II (Pol II).Such a heterodimer together with cofactors,is stabilized andtranslocated to the nucleus,where it binds to hypoxia responsive element sequence (HRE) and induces expression of many genes promoting angiogenesis, e.g. *VEGF*[71][62]. Hypoxic microenvironment dramatically shiftsthe glucose metabolism from aerobic cellular respiration to anaerobic glycolysis[71]. The resulting increased glucose uptake and activation of glycolysis are highly important compensatory responses to the reduction of intracellular ATP level due to the inhibition of cellular respiration[71]. Hypoxic conditions are also characterized bythe enhanced production of transforming growth factor-beta (TGF-β) and increased deposition of extracellular matrix (ECM) molecules[72]. Recent data indicate that hypoxia differentially enhances the effect of TGF-βisoforms on the secretion and deposition of GAGs and may hasten ECM remodelling associated with the pathological state of tissues[72].

Hypoxia affects the biology of CAFs. It has been shown that genes modulated by hypoxia induce CAF phenotype by down-regulation of caveolin-1[73]. Moreover HIF-1α overexpression in CAFs has a pro-metastatic effect and is responsible for increasing tumor hypoxia due to formation of aberrant vessels[73].

5.5.PODOPLANIN

5.5.1. The discovery and occurrence of podoplanin

Podoplanin was described for the first time in 1997 in puromycinaminonucleosidenephrosis (PAN), a rat model of human minimal change nephropathy[74]. Sequence identities revealed the presence of structurally related proteins in many normal cells from different species. It was found that podoplanin is a marker of rat glomerular epithelial cells(podocytes) and lymphatic vessels[75][76].Podoplanin was localized in high density on podocytesshowing an asymmetric distribution, with 90% in the luminal and 10% in basal cell membranes[74]. The protein was also found at the luminal surface of epithelial cells ofBowman's capsule but not at other locations in the kidney. Under the name OTS-8, it was identified in murine osteoblastic cells after their treatment with phorbol ester[74]. Podoplanin was also described as T1α or RTI40 in rat alveolar type I cells of the lung and E11 in rat bone. In canine Madin-Darby kidney (MDCK) cells as gp40 where it serves as receptor for influenza C virus[74][77]. In mouse cancer cells podoplanin was identified as aggrus (platelet aggregation inducing factor)[78], and gp38 in murine type I epithelial cells of the thymus and stromal cells in T-dependent cell areas of peripheral lymphoid tissues[79]. In human, podoplanin was called gp36 in placenta[80],PA2.26[77]inHeLa carcinoma cells and immortalized HaCaT keratinocytes[77].

5.5.2. Structure of podoplanin

Podoplanin is a166-amino-acid integral membrane protein with a single transmembrane domain composed by an hydrophobic stretch of 29 amino acids (amino acids 129 to 157)[74] (**Fig. 9B**). The N-terminal ectodomain contains 128 amino acids, with six serine/threonine residues at positions 3, 19, 71, 79, 110 and 122, providing potential *O*-glycosylation sites. Therefore, due tothe high contentin*O*-glycans, podoplanin is classified as a mucin-like glycoprotein. This highly glycosylated protein containssialic acid α(2-3) linkedto galactoselinked in β(1-3) to the N-acetylgalactosamine**(Fig. 9A)**[77]. The Short cytoplasmic domain iscomposed of nine amino acids, providingpotential phosphorylation sites for cAMP-dependent protein kinase (amino acids 158 to 161) and protein kinase C (amino acids 161 to 163)[74] and directly interacting with ezrin and moesin[81]. The biological role of podoplanin is still poorly understood. Mice withtheir podoplanin gene knocked-out die shortly after birth because of respiratory failure. A characteristic feature is dilation and malfunction of lymphatic vessels together with lymphedema [82][83]. In this context, it should be stressed thathighlevel of podoplanin expression is observed in the endothelium of lymphatic

vessels, but not in the endothelium of blood vessels. Thus it is widely used as a marker for endothelial cells from lymphatic vessels andforlymphangiogenesis[84]. The murine homologue of podoplanin (PA2.26) is over expressed during wound healing, which indicates that it can take part in the regeneration of tissues[85]. Under physiological conditions, podoplanin has an important role in the adhesion processasanti-adhesive or pro-adhesivemolecule[82][81]. It also participates in the regulation of podocyte shaping and regulatesblood filtration within the glomeruli[74][86][87].

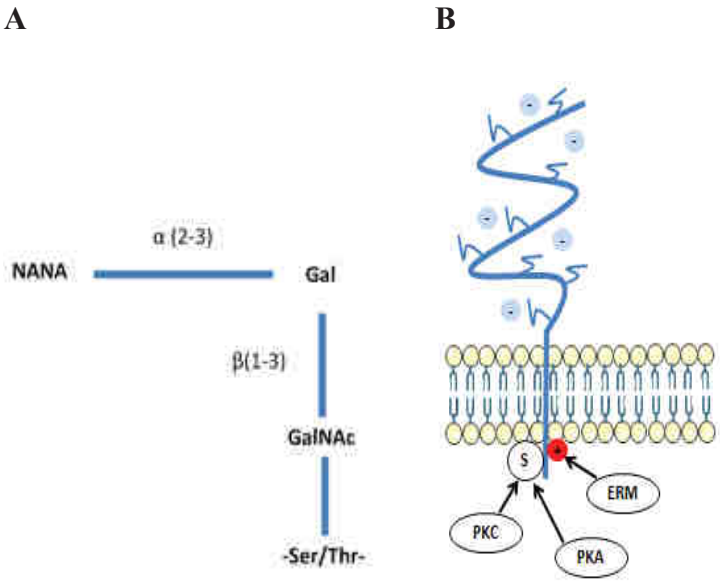

Figure 9. Structure of podoplanin.**(A)** O-glycan chains linked to Ser or Thr in the podoplanin ectodomain. NANA: N-acetylneuraminic acid (sialic acid); Gal: galactose; GalNAc: N-acetylgalactosamine. **(B)** Schematic representation of the podoplanin backbone showing the O-glycosylated ectodomain, positively charged site for thebinding of ezrin radixinmoesin (ERM) proteins and the potentially phosphorylated serine (S) in the endodomain.Adapted fromVillar et al. (2003), doi:10.1007/BF02710396

5.5.3. Podoplanin in cancer

Induction of podoplanin expression is observed in experimental animal tumors. For example, significant amounts of this glycoprotein were found both on the surface of murine epidermal keratinocytes as well as on stromal cells of tumors caused by animal treatment with 7,12-dimethylbenzo[a]anthracene (DMBA) or 12-O-tetradecanoiloforbolo-13-acetate (TPA)[85]. Increased amounts of podoplanin and its neo-expression have been demonstrated in several types of human cancers. It is present in squamous cell carcinoma of the esophagus[88] of the uterine cervix[89], larynx, oral cavity[90][91], skin[81], lung[92][93], also in ovarian germ cell tumors (dysgerminomas and granulosa cell tumors)[81], seminomas[81], non-small lung carcinomas[81], angiosarcomas[84], mesotheliomas[94], fibrous tumor of the pleura[95], follicular

dendritic cell tumors[81], colon adenocarcinoma[96]. Increased amounts of podoplanin is also observed in some tumors of the central nervous system, such as germinoma, brain[97] and the highly malignant glioblastomamultiformisascompared to anaplastic astrocytoma[97].

The presence of podoplanin in hemangioblastomas,helpsto distinguish this type of cancer from renal cell carcinoma[81]. Similarly, the presence of this glycoprotein on mesothelioma cells allows to distinguish it from adenocarcinomas[81]and seminomas from embryonalcarcinomas[81].

In the case of squamous cell carcinoma of the oral cavity, a high level of podoplanin expression correlates with the incidence of lymph node metastasis and shorter survival[91].Wicki et al. (2006) have shown that generally in squamous cell carcinoma, including esophageal, skin, larynx, cervical uterine and lung, as well as some adenocarcinomas podoplanin expression is limited to tumor cells forming the outer layer of invasive front. Interestingly, tumor cell in these cases, also expressed the E-cadherin next to podoplanin. A similar location of podoplanin-expressing cells was observed by Shimada et al. (2009) in lung squamous cell carcinoma. The presence of podoplanin in these primary tumors correlated with the absence of lymphatic invasion and improved survival of patients. Low podoplanin expression was also an unfavorable prognostic in squamous cell carcinoma of the uterine cervix, correlating withan increased infiltration of lymphatic vessels by cancer cells, increased incidence of metastases to regional lymph nodes and worse survival[89]. These results were not confirmed in studies of Longatto-Filho et al. (2007), who havecorrelatedthe lack of podoplanin expression on cancer cells with a shorter survival in patients with uterine adenocarcinoma and an increased incidence of metastases to regional lymph nodes as well asdistant organs.

Podoplanin may serve as a marker of cancer stem cells as shown for A431 cells of squamous cell carcinoma of the skin[81]. Its presence correlates with the ability of A431 cells to form a tumor in nude mice[81].

5.5.4. Interactions of podoplanin

Presence of podoplanin in tumor cells is linked to their ability to form aggregates with platelets which, in turn, enhancesthe metastatic potential[98][99]. Ectopic podoplanin expression in Chinese Hamster Ovary (CHO) cells increased their ability to develop metastases in athymic mouse model. This wasdirectly connected to the presence of CHO cells-platelet aggregates[99]. The interaction with platelets is mediated by the sequence EDxxVTPG, called platelet aggregation-stimulating (PLAG) domainpresentin theextracellular domain of podoplanin[96]. PLAG domain is bound by lectin-like platelet receptor CLEC-2 (C-type lectin-

like receptor 2), which recognizes thetype-1 core*O*-glycanattached to threonine at position 52 of the polypeptidicchain[92][100].

Podoplanin is not only involved in the binding of platelets to tumor cells, but also increases the migratory ability of cells, including cancer cells. It was shown that podoplanin neo-expression in normal human keratinocytes and human breast cancer MCF-7 cells significantly changed their morphology, what was associated with a spike-like formation of filopodia. In MCF-7 cells, migratory and invasive properties increased, even in the presence of E-cadherin, a tumor suppressor involved in cell-cell adhesion[93][85]. This causes an increased adhesion to fibronectin through integrinsβ1[93]. Invasiveness of MCF-7 tumor cells was correlated with the ectopicexpression of podoplanin. This is associated with the increased activity of matrix metalloproteases (MMPs)[101]. Moreover, the transformation of mouse embryonic fibroblasts and cells of the central nervous system with Src oncogene resulted in the induction of podoplanin expression and increased their motility[102].

Ezrin, radixin, and moesin (ERM) are proteins which participate in signal transduction pathways that regulate adhesion and cell motility by linking integral membrane proteins with cortical actin cytoskeleton[103]. Therefore, changes in the migratory properties caused by podoplanin may be explained by its interaction with ezrin and moesin[85][93][90][104]. Podoplanin promotes the epithelial-mesenchymal transition associated with increased invasive and metastatic features through redistribution of ezrin to cell-surface protrusions. This is associated with the reorganization of actin cytoskeleton[105]. It was also found that podoplanin modulates the activity of RhoA GTP-ase, which increases cell migration and leads to epithelial-mesenchymal transition[90]**.** To elucidate the role of podoplanin in the activation of RhoA protein, various mutated forms of podoplanin were expressed in canine MDCK cells[90]. Podoplanin-positive MDCK cells displayed an increased activation of RhoA protein as compared to podoplanin-negative MDCK cells. This indicated a direct role of podoplanin in the activation of this GTP-aseandsuggested that podoplanin may activate RhoA protein in a similar manner to CD44 protein. Podoplanin in a complex with ERM protein binds to GDP/GTP exchange protein (GEP). Next, PDPN-ERM-GEP complex interacts with Rho-GDI dissociation inhibitor which is associated with RhoA protein with GDP molecule (RhoA-GDP) **(Fig. 10)**. RhoA-GDP is released, allowing its activation through GDP to GTP exchange by GDP-GTP exchange factor **(Fig. 10)**. Phosphorylation of ERM proteins is due to increased activity of RhoA protein which activates RhoA-associated kinase (ROCK) and this enhances the interaction between podoplanin and the cell cytoskeleton**(Fig. 10)**[106][81].

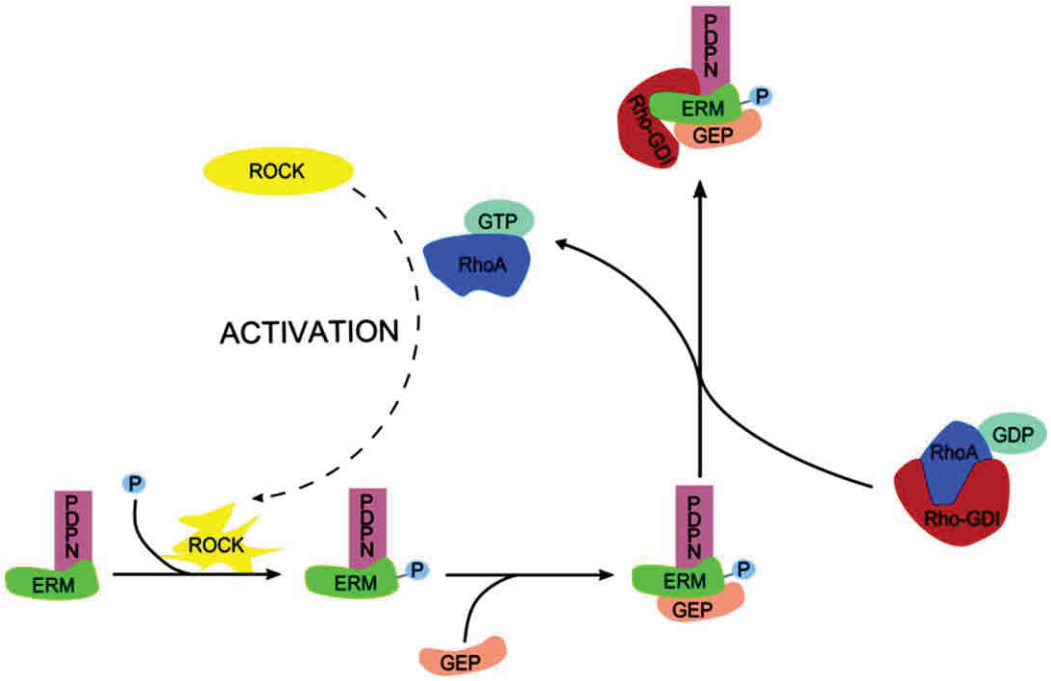

Figure 10. Schematic representation of RhoA activation by podoplanin and its interaction with ezrin radixin moesin proteins (ERM). Podoplanin (PDPN), RhoA-associated kinase (ROCK), exchange protein (GEP - GDP/GTP), dissociation inhibitor (Rho-GDI - Rho- GDP). Ugorski et al. (2016), 15;6(2):370-86. eCollection 2016.

5.5.5. Factors that stimulatespodoplanin expression

In the human breast cancerMCF-7 cells, podoplanin expression is induced by EGF, FGF2 and TNFα, in murine 3T3 fibroblasts by bradykinin[85][93], in human fibrosarcoma cells by TGFβ[99],and in the cutaneous lymphatic vessels by IL-3[107]. This suggests that podoplanin expression in tumor cells can be influenced by tumor microenvironment. As far as the endogenous factors which activate the expression of podoplanin are concerned,Foes protein was proposed[108], and in mouse embryonic fibroblasts transformed with malignant oncogene Src, podoplanin expression was induced by the intracellular signaling pathway comprising the Src oncogene and an adapter protein called Cry-associated substrate (CAS)[109].

5.5.6. Podoplanin in cancer-associated fibroblasts

Although podoplanin is expressed in many types of cancer, its expression was not found in tumor cells from several invasive adenocarcinomas, like breast[77], lung[110] or pancreas[111]. However, in such malignancies, this glycoprotein is highly expressed in cancer associated fibroblasts (CAFs)[81].Using newly

developed collagen invasion assay, Neri et al. (2015) foundthat, in lung adenocarcinoma, podoplanin-expressing CAFs invaded the collagen matrix more potently, and that more numerous cancer cells traveled within the "tracks" created by CAFs as compared to CAFs low-expressing thisglycoprotein. *Invivo* studiesconfirmed these data. When mice were injected intravenously with CAFs simultaneously with tumor cells, podoplanin-high CAFs invaded in larger amounts and promoted cancer cell invasion into the lung parenchyma as compared to podoplanin-low CAFs. When pancreatic cancer cells were co-cultured with fibroblasts with high podoplanin expression, their motility and invasiveness were increased in comparison to CAFs with low expression of *PDPN* gene. However, the suppression of PDPN in such cells by siRNA did not affect the biological properties of tumor cells, suggestingthatpodoplanin is not directly responsible for their migration and invasiveness. Podoplanin expression in CAFs of ductal breast carcinoma **(Fig. 11)** was associated with their degree of malignancy **(Fig. 12)**,blood vessel and lymphatic invasion by cancer cells, lymph node metastases, size of the tumor, shorter survival, expression of Ki67 and VEGF-C[22][81]. Similar observation was done for pancreatic and liver cancer[112][113]. Interestingly, podoplanin expression on CAFs in colon and squamous cell uterine cervix cancer correlated with longer survival[114][115]. Moreover the role of podoplanin expressed by CAFs in increased proliferation, survival and invasive properties of cancer cells through extracellular matrix remodeling, recruitment of progenitor endothelial cells, induction of angiogenesis, secretion of growth factors and chemokines, remain unclear. Recent studies using co-cultures of podoplanin-positive CAFs with lung adenocarcinoma cell lines display higher resistance of cancer cells in comparison to co-culture of cancer cells with control CAFs[116]. However, the molecular mechanism of podoplanin action in tumor progression is not explained. It was proposed that fibroblasts expressing podoplanin promote tumor formation by human lung adenocarcinoma cells through its interaction with RhoA protein[117]. A mutated form of podoplanin with deleted cytoplasmic domain resulted in a lowered potential of tumor formation[117]. The cytoplasmic domain of podoplanin regulates RhoA activity as confirmed in podoplanin-positive fibroblasts compared to podoplanin-mutated ones[117]. Thus the action of podoplanintowards cancer cells may be due to enhanced RhoA activity and further microenvironment remodeling. The direct effect of podoplanin in increasing the metastatic potential and tumorigenic activity was shown to involve human vascular adventitial fibroblasts (hVAFs) interacting with cancer cells and with the surrounding bloodvesselsduring the metastatic process[118]. The coinjection of hVAFs with human lung adenocarcinoma cell lines in comparison to co-injection with human lung tissue-derived fibroblasts (hLFs) lead to the rapid formation of tumor[118]. cDNA and flow cytometry analysis showed thatexpression of podoplanin is much higher inhVAFsthan in hLFs. Podoplanin positive hVAFs, upon sorting, showed higher ability to induce lymph node and lung metastasis of lung cancer cells, higher tumor formation compared to podoplanin-negative hVAFs. Moreover,the effect of tumorigenicityand colony formation *in vitro* decreased after podoplanin knockout whereas its overexpression accelerated tumor formation by

lungcancer cells [118]. Additionally patients with podoplanin-positive CAFs had high risk of recurrence and high rate of lymph node metastases[118].

Taken together, the role of podoplanin expressed by CAFs in cancer progression remains to be clarified.

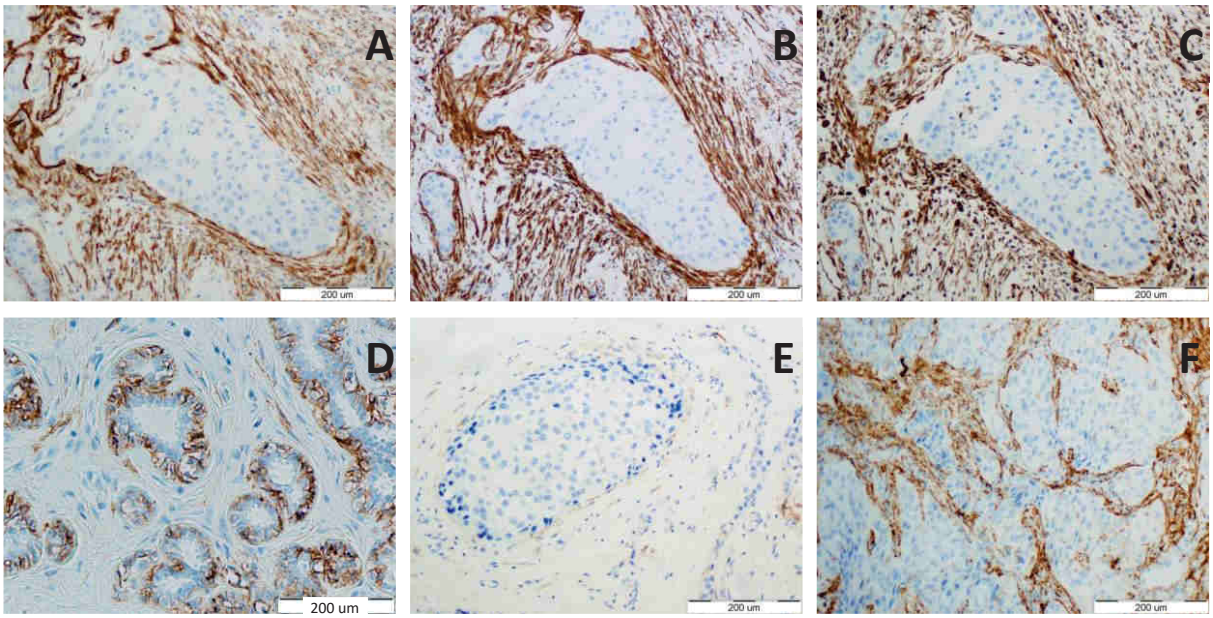

Figure 11. Immunocytochemical labeling of tissue sections.**(A)** Expression of podoplanin.**(B)** Expression of αSMA.**(C)** Expression ofvimentin in the stroma in ductal carcinoma of the breast.**(D)** No podoplanin expression was observed in the stroma in*dysplasia fibrocystica***(E)** and in breast cancer.**(F)**Its strong expression was observed in the stroma of ductal breast carcinoma. Bartosz Puła (Medical University, Wrocław).

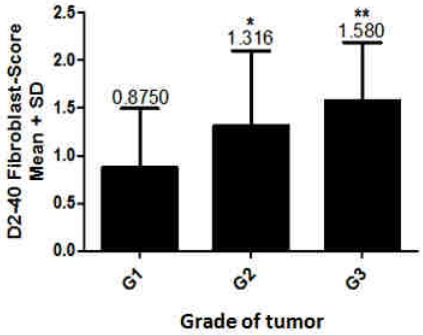

Figure 12. Podoplanin expression in the stroma, as a function of the degree of malignancy. The lowest expression was seen in cases of G1, and the highest in cancers G3. (* P <0.05 vs G1 G2; p <.005 G1 vs G3).G- degree of malignancy. Bartosz Puła (Medical University, Wrocław).

5.6. Micro RNAs

Podoplanin expressionisregulated by microRNAs (miRs) [119]. MiRsare a class of small noncodingRNAsofapproximately 22 nucleotides. They interfere with ribosomal machinery to regulate expression of genes and translation of proteins by targeting 3' untranslated regions (3' UTRs) of mRNAs, leading to their instability and suppressing translation. However, they can also activate genes[120] which are constitutively expressed. They usually have shorter 3' UTR sites and in consequence only fewer binding sites for miRNAsthan genes with multiple binding sites for minas[121]. Lin4 and let7 were the first discovered miRs, they are conserved among species what indicates an important role as regulatory factors, as they moreover can control hundreds of target mRNAs[122][123][124].

MiRNA genes are mostly transcribed by RNA polymerase II (Pol II) in the nucleus. The primary miRNAs (pri-miRNAs) are capped, spliced and polyadenylated (nature). Pri-miRNA can either produce a single miRNAormay contain two or more miRNAs. Long pri-miRNAs are cleaved to the 60–70-nucleotide precursor miRNAs (pre-miRNAs) by Microprocessor, which includes the double-stranded RNase III enzyme DROSHA and its cofactor, the double-stranded RNA (siRNA)-binding protein DiGeorge syndrome critical region 8 (DGCR8). The pre-miRNAs are processed by a ribonucleaseIII :DICER1into the mature miRNA. This process occurs in the cytoplasm where pre-miRNA is exported by exportin 5 (XPO5) from the nucleus. The guiding strand of mature miRNA is incorporated in the miRNA-induced silencing complex (miRISC), containing DICER1 and Argonaute (AGO) proteins. This complex directs the miRISC to target mRNAs by sequence complementary binding. Genes are suppressed by mRNA degradation and translational repression in processing bodies (P-bodies)**(Fig. 13A)**.

In cancer, the biogenesis of miRNA is deregulated at different steps during maturation. Hypoxia is one of the key regulator of pri-miRNA and pre-miRNA processing **(Fig. 13B)**.

A **B**

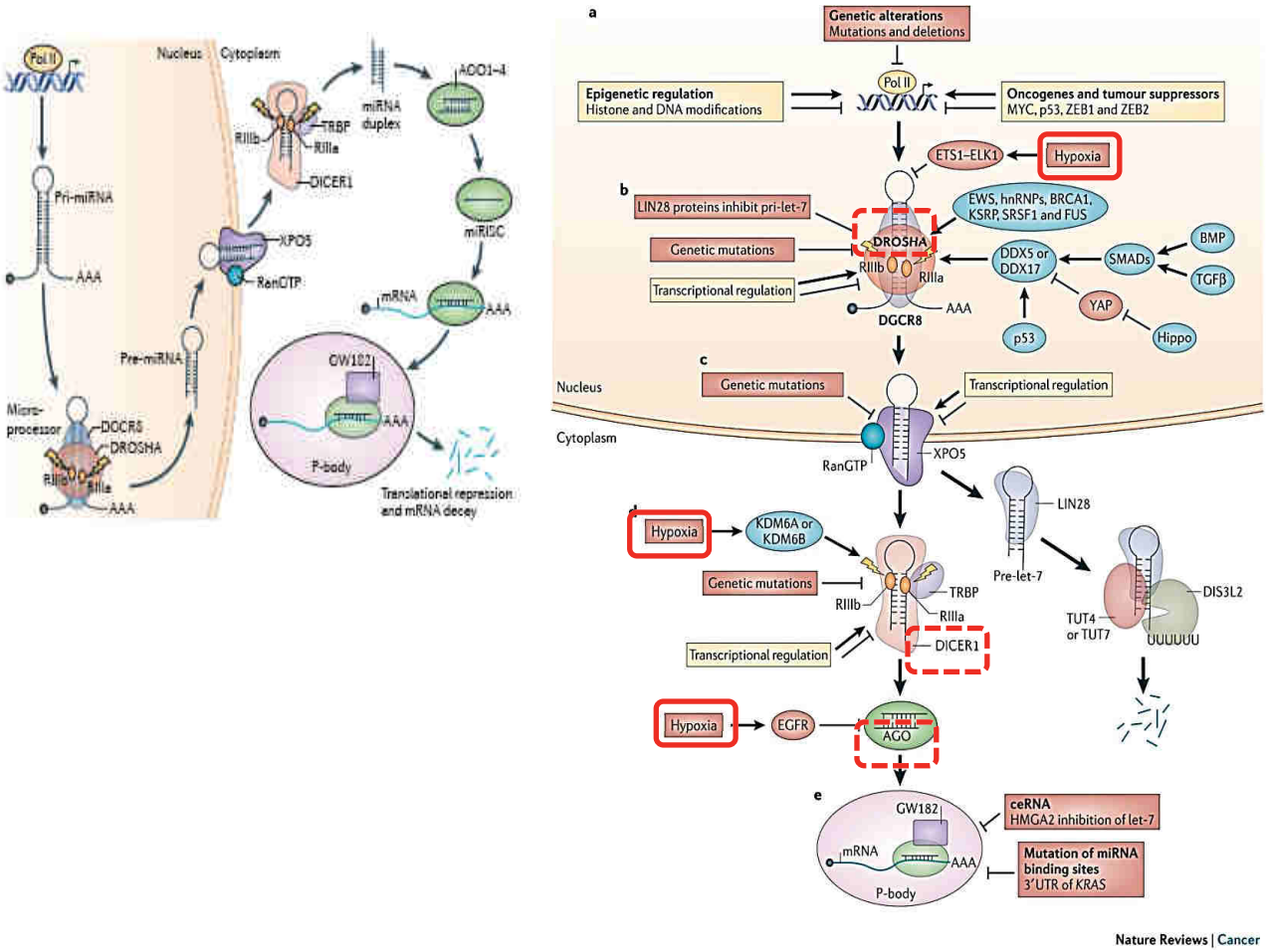

Figure 13. Normal and cancer-altered biogenesis of microRNAs. **(A)** Biogenesis of miRNA.RNA polymerase II (Pol II) transcribes miRNA genes as pri-miRNAs which are further cleaved by DROSHA and DGCR8 which are microprocessors to pre-miRNA. Then exportin 5 (XPO5) transfer pre-miRNA from nucleus to the cytoplasm where it is processed by DICER1 to mature miRNA. The guide strand of mature miRNA is loaded into miRISC complex which includes DICER1 and AGO proteins leading to target mRNAs. TRBP- transactivation-responsive RNA-binding protein. **(B)** Biogenesis of miRNA in cancer**. (a)** Regulation of pri-miRNA through oncogenes, tumor suppressors, genetic alterations and epigenetic modifications. **(b)** Hypoxia, transcriptional regulation and genetic mutations regulates pri-miRNA processing by controlling DROSHA and DGCR8 expression in cancer. Microprocessor activity is regulated by BRCA1, DEAD box protein 5 (DDX5) and DDX17.Pri-miRNA processing is regulated by cell signalling pathways as Hippo and BMP. Processing of pri-let-7 is blocked by LIN28 proteins. **(c)** Export of pre-miRNA if affected by regulation and mutations in XPO5. **(d)** Transcriptional regulation, mutations and hypoxia regulates pre-miRNA processing in cancer. **(e)** Function of miRNA is regulated through competing endogenous RNA (ceRNA**).** Pol II, RNA polymerase II; KDM6, lysine-specific demethylase 6; hnRNP, heterogeneous nuclear ribonucleoprotein; KSRP, KH-type splicing regulatory protein; ZEB, zinc-finger E-box-binding homeobox; RIII, ribonuclease III; YAP, Yes-associated protein; TGFβ, transforming growth factor-β; TRBP, transactivation-responsive RNA-binding protein; SRSF1, serine/arginine-rich splicing factor 1. Adapted from S.Lin (2015) Nature Reviews Cancer

Human and animal miRNAs target 3' UTR of mRNAs at position 2 to 7, called seed sequence because this is where complementarity occurs[125][126].Each miRNA may regulate many target genes and more than just one miRNA may bind to the same 3' UTR[127]. MiRNAs may be secreted and exchanged with other cells by exosomes and this mechanism is considered as a novel type of genetic exchange between cells[128]. Exosomes may be recognized by other cells. The latter may be distant thus achieving a paracrine action. MicroRNAs can reflect a biological state. This makes them useful diagnostic markers of diseases[129][130].MiRNAs may be located in introns of coding or non-coding genes or in exons so their transcription may be dependent on the host gene[131][132]. IntronicmiRNAs may be expressed together with their host gene but they also may have their own promoters and be expressed independently[133][134]. Stem loops of miRNAsare cut out from primary transcripts (pri-miRNA) in the nucleus by enzyme Drosha acting with DGCR8. This cut hairpin, 70-100nt length, called pre-miRNA,is nexttransported from the nucleus to the cytoplasm, in a GTP-dependent manner. Pre-miRNA is then cleaved by Dicer to form mature miRNA. Less stable 5' end strand is incorporated to the RISC complex byArgonaute protein[135][136]. Usually the second strand,calledmiRNA*, is degraded.MiRNAs localized in introns "mirtrons" are distinctly processed as the stem loop 3' end is cleaved by pre-mRNA splicing[137]. The"simtrons"groupofmiRNAsare splicing-independent. They are processed in a Drosha-dependent manner not requiring DGCR8, Dicer, Exportin-5 or Argonaute 2[138].

Expression of miRNA has been successively discovered in many types of cancer, firstly in adult leukemia and colorectal cancer[139][140]. Some of them, called oncomirs, behave as oncogenes and promotetumorigenesis by reducing the levels of proteins known to block proliferation, migration and activating apoptosis[141]. One of the best known oncomiRs called also hypoxamiR, miR-210,enhances the metastatic potential of hepatocellular carcinoma by targeting the „vacuole membrane protein 1"[142] which is associated with autophagy, cell adhesion and membrane trafficking[143]. Breast cancer cell migration and invasion are promoted by miR-135a by targeting HOXA10, which acts as metastasis suppressor in breast cancer[144]. A group of miRNAs inhibit the development of cancer and their inactivation together with accumulation of proteins that stimulate proliferation, migration and decrease apoptosis, cause cancer progression. Migration and invasion of breast cancer cells through regulation of uPA is mediated by miR-193b[145]. Angiomirs represent another group of miRNAs that modulate the development of new blood vessels[146]. MiR-126, anangiomir expressed in endothelium,enhances the pro-angiogenic action of VEGF and FGF[147]. Finally as miRNAs may be detected in body fluids, they can serve as biomarkers of diseases to monitor the development and progression of a disease. ThesecirculatingmiRNAs may be secreted from the cells to the blood, saliva, urine as free particles or in microvesicles as exosomes secreted by tumors[148][149]. Exosomes are small 50nm to 1μm micro-vesicles secreted by healthy or damaged cells in

response to stimuli as hypoxia and they are involved in communication between cells as mentioned above[150].Cancer cells communicate with endothelial cells to promote angiogenesis using exosomes as carrier for miRNA[151][152].

MicroRNAs have been shown to control tumor suppressor genes as PTEN (phosphatase and tensin homolog deleted on chromosome ten) or oncogenes. PTEN is associated with estrogen receptor and with the process of metastasis into lymph nodes[153]. Its expression is reduced in breast cancer, making it a potent prognostic marker. Moreover PTEN negatively controls PI3K-AKT-AP-1 signalling which regulates podoplanin expression. Podoplanin is a target of Fos transcription factor which is a part of AP-1 protein family. PTEN is a known target of miR-21[119].

Podoplanin may be regulated directly through miR-29b and miR-125a. These miRsinhibit proliferation, apoptosis and invasion of glioblastoma where they are down-regulated[154].

This work points to the understanding and defining the role of podoplanin expressed by fibroblasts in breast cancer in the context of hypoxia which is shown here to regulate podoplanin expression. Therefore its role in fibroblast migration, angiogenesis and tumor cells adhesiveness to tumor fibroblasts was further investigated.

6. MATERIALS AND METHODS

6.1.Materials

6.1.1. List of reagents

Reagent	Manufacturer
Agar	Roth
Agarose	Lonza
Acrylamide	Bioshop
Bovine serum albumin	POCH
Ethanol	POCH
Isoamyl alcohol	POCH
Isopropyl alcohol	POCH
Methyl alcohol	POCH
Ampicillin	Polfa
Bromophenol blue	Sigma
Coomassie Brilliant Blue R-250	Sigma
Ethidium bromide	Fluka
Butanol	POCH
Cell Tracker	Molecular Probes
Cyanate xylene	Sigma
Magnesium chloride	Chempur
Potassium chloride	Chempur
Rubidium chloride	Chempur
Sodium chloride	Chempur
Calcium chloride	Chempur
Chloroform	POCH
Deoxynucleotides (dNTPs)	EURx
Dimethyl sulfoxide (DMSO)	Merck
Yeast extract	Roth

Ethylenediaminetetraacetate (EDTA)	Sigma
Phenol	POCH
Phenylmethylsulfonylfluoride fluoride (PMSF)	Sigma
Glycerol	POCH
Glycine	Bioshop
Bicinchoninic acid	Sigma
2- [4- (2-hydroxyethyl) - 1piperazynylo]thanesulfonic acid (HEPES)	Roth
Morpholinepropanesulfonic acid (MOPS)	Roth
Glacial acetic acid	Chempur
Hydrochloric acid	POCH
L-glutamine	PPA
Methanol	POCH
β – mercaptoethanol	Fluka
N, N, N ', N'-tetramethylethylenediamine (TEMED)	Roth
N, N-methylene - bisacrylamide	Roth
Ammonium persulfate (APS)	Roth
Polyethyleneimine	Sigma
Sodium dodecyl sulfate (SDS)	Serva
Tris (hydroxymethyl) aminoethane (Tris)	Roth
Triton X-114	Serva
Tryptone	Roth
Tween 20	Sigma
Sodium hydroxide	Chempur
PBS	GmbH/Lonza
Puromycin	Sigma-Aldrich
IGEPAL Ca-630	Sigma
Fibronectin	Sigma

6.1.2. A ready to use sets of reagents

Name	Producer
Gel-Out Kit for the purification of DNA from agarose gels	A&A Biotechnology
Plasmid MINI Kit for isolation of up to 20 µg of plasmid DNA	A&A Biotechnology
Plasmid Midi AX Kit for isolation of up to 200 µg of plasmid DNA	A&A Biotechnology
RNeasy Mini Plus Kit for isolation of total RNA	Qiagen
miRNeasy Mini Kit for isolation of total and microRNA	Qiagen
Superscript First Strand Synthesis Kit for reverse transcription reaction	Invitrogen
NCode™ VILO™ miRNA cDNA Synthesis Kit and EXPRESS SYBR® GreenER™ miRNA qRTPCR Kit	Invitrogen
ExoQuick-TC™ Exosome Precipitation Solution	SBI System Biosciences

6.1.3. Buffers and solutions

Buffers and solutions	Composition
Buffer for SDS-PAGE	25 mM Tris-HCl, 192 mM glycine, 0.1% SDS
Protein transfer buffer	10 mM Tris-HCl pH 8.3, 150 mM glycine, 20% methanol
Loading LaemmLi buffer 6x (DNA)	0.09% bromophenol blue, 0.09% xylene diisocyanate, 60% glycerol, 60 mM EDTA
Sample buffer 4x (protein)	62.5 mM Tris-HCl, 2% SDS, 10% glycerol, 0.015% bromophenol blue
TAE buffer	40 mM Tris pH 8.0, 40 mM EDTA, 1 mM CH_3COOH
TBS buffer	24 mM Tris pH 7.6, 137 mM NaCl, 2.7

	mM KCl
TBST Buffer	24 mM Tris pH 7.4, 137 mM NaCl, 2.7 mM KCl, 0.1% Triton X-114
PBS	10 mM Na_2HPO_4 pH 7.4, 2 mM KH_2PO_4,137 mM NaCl, 2.7 mM KCl
RIPA buffer	50 mM Tris-HCl pH 8.0, 150 mM NaCl, 0.1% SDS, 1% IGEPAL Ca-630, 0.5% sodium deoxycholate
Coomassie blue solution	0.25% Coomassie brilliant blue R-250, 50% methanol, 10% CH3COOH
Transforming buffer I	100 mM RbCl,50 mM $MnCl_2$ pH 5.8,30 mM $CaCl_2$,100 mM CH_3COOH, 15% glycerol (v/v)
Transforming buffer II	100 mM RbCl pH 6.4 and 75mM CaCl2 20 mM MOPS 15% glycerol v/v
Buffer I	50 mM glucose, pH 8.0, 10 mM EDTA 25 mM Tris-HCl
Buffer II	0.1% SDS, 0.2 M NaOH
Buffer III	12% CH_3COOH 3 M CH_3COOK
"Strip" buffer	0.1% SDS, pH 2.2, 1% Tween 20, 1.5% glycine
FCI solution	phenol: chloroform: isoamyl alcohol 25:24:01 (v/v/v)
bicinchoninic acid solution	1000mL solution containing bicinchoninic acid, sodium carbonate, sodium tartrate, and sodium bicarbonate in 0.1 N NaOH (final pH 11.25).
cupric sulfate solution	25 mL solution containing 4% (w/v) copper(II) sulfate pentahydrate

6.1.4. Bacterial culture medium

LB Luria-Bertani nutrient solution	**SB Super Broth nutrient solution**	**SOC medium**
1% bacto-tryptone	3% bacto-tryptone	2% bacto-tryptone
1% NaCl		
0.5% Yeast extract	2% Yeast extract	0.5% Yeast extract
pH 7.0	1% MOPS pH 7.0	0.05% NaCl, 20 mM glucose, 2.5 mM KCl, 10 mM $MgCl_2$, pH 7.0

Solidified medium LB-agar: LB medium containing 1.5% agar
Solidified medium SB-agar: SB medium containing 1.5% agar

All media were sterilized in an autoclave for 30 min at 120°C and pressure of 1.2 Ba, followed by cooling to a temperature of approx. 50°C, the ampicillin was added to obtain final concentration 100 mg/mL.

6.1.5. The culture media and solutions used for cell cultures

OptiMEM medium MEM (Optimal Minimal Essential Medium) [Laboratory of General Chemistry IITD Academy of Sciences, Wroclaw; Invitrogen; Gibco, France]
trypsin/EDTA solution - aqueous solution of 0.05% trypsin and 0.02% EDTA [General Chemistry Laboratory IITD Academy of Sciences, Wroclaw; Gibco, France]
Dulbecco's Modified Eagle's medium[General Chemistry Laboratory IITD Academy of Sciences, Wroclaw; Gibco, France]
FBS [Cytogen; Invitrogen]
200 mM L-glutamine [Cytogen]
Solution “PenStrep” - 10 000 U/mLpenicillin and 10 mg/mL streptomycin [Cytogen; Invitrogen]
Complete DMEM medium - DMEM (Gibco, France) supplemented with 10% (vol/vol) of foetal bovine serum(BioWest), 0.2% of fungizone (Contains 250 μg of amphotericin B and 250 μg of sodium

desoxycholate per mL as a solubilizer in double distilled water, Gibco) and 1% ofPenicillin-Streptomycin (10,000 U/mL, Gibco).

Complete OptiMEM medium - (Gibco, France) supplemented with 2% (vol/vol) of foetal bovine serum (BioWest), 0.2% of fungizone (Contains 250 μg of amphotericin B and 250 μg of sodium desoxycholate per mL as a solubilizer in distilled water, Gibco) and 0.4% of gentamycin (10 mg/mL, Gibco).

6.1.6. Enzymes

Enzyme	**Buffer**	**Manufacturer**
EcoRI	buffer EcoRI	Fermentas
Bsu15I (ClaI)	buffer „Tango“	Fermentas
HindIII	buffer “RED”	Fermentas
KpnI	buffer KpnI	Fermentas
MLuI	buffer “RED”	Fermentas
NdeI	buffer “ORANGE”	Fermentas
Ligase T4	buffer “T4 ligase”300mM Tris-HCl (pH 7.8), 100mM MgCl2, 100mM DTT and 10mM ATP	Promega
Polymerase OptiTaq	buffer B	EURx
Power SYBR Green Mix		Applied Biosystems
SYBR Green Mix		Takara
SYBR Green Mix		Qiagen
Rnase A		Invitrogen

6.1.7. DNA and protein standards

DNA Standards	**Manufacturer**
GeneRuler ™ DNA Ladder Mix	Fermentas
GeneRuler 100 bp Plus Ladder	Fermentas

Protein Standards	**Manufacturer**
PageRuler Prestained ™ Protein Ladder	Fermentas

6.1.8. Oligonucleotides

Name	**Sequence**	**Protein**	**Use**
a-SMAF	5’-CTTGAGAAGAGTTACGAGTTG-3’	α-smooth muscle actin	Real-time PCR
a-SMAR	5’-AGGACATTGTTAGCATAGAGG3-’	α-smooth muscle actin	
PDPNF	5’-TAACAGGCATTCGCATCG-3’	podoplanin	
PDPNR	5’-ACAAACCATCTTTCTCAACTG-3’	podoplanin	
b-actF	5’-ACCACACCTTCTACAATGAGC-3’	β-actin	
b-actR	5’-GATAGCACAGCCTGGATAGC-3’	β-actin	
mTORF	Primers from Qiagen (QuantiTect Primer Assay) sequences not provided by the vendor	mTOR	
mTORR		mTOR	
AKTF		AKT	
AKTR		AKT	
PI3KF		PI3K	
PI3KR		PI3K	
PTENF		PTEN	
PTENR		PTEN	
VEGFAF		VEGFA	
VEGFAR		PTEN	
VEGFR1F		VEGFR1	
VEGFR1R		VEGFR1	

PDGFAF		PDGFA	
PDGFAR		PDGFA	
PDGFBF		PDGFB	
PDGFBR		PDGFB	
FGF-1F		FGF-1	
FGF1R		FGF-1	
U6 snRNA	5'-CGCAAGGATGACACGCAAATTC-3'	Micro RNAs	
U1 snRNA			
miR21			
miR29b	5'-TAGCACCATTTGAAATCAGTGTT-3'		
miR210			
miR125a	5'-GAGACCCTTTAACCTGTGAAA-3'		
reverse universal sequence primer	NCode VILO miRNA cDNA Synthesis Kit Invitrogen, sequence not provided by the vendor		
Hs PDPNfor	CGAATTCATGTGGAAGGTGTCAGCTC		Amplification of podoplanin cDNA and cloning into vector
Hs PDPNrev	GAACGCGTTTAGGGCGAGTACCTT		Amplification of podoplanin cDNA and cloning into vector

6.1.9. Viral Vectors

Set of third generation lentiviral vectors were obtained from W.R. A. Osborne(Division of Genetics and Developmental Medicine, Department of Pediatrics,University of Washington, USA):

pRRL - CMV - IRES-PUROtransferor vector

pMDL - g/p - RRE packaging vector

pRSV - REV vector with the gene for REV protein
PMK - VSVG (CMV) vector with gene of the coat protein of the VSV virus

6.1.10. Antibodies

Antibody	**Manufacturer**
Anti-Podoplanin/gp36 antibody [18H5] (FITC) (ab205333)	abcam
Mouse IgG1 [B11/6] (FITC) – Isotype Control (ab91356)	abcam
Anti-Human PodoplaninPE	e-Bioscience
Rat IgG2a K Isotype Control PE	e-Bioscience
Anti-Podoplanin Antibody, clone NZ1.2	Sigma
podoplanin Antibody (18H5): sc-59347	Santa Cruz
Anti-Mouse IgG (whole molecule)– Peroxidase antibody produced in rabbit	Sigma

6.1.11. Bacterial Strains

Escherichia coli strain DH5α ™ (F- φ80lacZΔM15 Δ(lacZYA-argF)U169 deoR recA1 endA1 hsdR17(rk-, mk+) phoA supE44 thi-1 gyrA96 relA1 λ-) (Promega)

6.1.12. Cell lines

293T-LentiX cells (Clontech) were derived from HEK293 cells (***h**uman **e**mbryonic **k**idney cells*) by transduction with human adenovirus type 5 DNA, and transfection with T antigencDNA. The cells are used aspackaging cell line because of their high efficiency transfection and production of high-titer lentivirus.

Human breast cancer MCF-7 cell line was obtained from Cell Lines Collection of Institute of Immunology and Experimental Therapy, PolishAcademy of Sciences in Wroclaw. The cells were derived from hormone-dependent, differentiated adenocarcinoma of the breastcharacterized by the expression of estrogen receptors (ER1α) and progesterone (PR).MCF-7 cell line is characterized by the presence of

estrogen and progesterone receptors. MCF-7 cells were referred to as epithelial-like luminal (Lacroix and Leclercq, 2004) and clinically responsible for cancers of highly-diverse features and representing the G1grade.

Human breast cancerMDA-MB-231 cell line was obtained from Cell Lines Collection of Institute of Immunology and Experimental Therapy, PolishAcademy of Sciences in Wroclaw. These cells were derived from adenocarcinoma of the breast. A characteristic feature of this cell line is a lack of receptors for estrogen, progesterone, and Her-2/neu (ErbB-2).MDA-MB-231 cell line is completely hormone-independent, highly invasive, display a high ability to migrate, an increased growth in semi-solid agar and the ability to form metastases in athymic mice model. They have been identified as mesenchymal-like (Lacroix and Leclercq, 2004), and they present a G3 grade.

Human skin endothelial microvascular HSkMEC cell line was established in prof. Claudine Kieda laboratory(Centre National de la Recherche Scientifique patent 99-16169). Human microvascular ECs were isolated and immortalized according to the method previously described and patented[155]. Their phenotype was shown to be stable in terms of adhesion molecules and typical EC characteristics.

Human fibroblasticMSU1.1 cell line (human fibroblasts N° CVCL_9S81) derived from human skin fibroblasts was obtained from Cell Line Collection of C. Kieda laboratory, Centre National de la Recherche Scientifique in Orleans.

Human aorta fibroblasts T/G HA-VSMC. Obtained from Cell Lines Collection of Institute of Immunology and Experimental Therapy, Polish Academy of Sciences in Wroclaw. Cell line has been derived from aorta (ATCC® CRL-1999™).

6.2.Methods

6.2.1. Preparation of chemically competent bacterial cells

For the preparation of chemically competent bacteria*E. coli* DH5α strain was used (**see chapter*6.1.11.***). Bacteria were streaking out on Petri dish with LB medium solidified with 1.5% agar and grownovernight at 37° C to obtain single colonies. Individual colonies were transferred to 10 mL of LB Broth and bacteria were grown again overnight at 37°C. Next day, 4 mL of bacterial suspension was collected and transferred to 300 mL of fresh LB Broth. After the bacterial culture reached an optical density OD_{600} = 0.5, bacteria were centrifuged at 2500xg for 10 minutes at 4°C, and their pellet was resuspended in 32 mL of transformation buffer I(cooled to 4°C). The bacteria were then centrifuged at 2500xg for 10 minutes, the pellet was resuspended in 9 mL of transformation buffer II (cooled to 4°C) and 100 µl of bacterial suspensions were transferred into Eppendorff tubes and frozen in liquid nitrogen. Chemically competent bacteria were stored at -80°C.

6.2.2. Bacterial transformation: the heat shock method

10 ng to 1 µg of DNA was added to 100 µl of competent bacteria suspension (**see chapter*6.2.1***) thawed on ice,the samples were incubated on ice for 20 minutes, and transferred to a water bath at 42°C for 50 seconds. After this time, the bacteria were placedagain on ice for 3 minutes. After this time, 1 mLof SOC medium wasadded, samples were transferred at 37°C, and incubated with gentle agitation for one hour. In the end, the suspension of bacterial cells was streakedon Petri dishes with LB medium solidified with agar and grown at 37°C overnight.

6.2.3. Purification of plasmid DNA using Plasmid Midi AX Kit

The day before plasmid DNA isolation, 100 mL of liquid LB Broth with addition of ampicillin (100 µg/mL) was inoculated with 4 mL of inoculum obtained after 6-hour bacterial culture established from a single bacterial colony (**see chapter*6.2.2***). The bacteria were grown at 37°C with shaking, for 16 - 20 hours. After this time, bacteria were centrifuged for 10 minutes at 2500xg and 4°C. The supernatant was discarded and the bacterial pellet was resuspended in 5 mL of buffer L1, followed by the addition of 5 mL of lysis

buffer L2. The samples were mixed carefully by inversion and left at room temperature for 5 minutes. Resulted bacterial lysate was neutralized by addition of 5 mL of buffer GL3, and samples were centrifuged using the manufacturer's filter inserts for 5 minutes at 1500xg. The filtrate was applied on a column provided by the manufacturer, column was washed with 20 mL of buffer K2, and plasmid DNA bounded to the column bed was eluted with 6 mL of buffer K3. Purified DNA was precipitated from the solution with 5 mL of isopropanol and 25mL of a "booster precipitation" (**see chapter*6.1.2.***). The sample was centrifuged for 15 minutes at 14 000xg and 4°C, supernatant was discarded and DNA pellet was washed with 2 mL of 70% ethanol by re-centrifugation for 5 minutes at 14000xg and 4°C. Purified DNA was solubilized in 200 µl of distilled H_2O. The end concentration of such DNA was 100 - 200 µg/µl, depending on isolation efficiency.

6.2.4. Isolation of plasmid DNA using Plasmid Mini AX Kit

Plasmid DNA was isolated from overnight, liquid bacterial culture that was carried out in 3 mL LB Broth with addition of ampicillin (100 µg/mL). Next day, the bacteria were centrifuged for 5 minutes at 8000 x g and the pellet was suspended in 600 µl of L1 cell suspension solution.The whole contents were transferred to the 2 mL Eppendorf tubes. 600 µl of L2 lysis solution was added and mixed gently, then incubated for 3 min at room temperature. 600 µl of L3T neutralizing solution was added and mixed gently until the disappearance of raspberry colour of the lysates. After addition of L3T neutralizing solution lysates were centrifuged for 5 min at 10 000-15 000 g. During centrifugation the Plasmid 20 columns were prepared, placed into the 20 mL tubes and set with tubes in the suitable rack. Then 1 mL of K1 equilibrating solution was applied onto each Plasmid 20 column and K1 equilibrating solution passed through the Plasmid 20 columns. The supernatants were applied onto pre-equilibrated Plasmid 20 columns and the lysates passed through the Plasmid 20 columns. 4 mL of K2 wash solution was added and passed through the Plasmid 20 columns. 300 µl of K3 elution solution was added and passed through the Plasmid 20 columns. The Plasmid 20 columns were transferred to new 2 mL precipitation tubes. 1 mL of K3 elution solution was added and passed through the Plasmid 20 columns. The Plasmid 20 columns were removed and 800 µl of PM precipitation mix was added to the eluted DNA. The samples were mixed by inverting the tubes a few times and samples were centrifuged for 5 min at 20 000 g. Supernatants were carefully discarded. 500 µl of 70% ethanol was added and samples were mixed and centrifuged for 3 min at 12 000 g. Supernatants were discarded carefully and DNA pellets were air dried for 5 min at room temperature in the up-side-down position. Dried DNA pellets were dissolved in 50 µl of DEPC water. The plasmid DNA was stored at +4 ºC to +8 ºC.

6.2.5. DNA electrophoresis in agarose gel

DNA electrophoresis was performed for the analytical or preparative purposes. It was performed on 1 to 2% agarose gel in TAE buffer, at a voltage of 90 - 130V. Due to the presence 0.5 µg/mLof ethidium bromide in the agarose gel,DNA fragments were detected under UV light using a gel documentation apparatus G: BOX manual (Syngene).

6.2.6. Isolation of DNA fragments from the agarose gel using Gel-Out kit

Small slices of gel (up to 200 mg) containing DNA fragmentswere excised from the agarose and transferred to Eppendorf tubes. Then,400 µl of buffer R7S was added and samples was left in a water bath at 50°C to completely dissolve the agarose. Now, 200 µl of isopropanol was added, samples were mixed again by inverting the tube, and centrifuged to remove residual fluid from the lid and walls. In the next step, the whole mixture was applied to the cartridge which was provided by a manufacturer and centrifuged for 30 seconds at 10 000xg. The supernatant was discarded, and the column was loaded with 600 µl of buffer A1. The samples were centrifuged at 10 000xg for 30 sec, supernatant was discarded and the column was loaded with 300 µl of buffer A1 and centrifuged again at 10 000xg for 2 minutes. After this time, the columns were placed in clean Eppendorf tubes,30 µl of distilled water was added and incubated for 3 minutes at room temperature. Samples were centrifuged at 10 000xg for 1 minute in order to elute DNA. The purified DNA was stored at -20°C.

6.2.7. Quantification of DNA

To determine the amount of plasmid DNA and degree of protein soilabsorbance at a wavelength of 260 nm and 280 nm on a spectrophotometer PicoDrop (Wrocław) or NanoDrop (Orleans) against water (blank) was measured. The amount of DNA was determined using the assumption that 50 µg/mL of plasmidDNA at a wavelength of 260 nm, gives an absorbance equal to 1. The ratio of absorbance atwavelength of 260 nm and 280 nm is indicative of the degree ofDNA and protein contaminationand it should be in the range of 1.7-2.0.

6.2.8. DNA digestion with restriction enzymes

Digestion of DNA with restriction enzymes was carried out in buffers recommended by the manufacturer, at 37°C for 1 to 16 hours. Usually, 10 U of enzyme per 1 µg of DNA was used, resulting in digestion for 1 hour. The final volume of the samples ranged from 10 µl to 50 µl.

6.2.9. Polymerase chain reaction (PCR)

PCR was performed in a thermocycler "Biorad". Reaction mixture composition and the conditions of reactions are shown below. PCR was performed using appropriate primers.

Composition of the PCR reaction mix	
5 - 50 ng of DNA template	1 µl
10x Buffer	2,5 µl
10 mM forward primer	1 µl
10 mM reverse primer	1 µl
1U OptiTaq polymerase (EURx)	1 µl
10 mM dNTPs	1 µl
25 mM MgCl2	2 µl
milliQ water	15,5 µl

Stage	**Temperature**	**Time**	**Cycle**
Initial denaturation	94 ºC	3 minutes	1
Denaturation	94 ºC	15-30 seconds	29
primer annealing	Tm ± 5 ° C	20 seconds	
elongation	72 ° C	1 min per 1000 bp	
final elongation	72 ° C	7 minutes	1

T_m - melting temperature of the primers

6.2.10. DNA ligation

Ligation reaction was used to connect covalently plasmid vectors and DNA inserts after their digestion with appropriate restriction enzymes. Relative ratios of insert to vector were 3: 1 or 2: 1. The reaction mixtures contained100 ng of total DNA in a suitable volume of 0.5 µl (1U) T4 ligase, 1 µl of buffer "T4 ligase buffer" (**see chapter*6.1.6)***and distilled water to a volume of 10 µl. The reaction was carried out at 15°C for 16 hours.

6.2.11. DNA sequencing

DNA sequencing was done by the company "Genomed" Sp. z o.o. (Warsaw, Poland). For sequencing primers were identical to the primers used for amplification of DNA fragments by PCR or "standard" primers supplied by the company "Genomed" for sequencing.

6.2.12. Isolation of total RNA using RNeasy Mini Plus Kit

RNA purification was carried out using the RNeasy Mini Plus Kit (**see chapter*6.1.2.***).Cells ($1x10^5$–$2x10^6$)were harvested from the culture dish by treatment with trypsin/EDTA solution (**see*6.1.5)***, rinsed twice with PBS buffer and centrifuged at 1200xg for 5 minutes at room temperature. Cell pellet was re-suspended in 350 µl of RLT buffer plus containing β-mercaptoethanol (10 µl of 14,3 M β-mercaptoethanol) and homogenized with a syringe. To remove genomic DNA, the lysate was applied onto "gDNA Eliminator" column(supplied by the manufacturer) andcentrifuged for 15 seconds at 10 000xg. Then,350 µl of 70% ethanol was added to the filtrate, sample was gently mixed by pipetting and applied onto the "RNeasy spin columns" (provided by the manufacturer), which was centrifuged for 15 seconds at 10 000xg. The filtrate was removed and column was washed with buffer RW1 (700 µl) and RPE (2x500 µl) by centrifugation for 15 seconds at 10 000xg, then transferred to the clean Eppendorf tube and centrifuged again for 2 minutes at 10 000x. In the end, 30 µl of RNase-free water was applied on the column, and after 3 minutes RNA bound to the column was eluted by centrifugation for 1 min at 1000xg.

6.2.13. Isolation of total RNA including miRNA using miRNeasy Mini Kit

Cells $1x10^6$ were washed twice with PBS and lysed by addition of 700 µl of Qiazol (**see chapter*6.1.2.***) directly to the culture dish. Lysates of cells were transferred to Eppendorf tubes and left for 5 minutes at room temperature to dissociate nucleoprotein complexes. Then the lysates were mixed with 140 µl of chloroform, shacked vigorously for 15 s and left for 2 minutes at room temperature. After that,samples were centrifuged at 12 000xg for 15 minutes at 4°C. The upper aqueous phase was transferred to new tube, mixed with 1.5 volume of 100% ethanol, and applied onto an RNeasy Mini spin column. After centrifugationfor 15 seconds at 8 000xg and room temperature, the column was washed once with 700 µl of RWT buffer and twice with 500 µl of RPE buffer. Bound RNA was eluted with 30-50 µl of RNase-free waterapplied directlyonto the RNeasy Mini spin column, which was centrifuged for 1 minute at 8 000xg.

6.2.14. Quantification of RNA and analysis of its purity and quality

RNA quantification was performed measuring the absorbance of the samples at 260 nmusing Nano-Drop ND-1000 Spectrophotometer (NanoDrop Technologies, Inc.), and the purity of RNA was determined by measuring the absorbance at 260 nm and 280 nm

The quality of RNA was assessed using Bioanalyzer 2100 (Agilent) **(Fig. 14A)** and RNA 6000 Nano Assay Kit with RNA Nano Chips**(Fig. 14B)**. RNA chip contains an interconnected set of microchannels that is used for separation of nucleic acid fragments based on their size as they are driven through it electrophoretically. RNA is detected by laser induced fluorescent detection. The results are displayed as chromatograms and electrophoresis pattern with estimated RNA Integrity Number (RIN). The electrodes of Agilent Bioanalyzer 2100 were decontaminated from RNAses using RNaseZAP solution and afterwards washed with RNase free water.The solution(550 µl)of gel matrix RNA 6000 Nanosupplied by the manufacturer**(Fig. 14C)**was added to a filter tube, which was centrifuged at 1500xg for 10 minutes. Then 1 µl of fluorescent dye concentrate supplied by the manufacturerwarmed to room temperature for 30 minutes was added to 65 µl of the filtered gel**(Fig. 14C)**. After vortexing, samples were centrifuged at 13 000xg for 10 minutes, and 9 µl of the gel-dye mix was loaded in the circled G well on the chip with pressure of a special syringe**(Fig. 14D)**, followed by pipetting of 9 µl of the gel-dye mix into the other 2G well and 5 µl of marker was pipetted to all other wells.In the meantime, the ladder RNA 6000 and RNA samples (25–500 ng/µl) were denatured at 70°C for 2 minutes and 1 µl of each sample was loaded on the chip, vortexed and fluorescence wasmeasured usingAgilent Bioanalyzer 2100. The results were analyzed with computer

program 2100 Expert Software (Agilent). Only RNA samples which had RINhigher than 7 were selected for further analysis.

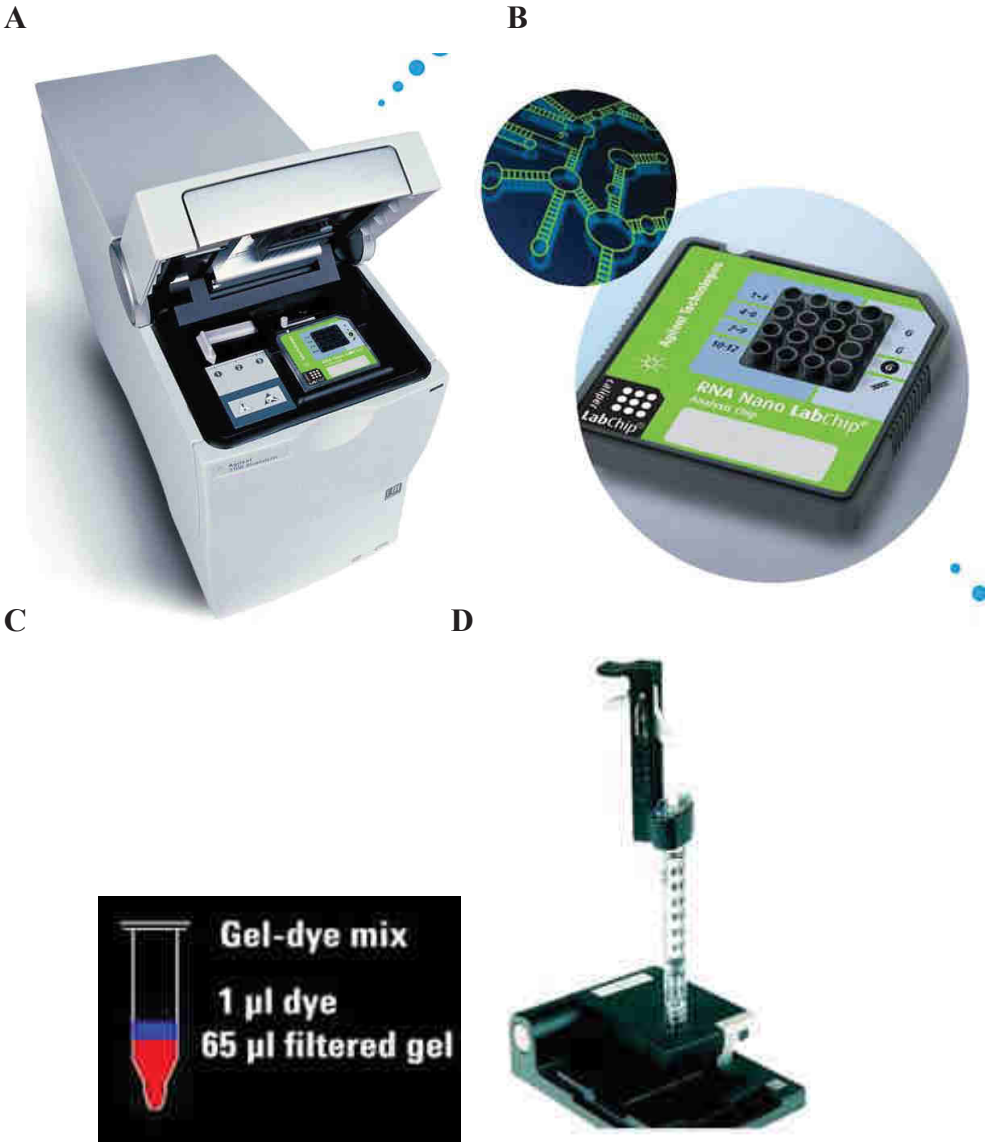

Figure 14. Diagram of Agilent RNA 6000 Nano Kit workflow.

6.2.15. cDNA synthesis (reverse transcription) using Superscript First Strand synthesis Kit

cDNA synthesis was performed according to the protocol provided by the manufacturer. To 8 µl (1 µg) of RNA solution in nuclease-free water, 1 µl of oligo(dT) at a concentration of 50 µM and 1 µl of 10

mM dNTPs (supplied by the manufacturer)were added and the sample was incubated for 5 minutes at 65°C. After this time, the sample was supplemented with10 µl of the reaction mixture (see table below) and incubated again at 50°C for 50 minutes. The reaction was stopped by leaving the tube in 85°C for 5 minutes. After chilling on ice, 1 µl of RNase H was added and sample was incubated for 20 minutes at 37 ° C. ObtainedcDNA was stored at -20 ° C.

Reagent	**Volume**
10x RT buffer	2 µl
25 mM $MgCl_2$	4 µl
0,1 M DDT	2 µl
Rnase OUT (40U/µl)	1 µl
SuperScript III RT (200 U/µl)	1 µl

6.2.16. cDNA synthesis using NCode™ VILO™ miRNA cDNA Synthesis Kit and EXPRESS SYBR® GreenER™ miRNA qRTPCR Kit

cDNA synthesis using NCode™ VILO™ miRNA cDNA Synthesis Kit and EXPRESS SYBR® GreenER™ miRNA qRTPCR Kit is a kit dedicated to synthesis of miRNA cDNA and further real-time qPCR. Following isolation of total RNA, all the miRNAs in the sample are polyadenlyated and reverse-transcribed using poly A polymerase, ATP, SuperScript™ III RT, and a specially designed universal RT primer in a single reaction **(Fig. 15)**. The first-strand cDNA is ready for analysis in qPCR using EXPRESS SYBR® GreenER™ detection reagents, the Universal qPCR Primer provided in the kit, and a forward primer designed by the user that targets the specific miRNA sequence of interest.

cDNA synthesis was performed according to the protocol provided by the kit manufacturer "NCode™ VILO™" , Invitrogen. To 1000 ng of RNA resuspended in appropriate amount of nuclease free water to obtain 16 µl of sample 4 µl of 5 x reaction mix and 2 µl of Super Script was added. Reaction was performed at 37 º C for 60 minutes and terminated at 95 º C for 5 minutes. Obtained cDNA was stored at -20 ° C.

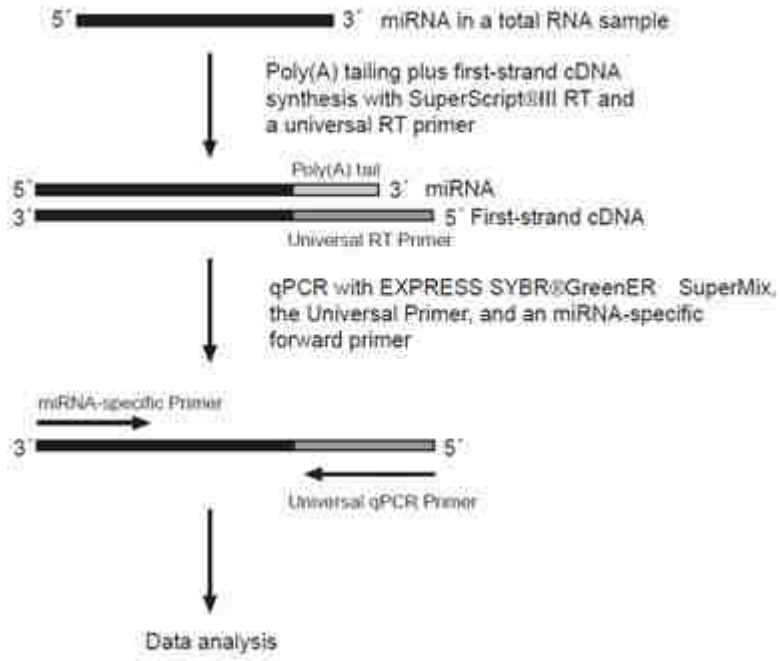

Figure 15. Diagram of miRNA cDNA synthesis kit workflow.

6.2.17. Real-time PCR

Melting curve analysis (60ºC -95ºC) was performed according to standard recommended programming in StepOnePlus™ Real-Time PCR Systems (Applied Biosystems) or LightCycler® 480 Real-Time PCR System (Roche).

The results were calculated using 2(-ΔΔCt) relative quantification method for independent in time *in vitro* experiments or 2(-ΔCt). SYBR Green I, used in the reaction, exhibits little fluorescence in solution, but emits a strong fluorescent signal upon binding to double-stranded DNA. Ct parameter (threshold cycle) is the cycle number at which the fluorescence emission exceeds the fixed threshold. ΔCt is equal to the difference: Ct value of gene of interest minus Ct value of reference gene. ΔΔCt is equal to the difference: ΔCt of experimental sample minus ΔCt of control sample.

Step	Temperature	TaKaRa	Cycles
Initial denaturation	95ºC	30 s	1
Denaturation	95ºC	5s	45
Annealing	60ºC	20 s	
Elongation	72ºC	15 s	

Step	Temperature	Qiagen	Cycles
Initial incubation	50ºC	2 min	1
Initial denaturation	95ºC	15 min	45
Denaturation	95ºC	15 s	
Annealing/Elongation	60ºC	60 s	

Expression levels of mRNAs and microRNAs were quantified using SYBR® Green QuantiTect Sybr Green PCR Kit (Qiagen) and SYBR® Premix Ex Taq^{TM} (TaKaRa) with either StepOnePlus™ Real-Time PCR Systems (Applied Biosystems) or LightCycler® 480 Real-Time PCR System (Roche) depending on the laboratory equipment (Poland or France). Prior to PCR, template cDNAs (**see chapter*6.2.15.*or *6.2.16.***) were diluted to the concentration of 10 ng/µl andthe reaction mix, in a final volume of 20 µl,was prepared. For template cDNA synthesized from mRNA, the mix consisted of 10 µl of Sybr Green fluorescent dye (supplied by the manufacturer), 1 µl of primer forward and 1 µl of primer reverse (supplied by manufacturer)and 6 µl of nuclease-free water. For miRNA-derived cDNA, the mix consisted of 7.5 µl of Sybr Green, 0.3 µl of miRNA primers and 0.3 µl of universal primer included in NCode VILO miRNA cDNA Synthesis Kitand 4.9 µl of nuclease-free water. Then 2 µl of not diluted cDNA was used. Melting curve analysis (60ºC - 95ºC) was performed according to recommended programming in StepOnePlus™ Real-Time PCR Systems (Applied Biosystems) or LightCycler® 480 Real-Time PCR System (Roche). The results were calculated employing the 2(-ΔΔCt) relative quantification method or 2(-ΔCt) for independent in time *in vitro* experiments. Ct parameter (threshold cycle) is the cycle number at which the fluorescence emission exceeds the fixed threshold. ΔCt is equal to the difference: Ct value of gene of interest minus Ct value of reference gene. ΔΔCt is equal to the difference: ΔCt of experimental sample minus ΔCt of control sample.

6.2.18. Production of lentivirus infectious particles in the packaging Lenti-X 293T cells

Packaging cells Lenti-X 293T (Clontech) were grown in two flasks T-75 in complete α-MEM medium until 50-60% of confluence was reached. For co-transfection of cells the following vectors were used: 20 µg of expression or control vectors, 10 µg pMDL-g/p-RRE, 5 µg pRSV-REV, 5 µg pMk-VSVG. To a mixture of the above vector, dissolved in 0.19 mL αMEM culture medium, 0.1 mL of PEI at a concentration of 1 mg/mL was added and kept for 15 minutes at room temperature in order to form PEI-DNA complexes. With thus-obtained reagent Lenti-X 293T cells were transfected by applying dropwise to the surface of the medium. After 16 - 18 hours of culture the medium was changed to 10 mL of fresh α-MEM containing 1% FBS. 72 hours after co-transfection, supernatant containing the infectious viral particles was collected in 50 mL tubes, which were centrifuged for 15 minutes at room temperature, 460xg in order to remove the packaging cells debris. The supernatant was then filtered using a 0.2 µm syringe filters (Millipore) and concentrated on Amicon Ultra-15 100 kDa (Millipore) filters by centrifugation for 10 minutes at room temperature, at 2460xg.

6.2.19. Cell transduction with lentivirus systemcontainingpRRL-CPPT-CMV-PDPN-IRES-PURO-PRE-SIN containing expression vector

Suspension of concentrated virus (**see chapter*6.2.18.***) (150µl)was added to 2 – 4x10^4 eukaryotic cells suspended in 0.9 mL of DMEM medium. Then, the sample was centrifuged for two hours at 2460x g, and 23°C. After this time, the supernatant was discarded and the cell pellet was re-suspended in complete DMEM medium and the cells were seeded into 24 well plate. Cells were selected with puromycin in appropriate concentration established in cytotoxicity test (1 µg/mL).

6.2.20. Preparation of cell lysates

Cells were rinsed three times with PBS, and then torn away from the surface of the culture vessel with a plastic scraper and centrifuged at 300xg for 5 minutes at 4°C. The cell pellet was re-suspended in RIPA lysis buffer (**see chapter*6.1.3.***)containing 1 mM PMSF and kept on ice for 15 minutes. The samples were then centrifuged at 8 000xg for 15 minutes at 4°C. The supernatant was collected into a clean Eppendorftube and protein concentration was determined by the biuret method using a bicinchoninic acid assay (**see chapter*6.2.21.***).

6.2.21. Bicinchoninic acid assay

For protein quantification, samples of cell lysates at a volume of 1 µl or 2 µl were supplemented up to a volume of 20 µl with distilled water. Subsequently, 200 µl of bicinchoninic acid solution (**see chapter*6.1.3***) mixed with cupric sulfate solution (**see chapter*6.1.3***) ata ratio of 50: 1 (v/v) were added to the lysates and the samples were incubated at 37°C for 30 min. Absorbance was measured at 562 nm, against blank sample in a spectrophotometer EL 311 (Behring). For the standard curve, serial dilutions (0.1 mg/mL, 0.25 mg/mL, 0.5 mg/mL, 0.75 mg/mL, 1 mg/mL) of BSAstandard (10 mg/mL) were used.

6.2.22. Sodium dodecyl sulphate polyacrylamide gel electrophoresis (SDS-PAGE)

SDS-PAGE was performedin gradient polyacrylamide gel (8% - 15%) or 13% polyacrylamide gel. Protein lysate (50 µg) was added to 6-fold concentrated Laemmli sample buffer (**see chapter*6.1.3.***) and the sample was placed inboiling water bath for 5 minutes. The sample and protein standard "PageRuler Prestained ™ Protein Ladder" (**see chapter*6.1.7.***) were applied to the wells in stacking polyacrylamide gel. Protein separation was performed in electrophoresis buffer (**see chapter*6.1.3.***), initially at a voltage of 70 V which, after incorporation of samples into the gel,was increased up to 120 V. Electrophoresis was carried out for 3 hours at room temperature. In order to detect the separated proteins, the gel was left overnight at room temperature in the solution of Coomassie Brilliant Blue(**see chapter*6.1.1.***). Then, the gel was placed in a solution of 25% methanol and 7.5% acetic acid to wash out the dye.

6.2.23. Immunoblotting (Western blotting)

To detect the specific protein bands, all proteins after separation in a polyacrylamide gel were transferred by electroblotting to a nitrocellulose membrane (BioRad) in electrotransfer buffer (**see chapter*6.1.3.***)for 60 minutes, at intensity of the current 200 mA. Then, the nitrocellulose membrane was incubated for 1 hour at room temperature in 5% solution ofmilk powder (Dairy Cooperative "Gostyń") dissolved in TBS buffer. After this period, proteins transferred to nitrocellulose were incubated at room temperature with the corresponding antibody diluted with TBS buffer containing 0.2% Tween-80 for 16 hours at 4°C. After washing the membrane three times with TBS buffer containing 0.2% Tween-80, the nitrocellulose was incubated with appropriate secondary antibody conjugated with HRP diluted 1 000 times with TBS containing 0.2% Tween-80. After washing away unbound antibody three times with TBS

containing 0.2% Tween-80, the nitrocellulose was placed in 2mL of SuperSignal West PicoChemiluminescent Substrate (Thermo Scientific) obtained by mixing equal parts of the Stable Peroxide Solution and the Luminol/Enhancer Solution and incubated for 5 minutes.Then the chemiluminescent signal was taken in a G-BOX (Syngene).

6.2.24. Removal of antibodies bound to the nitrocellulose (stripping)

In order to reuse the nitrocellulose membrane with bound antibodies, they were removed by treating the membrane twice, each time for 10 min, with a special "strip" buffer pH 2.2 (**see chapter*6.1.3.***). Then, the nitrocellulose membrane was washed twice with PBS and twice with TBS for 10 minutes, and treated second time with 5% solution of milk powder (Dairy Cooperative "Gostyń") in TBS buffer for 1 hour at room temperature.

6.2.25. Cell culture

The cell cultures were carried out in culture vessels (Sarstedt) in a complete DMEM or OptiMEM medium (**see chapter*6.1.5***), at a temperature of 37°C and 5% CO_2. When the cells reached the state of maximum growth density medium was harvested from the cells and rinsed with PBS (**see chapter*6.1.3***). Then 0.5 mL to 10 mL (depending on the size of the culture vessel)0.25% trypsin in 1 mM EDTA was added to the cells and incubated at 37 ° C until detachment of the cells from the bottom of the culture vessel. These cells were resuspended in 5 mL of medium α-MEM and centrifuged at 4 ° C, at 300 x g for 5 minutes. After removing the supernatant, the cell pellet was resuspended in an appropriate volume of complete DMEM or OptiMEM medium and seeded into a culture vessel of appropriate size. Human fibroblasts and breast cancer cells were cultured in complete DMEM complete medium.

6.2.26. Cell freezing

Cells were detached from culture dish with a solution of trypsin/EDTA (**see chapter*6.1.5***) and transferred to a sterile 15 mL (Sarstedt)test tube, complete DMEM medium was added and cell suspension was centrifuged at 300xg for 5 minutes at 4 ° C. The supernatant was discarded and the cells were suspended in 0.5 mL DMEM medium and 0.5 mLof 20% DMSO in FBS was added dropwise. After mixing, the cell suspension was transferred into ampoules for freezing cells (Nunc), which was then placed in a container

with isopropanol and left for approx. 24 hours at -80 ° C. After this time, the vial was transferred to a container with liquid nitrogen.

6.2.27. Cell culture in hypoxic conditions

To maintain cells under hypoxic conditions (1% O_2) a hypoxic chamber was used. Cells were exposed to a gas mixture (1% O_2, 5% CO_2, 94% N_2) in an automated PROOX *In Vitro* Chamber (C-174, BioSpherix, USA), controlled by the PROOX (Carbon Dioxide and Oxygen Controller), model 110 (BioSpherix, USA) in which the atmosphere was humidified. The chamber was located in an incubator, at 37°C.

6.2.28. Flow adhesion assay with Bioflux system

The BioFlux plates contain an array of microfluidic flow channels arranged on a well plate format (24 or 48 wells plates)**(Fig. 16B)**. Each flow channel connects to one input well (for 48 wells plate) or two input wells (for 24 wells plate) and an output wellon the plate**(Fig. 16C)**. The BioFlux Pressure Interface couples to the top of the well plate andapplies a controlled pneumatic pressure from the control instrument to the top of thewells which drives the fluid through the channels at a user-defined flow rate**(Fig. 16C)**. Reagentsin the channel flow across an observation area which is situated between the wells**(Fig. 16C, D)**. Theflow profile in BioFlux plates is uniform and laminar.Experiments with Bioflux (Fluxion Biosciences Inc, San Francisco) wereperformed on 24 or 48 wells plate. On 24 wells plate, the viewing windows allow visualizing 4 different channels and there are two viewing windows, whatallows setting 8 different conditions. For one condition, there are three wells, 2 inputsand 1 output. Output wells are used for cell seeding, whereas input wells are used to create cell flow and for washing with basal medium. 48 well plates possess 12viewingwindows, each permitting to visualize two different channels, what allows setting 24 different conditions on one plate**(Fig. 16B, D)**. Additionally, 48 well plates possess only 1 output and 1 input well, which requires taking off cell suspension and put basal medium for washing step. CMFDA-stained breast cancer cells MDA-MB-231 were resuspended in basal DMEM medium at aconcentration of 1 x 10^6cells/mL. 400 µl for 24 well plates or 200 µl for 48 well plates ofcellsuspension were added to the output wells. Plates were covered with the interface plate connected to the machine which creates pressure by plastic tubes. TheBioflux plate with tubes was placed under the Axiovert 200 epifluorescence invertedmicroscope (Zeiss, Germany) to enable the observation of cell monolayers in theviewing windows.

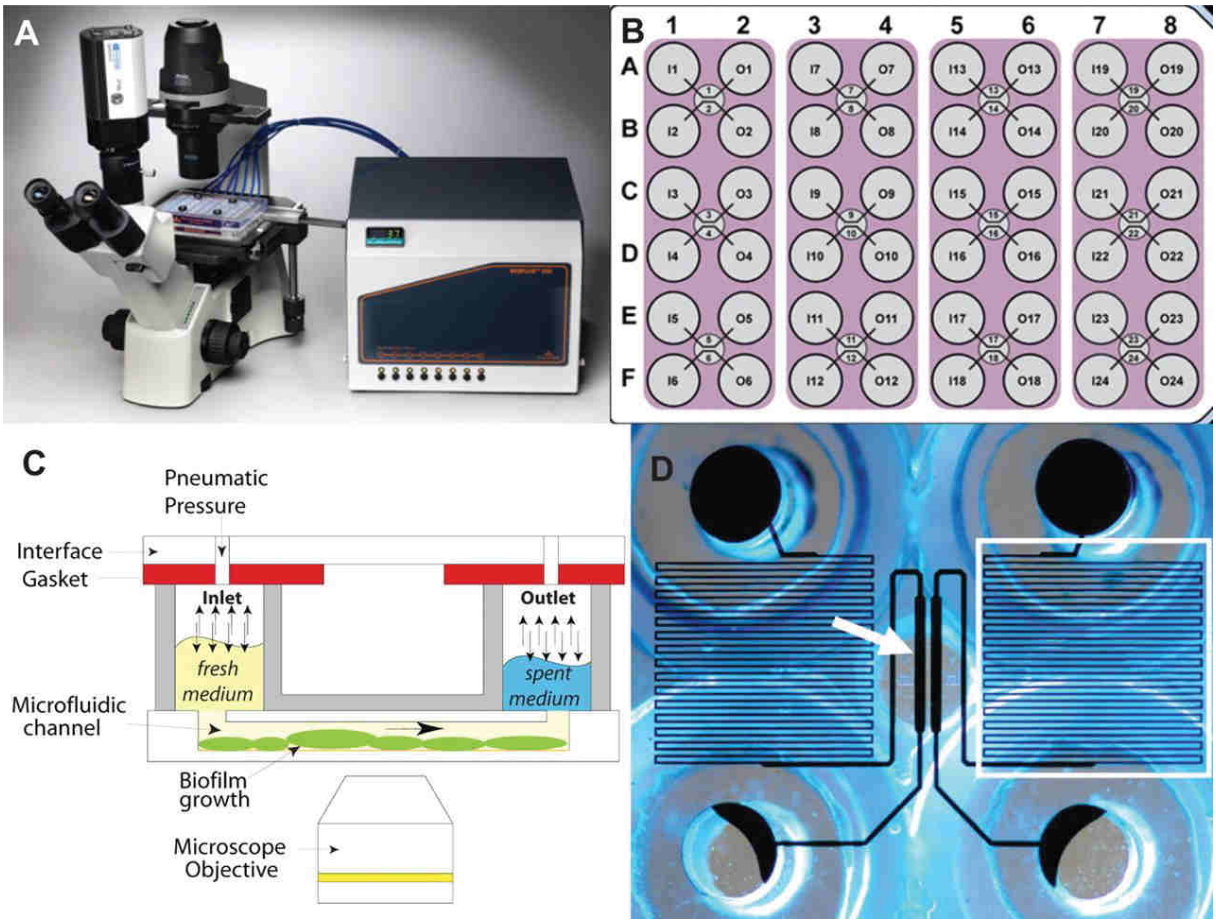

Figure 16. Bioflux system workflow.**(A)**Pump with 48 well plate under the microscope.**(B)**Scheme of input and output wells on 48-well plate.**(C)**Principle of cell monolayer (biofilm) seeding.**(D)**System of microchannels outgoing from input and output wells with viewing windows marked with white arrow.

6.2.28.1. Fibronectin coating prior to cell seeding in bioflux system

Human fibronectin (**see chapter*6.1.1***),was diluted to a concentration of50 µg/mL in PBS. 200 µl of PBS was added to each «exit» well, on the top of the centralring and push for 10 s at 10 dyn/cm^2 to prime the plate. PBS was removedfrom the «exit» wells and 200 µl of fibronectin(50 µg/mL) were added and pushed for 10 s at 5 dyn/cm^2 in 24 well plates or 5 s in 48 well plates. Plates wereincubated at room temperature for 1 hour.

6.2.28.2. Fibroblast seeding in bioflux system

In Bioflux plates, after incubation (**see *6.2.28.1***), solution of unbound fibronectin was removed) and 1 mL of appropriate complete DMEM medium as added into exit wells and pushed for 5 min at 5 dyn/cm^2 **(Fig. 16C)**. Medium was removed and 200 µl of cellsuspension (MSU1.1 NC or MSU1.1 PDPN) at 1 x 10^7 cells/mL was added in «exit» wells and pushed 10 s at 5 dyn/cm^2 for 24 well plates or 5 s for 48 well plates. Cell suspension was removed and 2 mL for 24 well plates or 1mL for 48 well plates of complete medium were added in all wells. Then, plates were incubated at 37°Cin a 5% CO2 and 95% air atmosphere. After at least 1 hour, cell adhesion was checked in the viewing windows and if cells were adhered, medium from the «exit» wells was removed to allow a passive flow of medium from the «entry» wells to the «exit» wells, so that the cells were oxygenated.

6.2.28.3. CCL21 pre-treatment of endothelial cell monolayer

The solution of the CCL21chemokine was prepared in basal medium at aconcentration of 0.2 µg/mL for cell culture slides or 0.6 µg/mL for Bioflux plate. After 48 hours of culture, medium was removed from cell culture slides or from wells of theBioflux plate. Then, 1 mL of CCL21 solution was added directly on slide. For Biofluxplate, 200 µl of CCL21 were added per well and pushed at 5 dyn/cm^{2}for 10 s. Thenslides or plates were incubated for 1 hour at 37°C.

6.2.29. 2D migration assay

4 x 10$^{5/}$mL (applied in 70 µl per well of an IbidiCulture-Insert, Ibidi GmbH, integratedBioDIagnostic)MSU1.1 NC, MSU1.1 PDPN, HSkMEC, MDA-MB-231, MCF-7 cells were seeded (**Fig. 17**) in each compartment of an insert placed in 24 - well plate (**Fig. 17**) and grown to full confluence in OptiMEM, 2% FBS medium. After the confluence was reached during 24 hours the insert was removed with tweezers and the cell-free gap (500 µm ± 50 µm) was generated. Photographs were taken each hour up to 48 hours after the injury, always from the same place (3 pictures per well), and analyzed using ImageJ software (National Institute of Health, available from the website http://rsb.info.nih.gov/ij). Cell-free area was calculated.

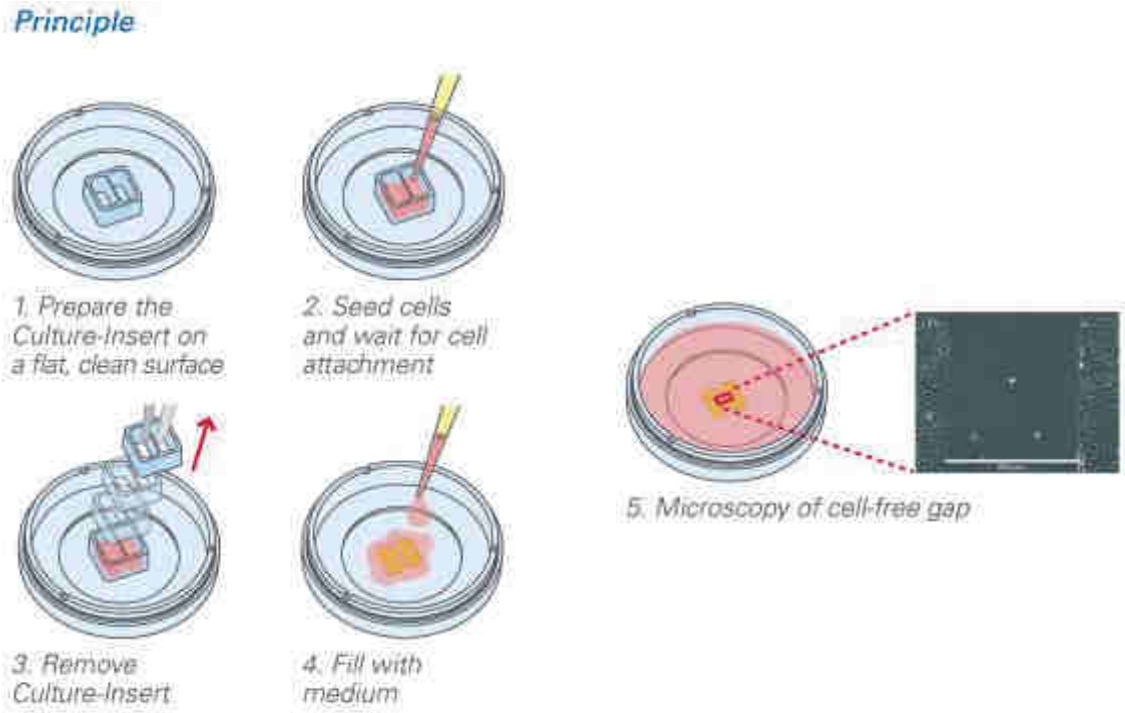

Figure 17. Principle of cell seeding using an Ibidi inserts.

6.2.30. Angiogenic assays with skin microvascular endothelial HSkMEC cells and fiboblasts

Fibroblasts were cultured in 10 cm^2 dishes in complete OPTI-MEM media one week prior to the experiment. Fibroblast cells and HSkMEC cells were labeled, respectively, with fluorescent dye DiO (Invitrogen) and fluorescent dye DiD (Invitrogen) according to the manufacturer's protocol. For angiogenic assay, HSkMEC cells were used at the density of $1x10^5$ cell/mL and MSU1.1 NC or MSU1.1 PDPNfibroblasts at a density of $0.5x10^5$ cell/mL. For the purpose of the assay, the wells of a 96-well plate (Sarstedt, Germany) were covered with 40 µl of Matrigel™ Growth Factor Reduced GFR (Corning) and left at 37°C for 30 min. Then 100 µl of each cell suspensions (fibroblasts or endothelial cells) or both cell suspensions (fibroblast-endothelial co-cultures) were added to the wells and cells were grown for 24 h at 37°C. Endothelial tube formation was analyzed by taking photographs every half hour with videomicroscope Zeiss Axiovert 200M and AxioVision Software (Zeiss). A toolset of Image J software was used for analysis of cellular networks (DeCicco-Skinner et al., 2014). The number of nodes and number of meshes were quantified on fluorescence images of HSkMEC, MSU1.1 NC and MSU1.1 PDPN cells after 12 hours. A node was defined as pixels that have at least 3 neighbors, corresponding to a bifurcation. The meshes were defined as areas enclosed by the segments. Quantitative statistical co-localization on two-color images using

a software tool to calculate the Pearson and Spearman correlation coefficients ('Pearson–Spearman correlation colocalization' ImageJ plug-in) across regions of interest within the image was used. A quantitative estimate of the amount of co-localization in the images was given as the result.

6.2.31. Exosome isolation using ExoQuick-TC™ Exosome Precipitation Solution

10 mL of medium from the cells ($1x10^6$) culturedeither in normoxia or hypoxia for 24 hours in 6 well plateswas collectedandcentrifuged at 3000 x g for 15 minutes to remove cells and cell debris. Culture supernatants transferred to a sterile 15 mL falcon tubeswere mixed with 2 mLof ExoQuick-TC Exosome Precipitation Solution (supplied by manufacturer) by inverting the tube. The samples were incubated overnight at 4ºC and centrifuged at 1500 x g for 30 minutes at 4°C. Supernatant was aspirated, the residual exoqiuck solution was spinned down bycentrifugation at 1500 x g for 5 minutes, andall traces of fluid was aspirated.Exosome beige pellet was resuspended in 700µl of Qiazol lysis buffer (supplied by manufacturer) for miRNA extraction (**see chapter*6.2.13.***).

6.2.32. Statistical analysis

Prism 5.0 software (GraphPad, La Jolla, CA, USA) was utilized to analyze the data. Statistical analysis of the results was performed using two-tailed Student's t-test. Differences at the level of $p<0.05$ were considered as statistically significant. All data are presented as mean + SEM. The Mann-Whitney test was used to compare the groups of data that not meet the assumptions of the parametric test when evaluating the significance of the differences between the tube formation curves in the angiogenic assay on Matrigel. Two-way ANOVA with the Bonferroni multiple comparison test was used to analyze the differences between the analyzed cell lines. In all analyzes, the results were considered statistically significant when $p < 0.05$. Image J software (open source) was used to calculate the amount of co-localization in the selected images. Pearson and Sperman correlation coefficient was measured and the amount of co-localization in the images was given as the result.

7. Aim of the study

„Wpływ hipoksji na ekspresję podoplaniny w fibroblastach towarzyszących nowotworom (CAF) i jej udział w progresji raka piersi
„The influence of hypoxia on podoplanin expression in cancer-associated fibroblasts (CAF) and its role in progression of breast cancer"

According to the present view, a tumor is a kind of tissue including, in addition to cancer cells, a modified extracellular matrix, endothelial cells, blood vessels and lymphatic vessels, various immune and inflammatory cells as well as activated fibroblasts called cancer-associated fibroblasts (CAF). Tumor microenvironment plays an important role in both tumor development and metastasis (Liotta and Kohn, 2001). However, the knowledge about individual components of the cellular microenvironment, matrix proteins and glycoproteins and their role in tumor progression is very limited, especially at the molecular level. Recent studies have shown that podoplanin (PDPN), a mucin-type glycoprotein, is expressed in tumor cells and/or tumor-associated fibroblasts (CAFs) and its expression is dependent on the tumor type (Aishima et al, 2008; Yamanashi et al, 2009). Previous studies have shown that, in breast cancer, the number of podoplanin-expressing CAFs correlated positively with tumor size, grade of malignancy, lymph node metastasis, lymphovascular invasion and poor patients' outcome [22]. **Therefore, the aim of the thesis was to better understand and define the role of podoplanin expressed by CAFs in breast cancer.** Research aimed: 1. to determine the role of CAFs expressing podoplanin in terms of migration, invasion, angiogenesis and adhesion properties of breast cancer and endothelial cells 2. to identify the factors of the tumor microenvironment which may induce the expression of podoplanin in CAF. In this view our study also focused on determining the influence of hypoxia on the expression of podoplanin and of the related microRNAs in CAFs as well as the influence of CAFs-produced factors upon overexpression of podoplanin on angiogenesis.

The above-cited major goals required to achieve the following steps.

1. The design of a cell model displaying overexpression of podoplanin, including :
    a. Construction of an expression vector pRRL-CPPT-CMV-PDPN-IRES-PURO-PRE-SIN containing the cDNA sequence for podoplanin coding
    b. Characterization of the human fibroblastic cell lines overexpressing podoplanin
2. The demonstration of the impact of hypoxia on the expression of podoplanin in human fibroblastic cells
3. The demonstration of the impact of podoplanin on fibroblasts, cancer cells and endothelial cells migration in the context of hypoxia

4. The demonstration of the role of podoplanin on adhesion of cancer cells in the context of hypoxia
5. The study of the effect of podoplanin expressed by fibroblasts on angiogenesis under hypoxic and normoxic conditions
6. The elucidation of the effect of podoplanin expression together with hypoxia on the expression of proangiogenic factors in human fibroblastic cells
7. The description of specific miRNAs expressed by non-activated fibroblasts and fibroblasts overexpressing podoplanin as well as their secretion mechanism via exosomes in the context of hypoxia

8. RESULTS

8.1. Characterization of human fibroblastic cell lines according to the expression of podoplanin

The human fibroblastic MSU1.1 cell line was used and smooth muscle T/G HA-VSMC cell line was chosen because it presents a fibroblastic morphology and putatively expresses podoplanin, constitutively. The cells were analyzed for the expression of podoplanin. Using real-time PCR, immunocytochemistry, western blotting and fluorescent staining of living cells it was found that T/G HA-VSMC cells only express podoplanin at the levels of mRNA **(Fig.18C)** as well as protein expression **(Fig. 18A, B, D)**.

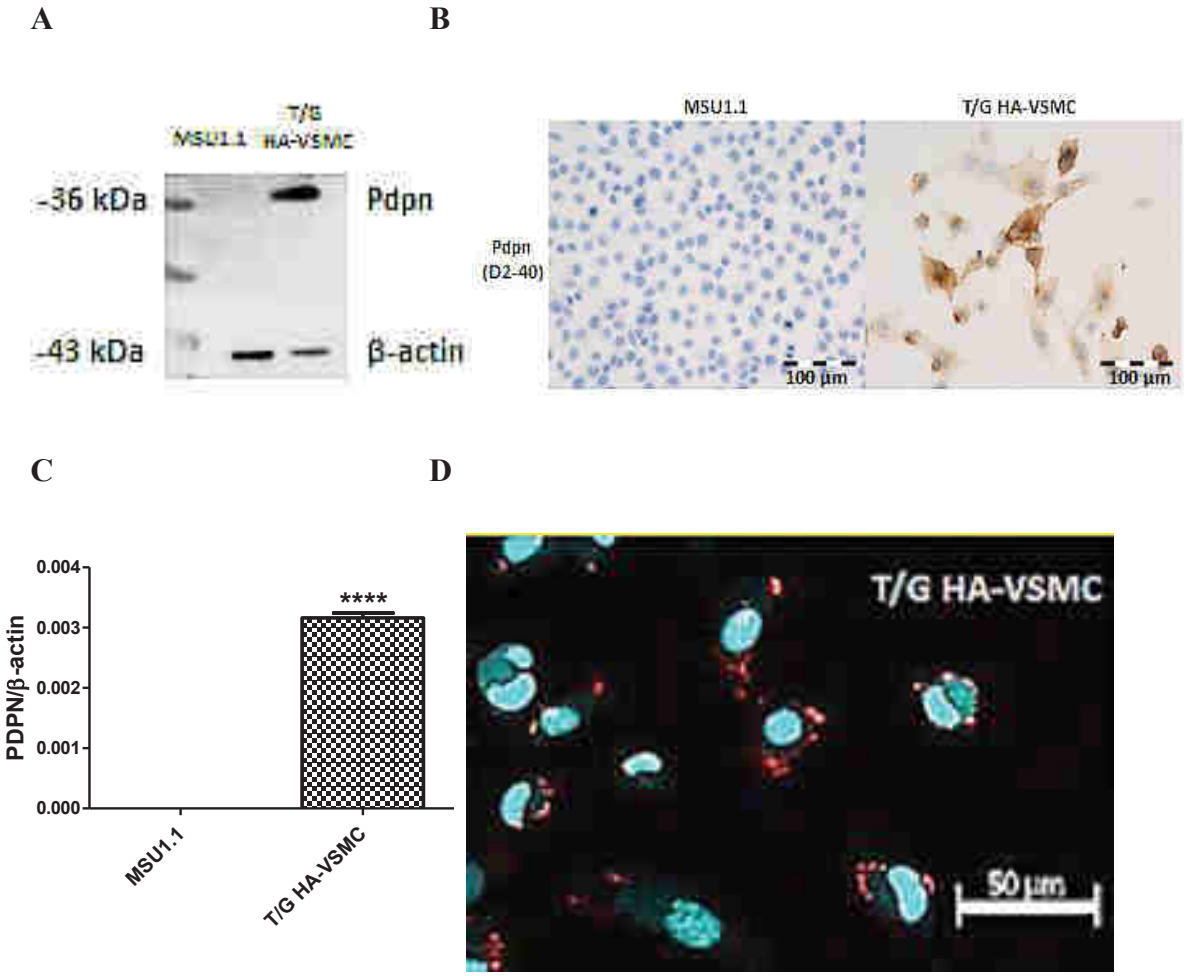

Figure 18. Characterization of human cell lines for expression of podoplanin. Expression of podoplanin in fibroblastic MSU1.1 cells and vascular smooth muscle T/G HA-VSMC cells at protein and mRNA levels. **(A)** Binding of rabbit polyclonal anti-podoplanin antibody to MSU1.1 and T/G HA-VSMC lysates and Western blotting. **(B)** Binding of mouse monoclonal anti-podoplanin antibody to MSU1.1 and T/G HA-VSMC cells. **(C)** podoplanin mRNA level in MSU1.1 and T/G HA-VSMC cell lines. **(D)** Binding of mouse monoclonal anti-podoplanin antibody to T/G HA-VSMC. **(A)** Western blotting revealed with anti-podoplanin rabbit polyclonal antibodies detect podoplanin in cell lysates. **(B)** Immunocytochemistry with mouse monoclonal anti-podoplanin antibodies was used to detect podoplanin on fixed cells (performed by Aleksandra Jethon-Jabłońska, Medical University, Wrocław). **(C)** Real-time RQ-PCR was used to analyze podoplanin mRNA. Podoplanin levels were normalized against *ACTB* gene expression. Results are expressed as mean RQ values. **(D)** Binding of mouse monoclonal fluorescent anti-podoplanin antibody to T/G HA-VSMC was used to detect podoplanin on living cells. Binding was evidenced by TRITC-conjugated goat anti–mouse IgG. Pictures were taken on a Zeiss Axiovert 200M inverted fluorescence microscope equipped with Apotome.

Due to the fact that T/G HA-VSMC are smooth muscle cells from vascular origin they cannot be representative for fibroblasts. Thus it was decided to build a fibroblastic cell model overexpressing podoplanin using MSU1.1 cells, in which the protein is naturally absent.

8.2. Generation of human fibroblastic cells overexpressing podoplanin

In order to study the role of podoplanin in CAFs and avoid the influence of other factors/proteins produced by those cells *in vitro*, a fibroblastic cell line was established from MSU1.1 which was shown above, not to express naturally podoplanin. The study was performed by designing a "gain-of-function" phenotype.

8.2.1. Construction of expression vector pRRL-CPPT-CMV-PDPN-IRES-PURO-PRE-SIN containing podoplanin cDNA

To obtain podoplanin cDNA a cDNA library was created from total RNA isolated from human embryonic kidney HEK-293T cells. The podoplanin cDNA was amplified by PCR reaction (**Fig. 19**) into the plasmid:pRRL-CPPT-CMV-IRES-PURO-PRE-SIN. Primers PovMLuI_Rand PovEcoI_F were used to introduce restriction sites in the resulting product. The PCR product was further purified by preparative electrophoresis in 1% agarose gel. DNA was eluted using a set Gel-Out extraction kit.

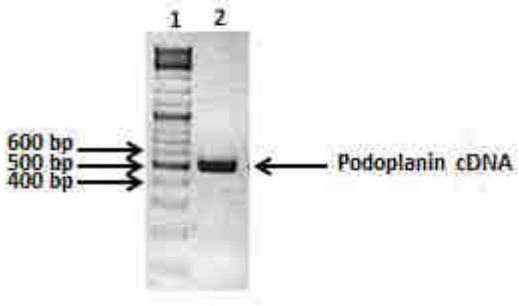

Figure 19. Agarose gel electrophoresis of podoplanin cDNA obtained from HEK-293T cell cDNA library by PCR using primers PovMLuI_R and PovEcoI_F. Lane 1 - standard DNA "GeneRuler^{TM} 100 bp Plus Ladder" (Fermentas); lane 2 – podoplanin cDNA.

Insert and pRRL-CPPT-CMV-IRES-PURO-PRE-SIN vector were overnight digested by restriction enzymes: MLuI and EcoRI. After digestion, the DNA fragments were purified and ligated by T4 ligase. The entire volume of the ligation mixture was used to transform *E. coli* DH5α. Bacteria were grown overnight on Petri dishes with LB medium solidified with agar containing ampicillin. Individual colonies were cultured in 3 mL of SB medium and plasmid DNA was purified by phenol extraction method. Purified DNA was subjected to restriction analysis with MLuI and EcoRI (**Fig. 20**).

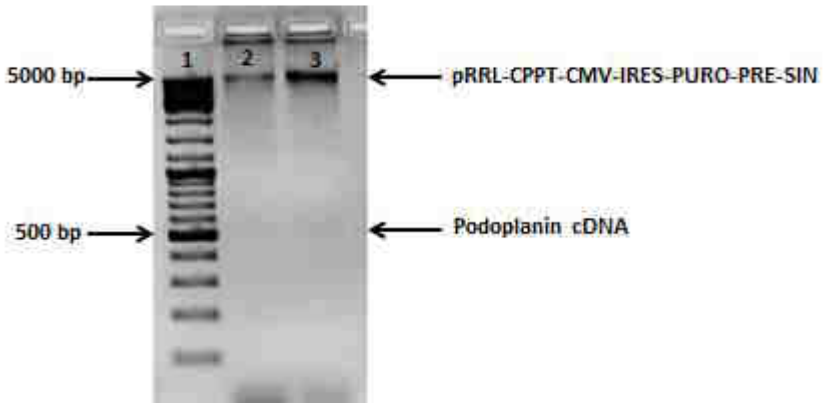

Figure 20. Restriction analysis of vector pRRL-CPPT-CMV-PDPN-IRES-PURO-PRE-SIN after action of restriction enzymes MLuI and EcoRI.Lane 1- DNA standard "GeneRuler^{TM} 100 bp Plus Ladder" (Fermentas); lanes 2 and 3 – plasmid DNA obtained after ligation of podoplanin cDNA with resulting construct.

Resulting construct, schematically represented on figure4, was named pRRL-CPPT-CMV-PDPN-IRES-PURO-PRE-SIN (**Fig. 21**), and further analyzed by DNA sequencing with primersPovMLuI_Rand PovEcoI_F (annex 1).

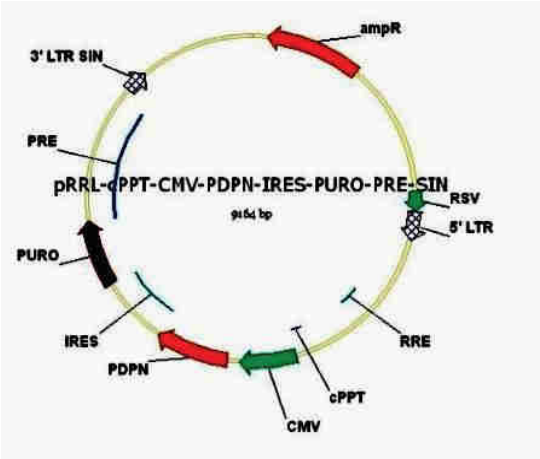

Figure 21. Schematic representation of the vector pRL-CPPT-CMV-IRES-PDPN PURO-PRE-SIN containing podoplanin cDNA.

8.3. Characteristics of human fibroblastic MSU1.1 cells overexpressing podoplanin

To design a fibroblastic cell line overexpressing podoplanin, MSU1.1 fibroblasts were transduced by the expression vector: pRRL-CPPT-CMV-PDPN-IRES-PURO-PRE-SIN containing the cDNA for podoplanin as a part of III Generation lentiviral system. Transduced cells were grown in the presence of puromycin and after selection, puromycin-resistant cells were analyzed for podoplanin expression at the mRNA level by real time PCR (**Fig. 22A**), at the protein level by Western blotting using rabbit polyclonal anti-podoplanin antibodies (**Fig. 22B**) and by flow cytometry using mouse monoclonal anti-podoplanin antibody (**Fig. 22C**). The cells with high expression of podoplanin were called MSU1.1 PDPN. The control MSU1.1 cells, named MSU1.1 NC, were obtained by transduction of MSU1.1 fibroblasts with vector: pRRL - CPPT - CMV - IRES - PURO - PRE – SIN alone.

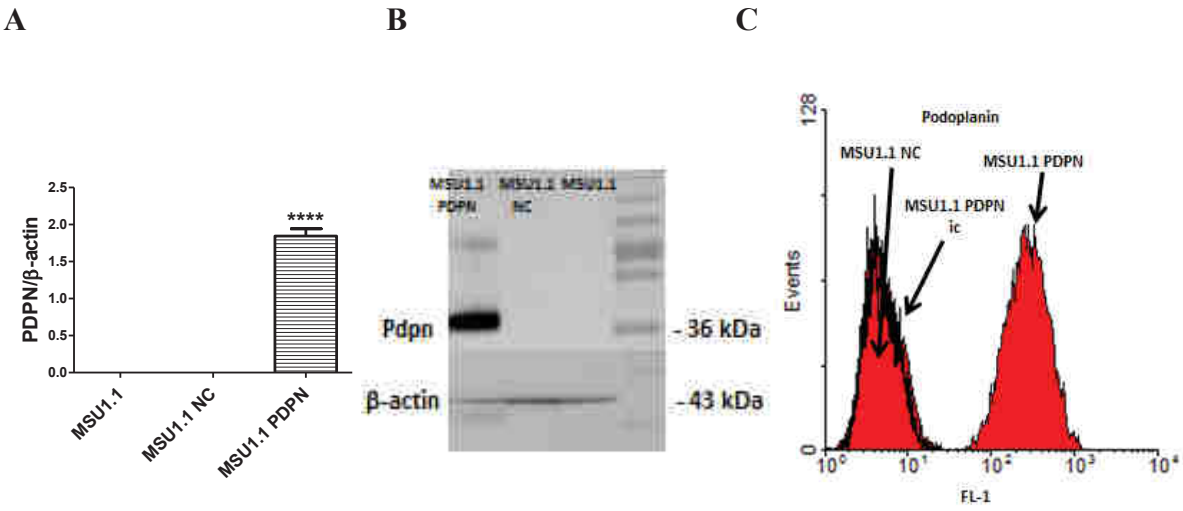

Figure 22. Characterization of human fibroblastic cell lines for overexpression of podoplanin. Expression of podoplanin in fibroblastic MSU1.1 PDPN cells transduced with pRRL-CMV-PDPN-IRES-PURO vector containing podoplanin cDNA and control MSU1.1 NC cells transduced with vector alone at **(A)** mRNA and **(B, C)** protein levels. **(A)** Real-time RQ-PCR was used to analyze podoplanin mRNA. Podoplanin levels were normalized against *ACTB* gene expression and cell line MSU1.1 NC was assigned as a calibrator sample. Results are expressed as mean values. **(B)** Western blotting with anti-human podoplanin rabbit polyclonal antibodies was used to detect podoplanin in cell lysates. **(C)** Binding of mouse fluorescent monoclonal anti-human podoplanin antibody to MSU1.1 PDPN and MSU1.1 NC cells using flow cytometry. Red positive histogram represents MSU1.1 PDPN labelling, red negative histograms represent MSU1.1 NC labelling and MSU1.1 PDPN labeling by isotypic control (MSU1.1 PDPN ic).

In addition, the presence of podoplanin and its localization in transduced cells were detected by cytochemistry and fluorescence microscopy (**Fig. 23**). Using mouse monoclonal anti–human podoplanin antibody and Alexa Fuor-conjugated goat anti–mouse IgG, PDPN was found mainly as membrane-

associated as shown on figure 23 A as compared to the control figure 23 B and to the MSU1.1 devoid of podoplanin shown on figure 23 C, D.

A **B**

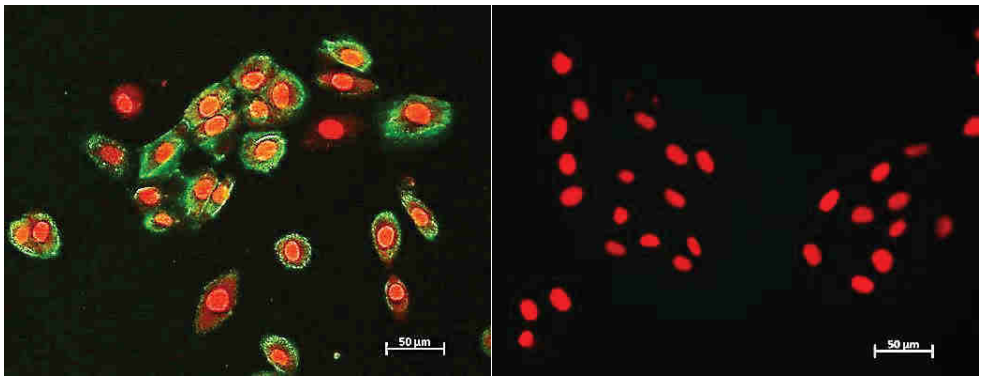

C **D**

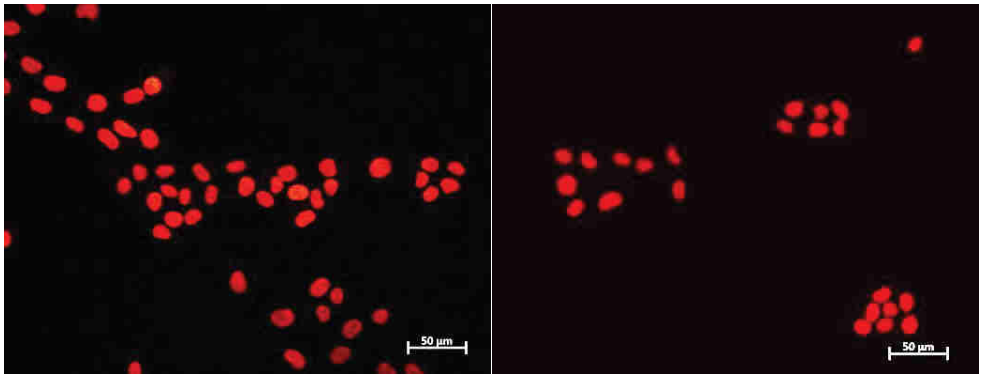

Figure 23. Localization of podoplanin in fibroblasts MSU 1.1 PDPN by fluorescence microscopy.**(A)** MSU1.1 PDPN cells incubated with murine monoclonal anti-human podoplanin antibody18H5; **(B)** MSU1.1 PDPN cells incubated with isotypic control; **(C)** MSU1.1 NC cells incubated with murine monoclonal anti-podoplanin antibody18H5; **(D)** MSU1.1 NC cells incubated with isotypic control. Binding was evidenced by AlexaFuor-conjugated goat anti–mouse IgG. Pictures were taken on a Zeiss Axiovert 200M inverted fluorescence microscope equipped with Apotome.

Data presented above demonstrate that the transfected MSU1.1 PDPN cells and the control MSU1.1 NC cells constitute a cell model which enables the study of the biological properties conferred by the presence of podoplanin in fibroblasts. Tumor microenvironment is highly hypoxic as it was mentioned above thus the further studies concerned the status of PDPN in hypoxia.

8.4. Effect of hypoxia on the expression of podoplanin in human fibroblastic cells

It has been shown previously that hypoxia increases the expression of podoplanin in several cell types[156]. Therefore, to further clarify the functional role of hypoxia in the regulation of podoplanin expression, T/G HA-VSMC cells were used as positive control **(Fig. 24E)** and, similarly to MSU1.1 cells, were grown in low pO2 level (1% O_2) conditions for 24 hours (hypoxia) or in usual cell culture conditions pO2 level (18.75% O_2) for 24 hours (noted normoxia). Podoplanin expression was detected at mRNA level. In hypoxic conditions an increase in podoplanin mRNA expression was observed only in T/G HA-VSMC fibroblasts (**Fig. 24A**). Indeed, this phenomenon was not observed in the case of MSU1.1 cells (**Fig. 24B**) nor in cells transduced by the control vector MSU1.1 NC **(Fig. 24C)** (it was assumed that hypoxia increases the expression levels of podoplanin, but it does not induce its expression). The effect of hypoxia on podoplanin expression was clearly shown in MSU1.1 PDPN cells, as its expression is under the control of the CMV promoter sensitive to hypoxia[157]. Indeed, using real-time PCR, MSU1.1 PDPN fibroblasts grown in hypoxia, were shown to express higher level of podoplanin mRNA than in normoxia (**Fig. 24D**). Nevertheless the sensitivity of PDPN induction to hypoxia is confirmed by its increase in T/G HA-VSMC cells **(Fig. 24A)**.

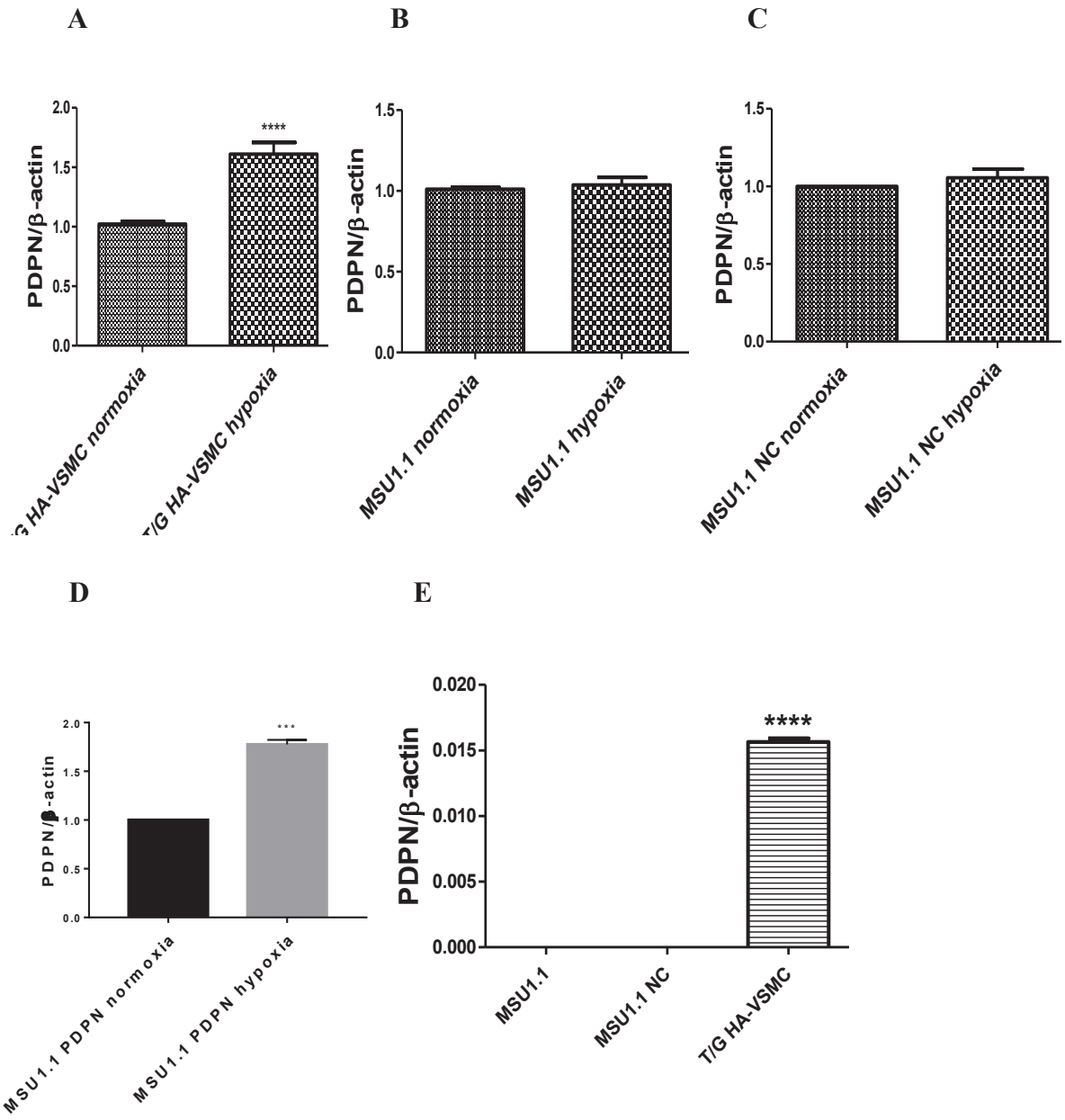

Figure 24. Effect of hypoxia on podoplanin expression.

Podoplanin expression was analyzed in **(A)** T/G HA-VSMC cells, **(B)** MSU1.1 cells, **(C)** MSU1.1 NC **(D)** MSU1.1 PDPN and cells in hypoxia (1% O_2) and normoxia (18.75% O_2). **(E)** MSU1.1, MSU1.1 NC and T/G HA-VSMC cells in normoxia. Real-time RQ-PCR was used to assess for podoplanin mRNA. Podoplanin levels were normalized against *ACTB* gene expression and cell line MSU1.1 NC was assigned as a calibrator sample. Results are expressed as mean values $\pm$ SEM. N = 3, *** $p < 0.001$,**** $p < 0.0001$.

8.5. Effects of podoplanin and hypoxia on migratory properties of fibroblasts, cancer cells and endothelial cells

It has been suggested that CAFs overexpressing podoplanin stimulate tumor cell migration and invasiveness. However, the role of this glycoprotein in both processes remains unclear[158][112]. Therefore, to further clarify the functional role of podoplanin present on the surface of fibroblasts towards the migratory properties of cancer cells and other cells present in tumor microenvironment, their ability to migrate towards one another was assayed for the putative influence of podoplanin on cell migration in both hypoxic and normoxic conditions.

8.5.1. Effect of podoplanin expression by fibroblasts on migratory properties of breast cancer cells in normoxia and hypoxia

Migration of fluorescently labelled breast cancer MCF7 or MDA-MB-231 cells cultured in distinct areas with MSU1.1.PDPN fibroblasts or control MSU1.1 NC fibroblasts was performed. No difference in the migration of tumor cells was evidenced whether or not podoplanin was expressed by fibroblasts **(Fig. 25A, B).**

These results indicate that podoplanin present on the surface of fibroblasts does not influence the migratory ability of breast cancer cells. The data show that the fibroblasts migrate towards cancer cells in all cases in normoxia (A). MCF-7 are migrating faster towards fibroblasts in hypoxia, independently of PDPN (B). Fibroblasts migrate towards MDA-MB-231 in normoxia (A) while MDA-MB-231 and fibroblasts are more or less equally migrating towards one another in hypoxia (B)

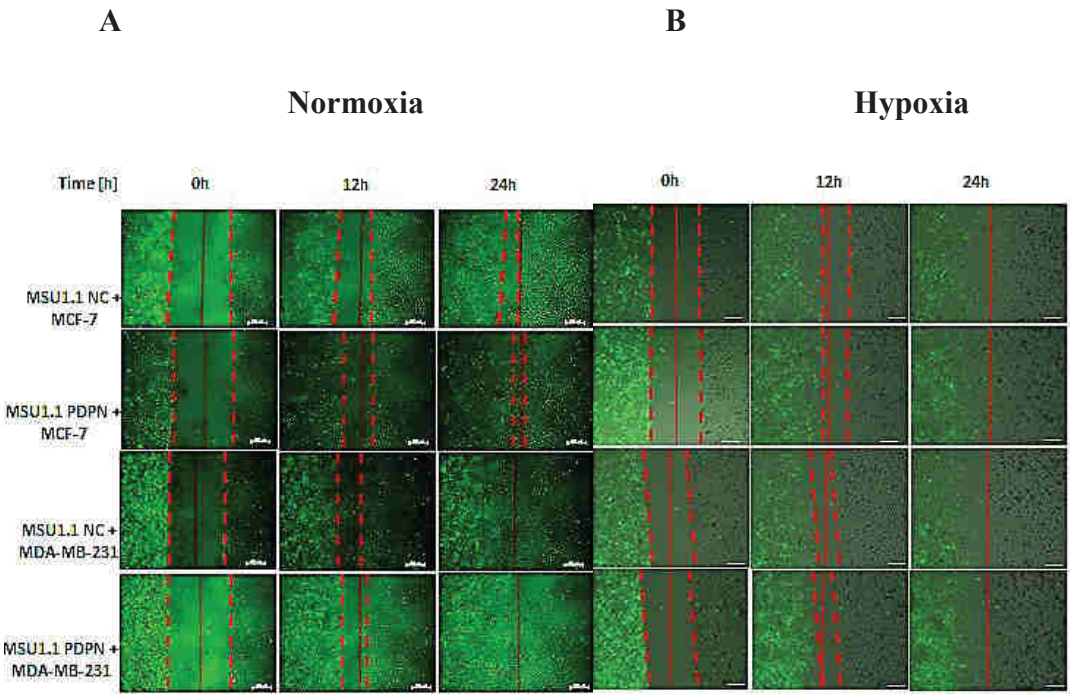

Figure 25. Migratory capability of human breast cancer cell lines co-cultured with human fibroblasts expressing different amounts of podoplanin. Pictures presenting cell free area between cell monolayers in normoxia (18.75% O_2)**(A)** and in hypoxia (1% O_2) **(B)**. MSU1.1 NC and MSU1.1 PDPN were labelled by DiD (green) and MCF-7 and MDA-MB-231 cancer cells were not labelled.

8.5.2. Effect of hypoxia on migratory properties of breast cancer cells in the presence of fibroblasts

Migration, all along the 36 hours experiment, of breast cancer MCF-7 cell line is strongly influenced by hypoxia **(Fig. 26A, B), (Fig. 27A).** This occurs both in the presence or absence of fibroblasts and the presence of PDPN did not show any influence **(Fig. 26A, B)**. This effect was not shown in the case of aggressive breast cancer cell line MDA-MB-231 where hypoxia does not influence migration of MDA-MB-231 cells alone **(Fig. 26C, D).** Hypoxia, on the contrary, reduced the speed of wound closing when MDA-MB-231 cells were in the presence of fibroblasts. This effect was more evident when fibroblasts MSU 1.1 expressed PDPN. These data are summarized on figure 26 (A, B, C and D)

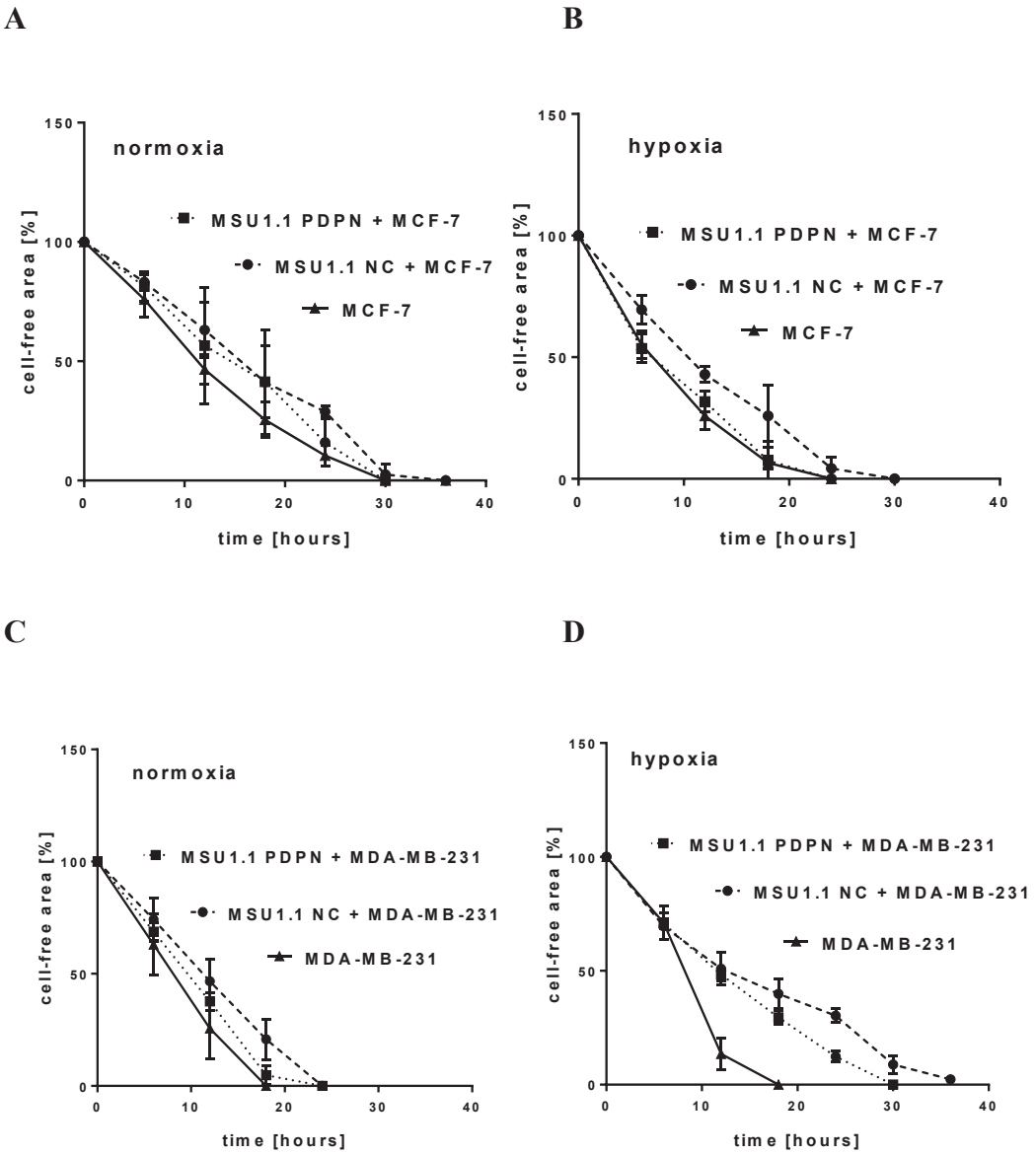

Figure 26. Migratory capability of human breast cancer cell lines co-cultured with human fibroblasts expressing different amounts of podoplanin. Quantification of cancer cells motility in co-culture of **(A)** MCF-7 with MSU1.1 PDPN fibroblasts or MSU1.1 NC in normoxia (18.75% O_2), **(B)** MCF-7 with MSU1.1 PDPN fibroblasts or MSU1.1 NC in hypoxia (1% O_2), **(C)** MDA-MB-231 with MSU1.1 PDPN fibroblasts or MSU1.1 NC in normoxia, **(D)** MDA-MB-231 with MSU1.1 PDPN fibroblasts or MSU1.1 NC in hypoxia. Graphs are expressing the percent of cell free area between cell monolayers. N = 3; * $p<0.05$.

The effect of hypoxia on MCF-7 non aggressive breast cancer cell line is presented on figure 27A, and the lack of such an effect on MDA-MB-231 aggressive breast cancer cell line is presented on figure 27B.

A **B**

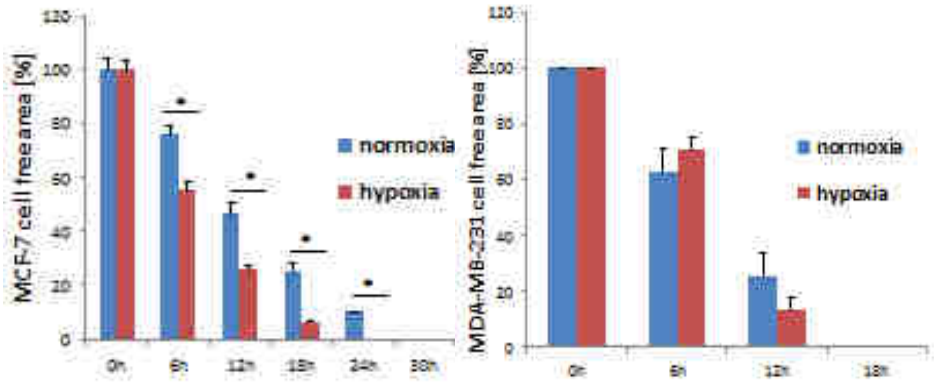

Figure 27.Comparison of the migratory capability of human breast cancer cell lines under normoxic or hypoxic conditions. (A) Graphs presenting cell free area between cell monolayers. Quantification of MCF-7 cancer cells motility in normoxia (18.75% O_2) vs hypoxia (1% O_2). **(B)** Quantification of MDA-MB-231 cancer cells motility in normoxia vs hypoxia. Graphs are expressing the percent of cell free area between cell monolayers. N = 3; * $p<0.05$.

Podoplanin expressed by CAFs has no effect on cancer cell migration. While hypoxia accelerates the motility of non-aggressive breast cancer cell line MCF-7, it has no effect on aggressive MDA-MB-231 cell line. Therefore further analysis of podoplanin expression on CAFs and hypoxia on fibroblasts migration were carried out.

8.5.3. Effect of podoplanin and hypoxia on migratory properties of fibroblasts

In contrast to the above results, when migratory properties of fluorescently labelled MSU1.1 PDPN and MSU1.1 NC fibroblasts were analysed separately, by the same migratory assay, a statistically significant increase in the speed of wound closure was found in the case of fibroblasts overexpressing PDPN **(Fig. 28A, B)**. These data show that podoplanin expressed by fibroblasts increases their mobility as it was shown for other cells (Martin-Villar et al., 2005; Wicki et al., 2006; Kunita et al., 2011). Interestingly hypoxia reduced this effect and reduced the speed of healing for both MSU1.1 PDPN and MSU1.1 NC **(Fig. 28C, D)**.

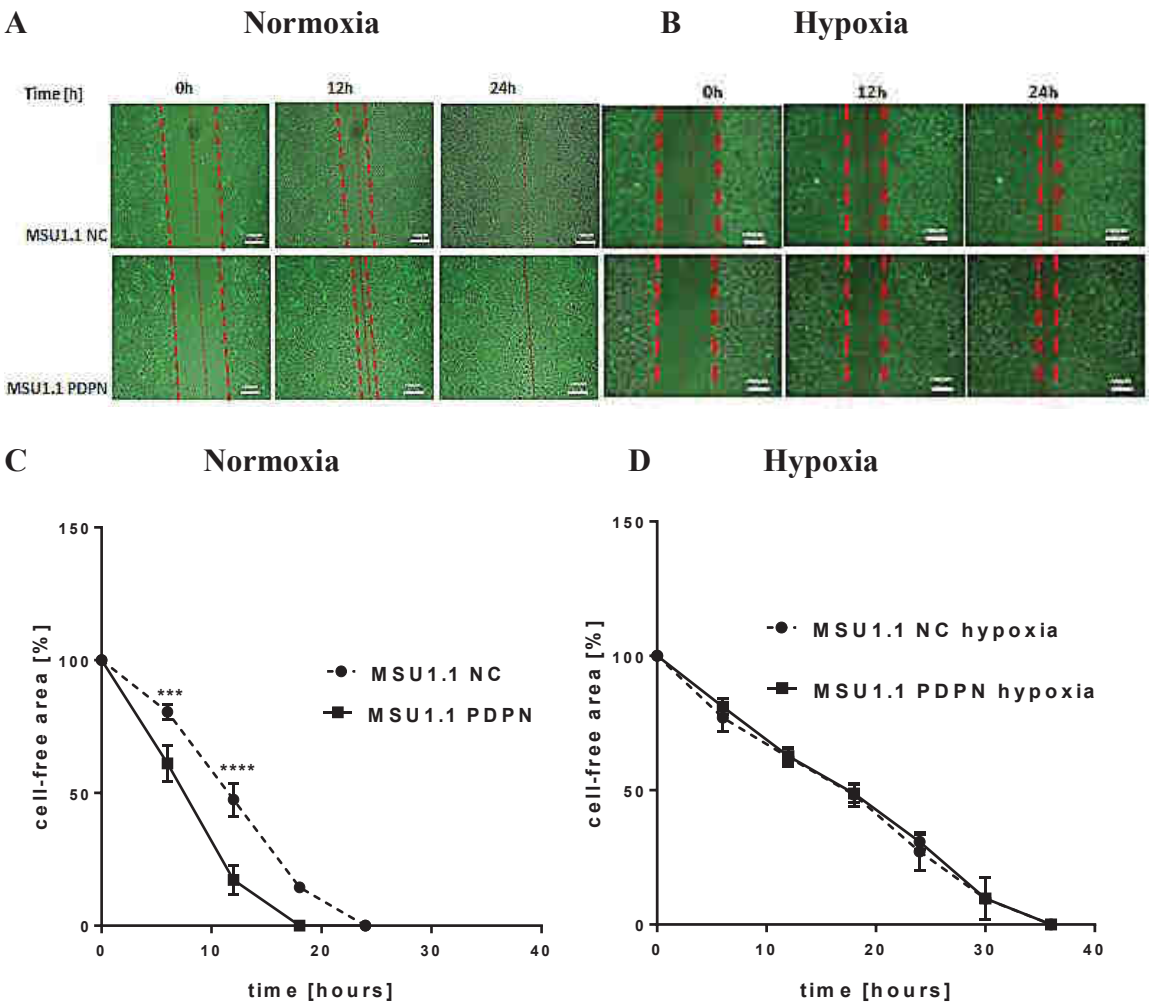

Figure 28. Migratory capability of human fibroblastic cell lines expressing different amounts of podoplanin. (A) Pictures presenting cell free area between cell monolayers in normoxia (18.75% O_2). **(B)** Pictures presenting cell free area between cell monolayers in hypoxia (1% O_2). **(C)** Quantification of MSU1.1 NC and MSU1.1 PDPN cells motility in normoxia. **(D)** Quantification of MSU1.1 NC and MSU1.1 PDPN cells motility in hypoxia. Graphs are expressing the percent of cell free area between cell monolayers. N = 3; * p<0.05, *** p < 0.001,**** p< 0.0001.

Hypoxia not only decreases the podoplanin mediated motility of fibroblasts but also lowers the speed of fibroblasts non-expressing podoplanin. Therefore the effect of podoplanin positive CAFs and hypoxia was further analysed for endothelial cells which the angiogenesis forming cells.

8.5.4. Effect of podoplanin expressed by fibroblasts and hypoxia on the migratory properties of human microvascular endothelial cells HSkMEC

Migratory properties of fluorescently labelled MSU1.1 PDPN and MSU1.1 NC fibroblasts cultured in distinct areas with endothelial HSkMEC cells were analysed by the same migratory assay. A statistically significant increase in the speed of wound closure was observed when fibroblasts overexpressed PDPN **(Fig. 29A, C)**, and this effect was blocked by hypoxia **(Fig. 29B, D).** This data confirmed that podoplanin expressed by fibroblasts increases their mobility **(Fig. 29C)**.

Moreover hypoxia is clearly influencing the mobility of fibroblasts showing a reducing effect on the healing.

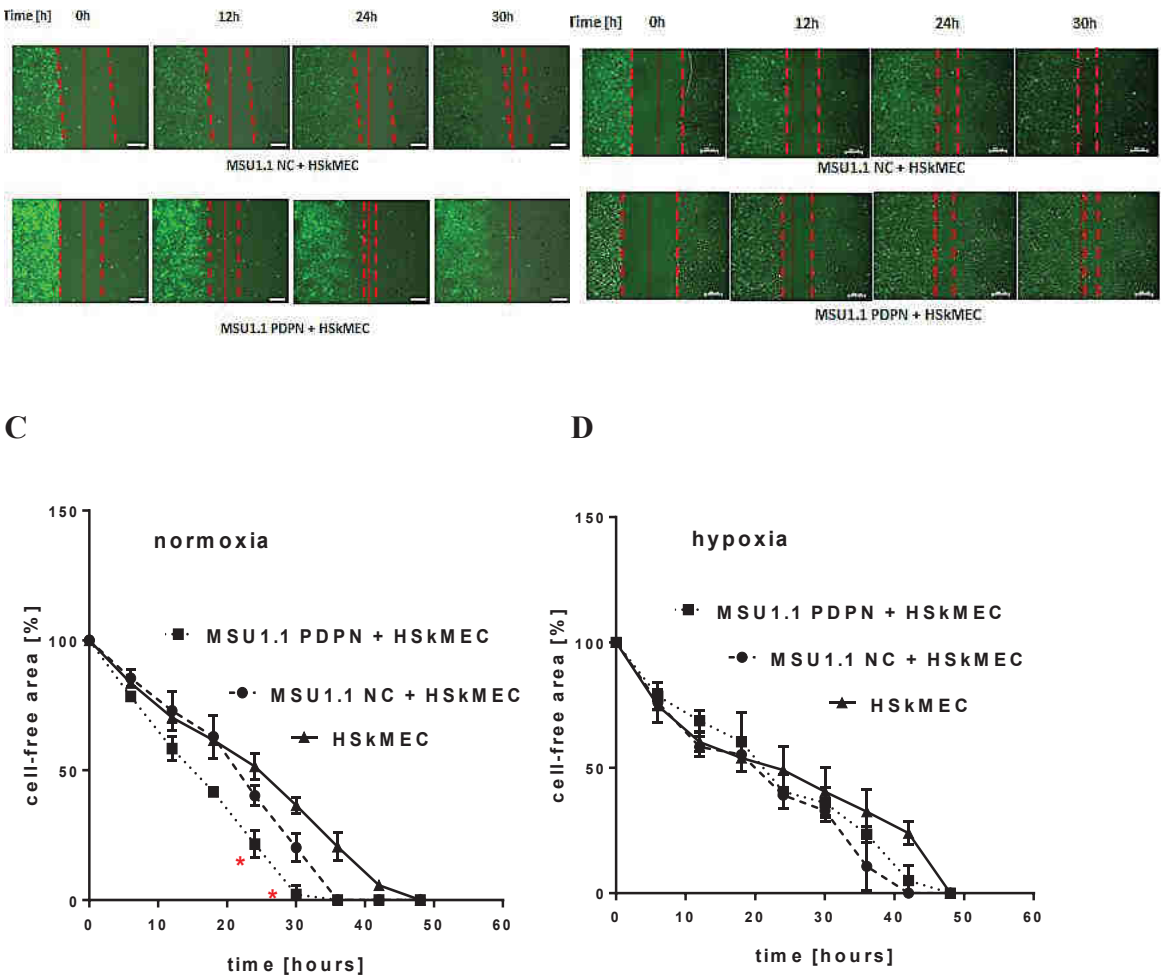

Figure 29. Migratory capability of human microvascular endothelial cells HSkMEC co-cultured with human fibroblasts expressing different amounts of podoplanin. (A) Pictures presenting cell free area between cell monolayers in normoxia(18.75% O2). **(B)** Pictures presenting cell free area between cell monolayers in hypoxia (1% O2). Quantification of human microvascular endothelial cells HSkMEC motility in co-culture with **(C)** MSU1.1 PDPN fibroblasts or MSU1.1 NC in normoxia **(D)** MSU1.1 PDPN fibroblasts or MSU1.1 NC in hypoxia. Graphs express the percent of cell free area between cell monolayers. N = 3; * $p<0.05$. MSU1.1 NC and MSU1.1 PDPN were labelled with DiD (green) and HSkMEC endothelial cells were not labelled.

It can be concluded that PDPN influences the migration of fibroblasts either alone or in the presence of other cells. This effect is observed in normoxia and annihilated in hypoxia.

8.6. Effect of podoplanin expressed by fibroblasts and hypoxia on the adhesion of breast cancer cells to fibroblasts

It has been shown that podoplanin plays a role in tumor cells communication with ECM or ECM-mediated cell adhesion [159]. Therefore, to analyze the role of podoplanin in adhesion of breast cancer cells to components of tumor stroma, namely fibroblasts, the experiments were performed with the help of the "bioflux" setting in normoxia and hypoxia. The "bioflux" device enables to create a static monolayer phase composed of fibroblasts expressing, or non-expressing, podoplanin and a dynamic phase composed of cancer cells. One phase is moving over another one in flow conditions. This is performed in the purpose of mimicking the tumor microenvironment dynamic processes. For this aim, human breast cancer MDA-MB-231 cells and MSU1.1 PDPN cells with overexpression of podoplanin were used. Figure 30 shows that, in normoxia, significantly less MDA-MB-231 cells were able to adhere to MSU1.1 PDPN cells monolayer as compared to MSU1.1.NC cells as control devoid of PDPN **(Fig. 30A and B).** A comparable effect was observed in hypoxia **(Fig. 30C and D)**. Moreover, upon quantification of the adhesion it appears that hypoxia has no significant effect on the binding of MDA-MB-231 cells to MSU1.1 NC fibroblasts **(Fig. 31A),** but hypoxia reduced considerably the binding of MDA-MB-231 cells to MSU1.1 PDPN cells **(Fig. 31B)**.Taken together, these results suggest that podoplanin can act as an anti-adhesive molecule and hypoxia increases this effect.

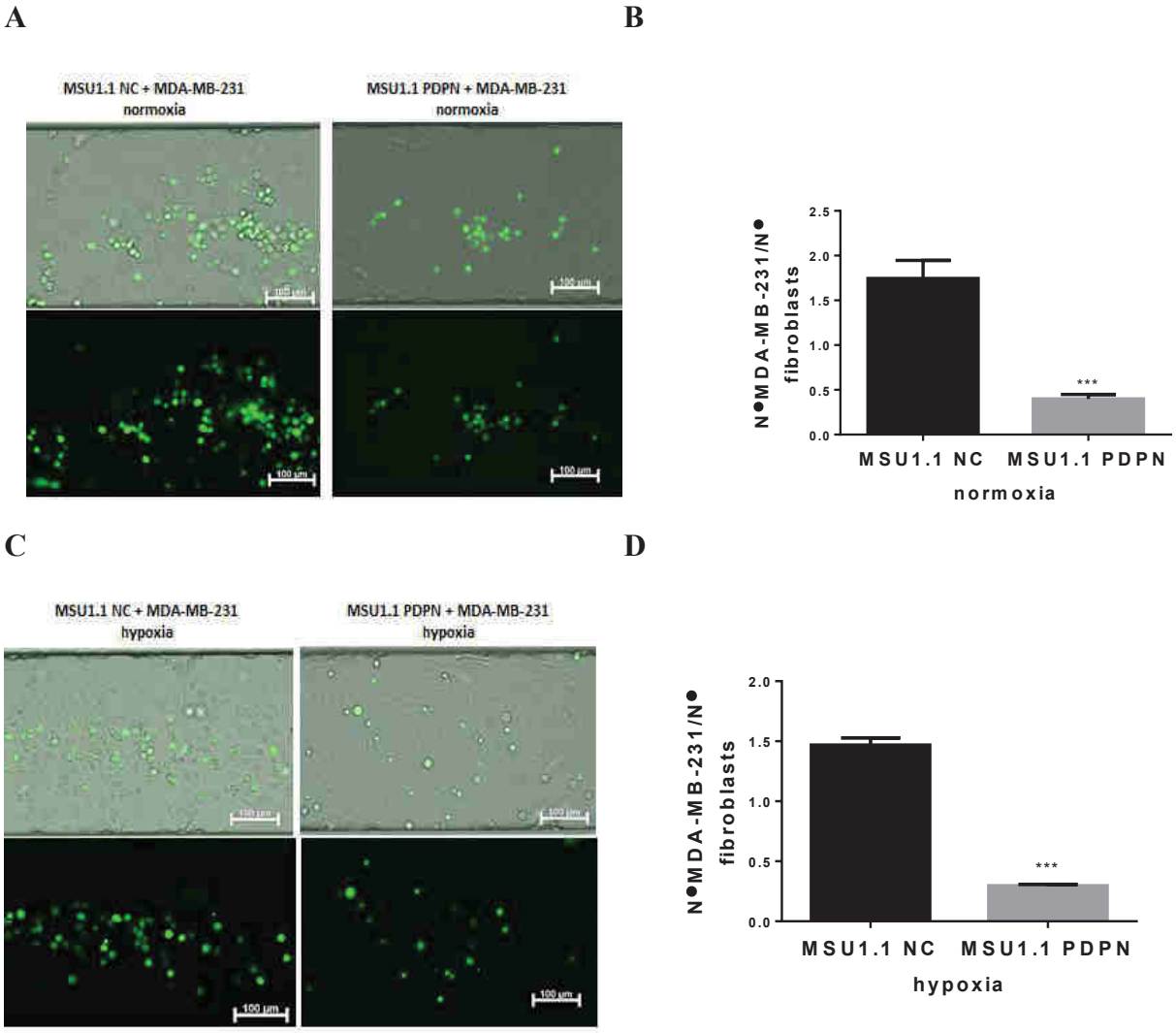

Figure 30. Visualization and quantification of the adhesion of MDA-MB-231 cancer cells to MSU1.1 PDPN and MSU1.1 NC, effect of podoplanin and hypoxia. (A) Picture of DiO-labeled MDA-MB-231 cells adhering to MSU1.1 NC or MSU1.1 PDPN monolayers in normoxia(18.75% O2). **(B)** Diagram representing the adhesion of MDA-MB-231 cells to MSU1.1 NC or MSU1.1 PDPN monolayers in normoxia. **(C)** Picture of DiO-labeled MDA-MB-231 cells adhering to MSU1.1 NC or MSU1.1 PDPN monolayers in hypoxia (1% O2). **(D)** Diagram representing the adhesion of MDA-MB-231 cells to MSU1.1 NC or MSU1.1 PDPN monolayers in hypoxia. Each bar represents mean $\pm$ SEM, N = 3, *** $p < 0.001$. (scale bar 100µm).

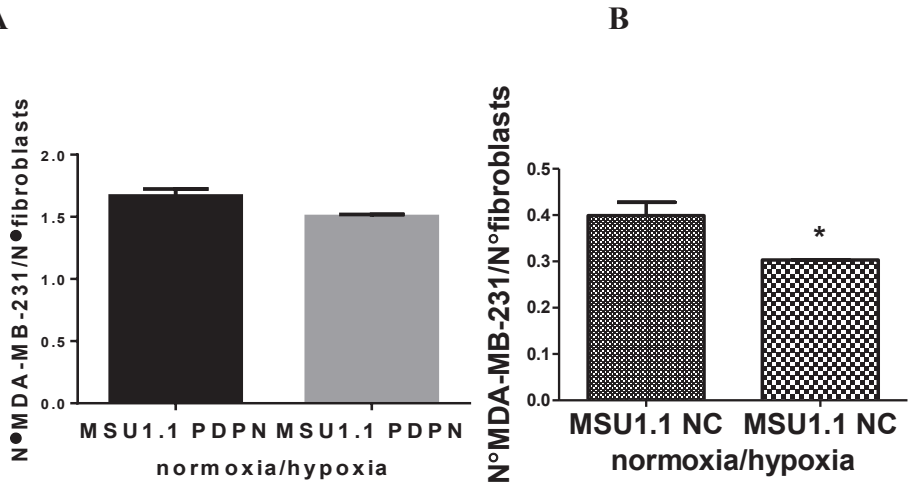

Figure 31. Comparison of the adhesion process of MDA-MB-231 cancer cells to MSU1.1 PDPN and MSU1.1 NC, in normoxia and hypoxia. (A) Diagram representing adhesion of MDA-MB-231 cells to MSU1.1 PDPN monolayer in normoxia(18.75% O2) vs hypoxia (1% O2). **(B)** Diagram representing adhesion of MDA-MB-231 cells to MSU1.1 NC monolayer in normoxia vs hypoxia. Each bar represents mean ± SEM, N = 3, * $p < 0.05$. (scale bar 100µm).

Breast cancer metastasis occurs firstly in lymphatic vessels where CCL21 and podoplanin are naturally expressed. CCL21, which is a potent chemoattractant for CCR7+ cells as MDA-MB-231, binds to podoplanin[160]. Therefore it was of high interest to determine the role of podoplanin in the CCL21/CCR7 axis in breast cancer cells adhesion.

8.6.1. CCL21/CCR7 implication in tumor cells adhesion to fibroblasts expressing podoplanin.

The mechanism of the tumor to fibroblasts cross talk was further analysed through the chemokines and their receptors. More precisely, the involvement of the CCL21/CCR7 axis in the breast tumor microenvironment was analysed for tumor cells interaction with stromal cells, namely the cancer associated fibroblasts. For this purpose the human breast cancer model MDA-MB-231 was chosen for its aggressive properties and expression of CCR7, as shown in annex 2, as compared to the non-aggressive MCF-7 breast cancer cell line. The role of PDPN in the adhesion process of MDA-MB-231 cells to CAFs was studied. MDA-MB-231 adhered more efficiently in normoxia **(Fig. 32A)** than in hypoxia **(Fig. 32B)** on MSU1.1 PDPN. Upon preincubation of the MSU1.1 PDPN in the presence of CCL21 no significant change was observed in the adhesion when performed in normoxia **(Fig. 32A)** while it significantly increased the adhesion of MDA-MB-231 cells in hypoxia **(Fig. 32B)**. In both oxygen tension conditions, adhesion was

inhibited by preincubation of the cancer cells MDA-MB-231 in the presence of neutralizing anti-CCR7 antibodies **(Fig. 32A, B)** which bound efficiently to MDA-MB-231 (annex 2). This effect is obtained in hypoxic conditions **(Fig. 32B).** Indeed, when MSU1.1 PDPN cells were pre-incubated with exogenous CCL21, the adhesion level of MDA-MB-231 cells was clearly (2 fold) increased **(Fig. 32B)**. This increased adhesion, which was displayed after CCL21 treatment in hypoxia only, was totally inhibited upon blocking the CCR7 receptors on the MDA-MB-231 cancer cells (annex 2) by pre-incubation with anti-CCR7 neutralizing antibodies **(Fig. 32B)**. This shows the involvement of the CCL21/CCR7 axis in the tumor cell to cancer associated fibroblast recognition. Figure 32C displays the same type of experiment on PDPN non-expressing MSU1.1 NC fibroblasts, in normoxia, pointing to the higher adhesion activity of MDA-MB-231 cells. In normoxia, the CCR7 inhibition effect indicates that CCL21/CCR7 axis is involved in the recognition similarly to PDPN expressing fibroblasts in normoxia **(Fig. 32A).** Indeed, CCL21 has no effect on MSU1.1 NC adhering capacity pointing to a PDPN/CCL21 interaction, evidenced in hypoxia, on CAFs. The data obtained upon adhesion of MDA-MB-231 on MSU1.1 NC non expressing PDPN in hypoxia **(Fig. 32D)** were similar to normoxia, confirming that in CAFs, PDPN can interact with CCL21 to bind CCR7+ cells. It has to be remarked that NKL3 cells are, similarly to MDA-MB-231 cancer cells, adhering less to PDPN expressing fibroblasts, confirming an anti-adhesive effect of PDPN in the tumor stroma (annex 3). While this effect is compensated upon addition of CCL21 in vitro, no increase of CCL21 level was observed upon hypoxia in fibroblasts (annex 4).

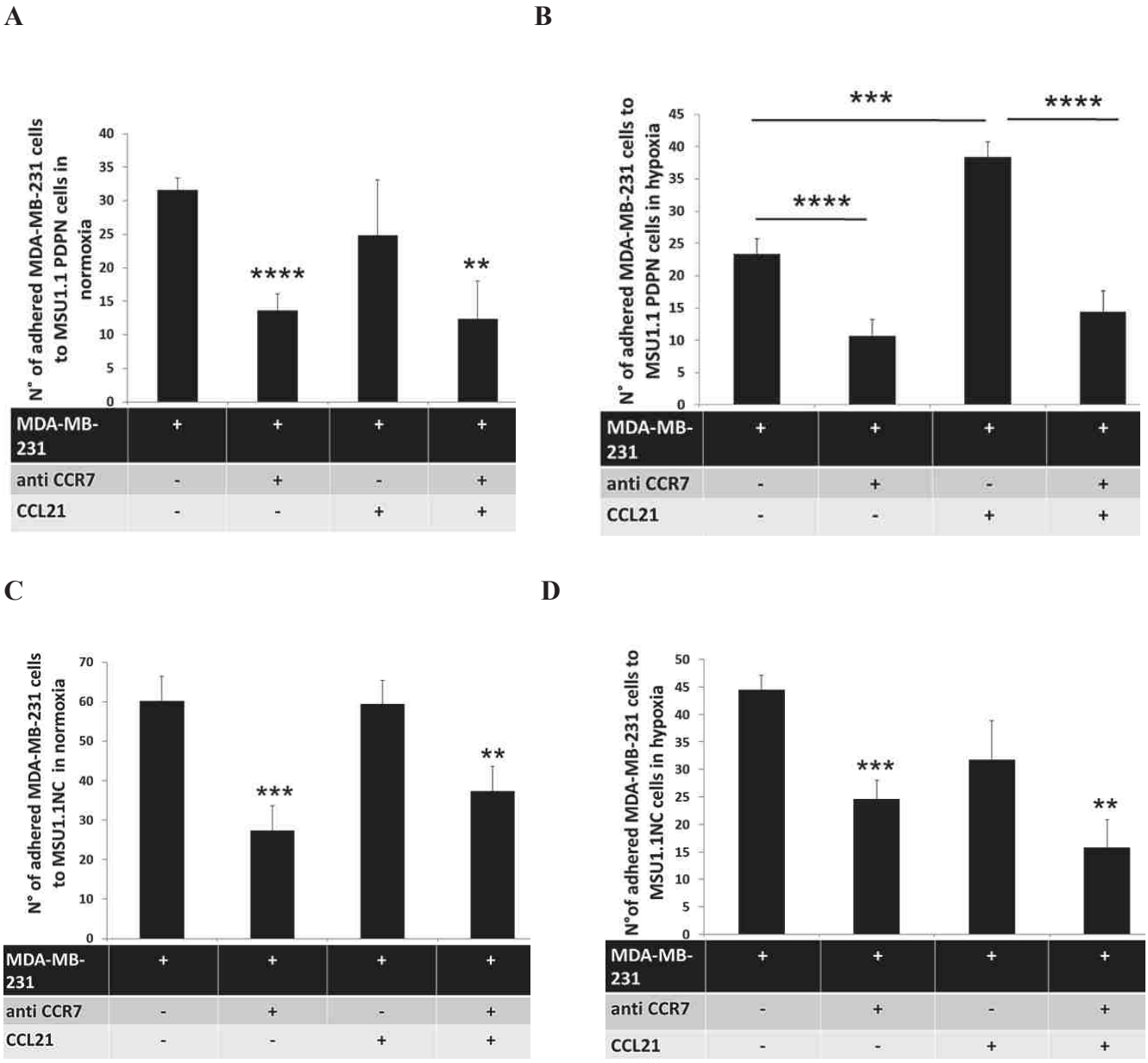

Figure 32. Impact of podoplanin/CCL21 interaction on MDA-MB-231 cells adhesion to MSU1.1 NC and MSU1.1 PDPN cells surface in normoxia(18.75% O2) and hypoxia (1% O2). Quantification of the MDA-MB-231 cells adhesion to MSU1.1 NC and MSU1.1 PDPN cells surface. MDA-MB-231 cells were counted on the surface of MSU1.1 NC or MSU1.1 PDPN cells (ten representative fields were counted) after flow adhesion in normoxia and in hypoxia. * $p<0.05$, N = 3 (mean from ten representative fields). **(A)** Effect of CCL21/CCR7 interaction on MDA-MB-231 cell adhesion onto MSU 1.1 PDPN cells in normoxia. **(B)** Effect of CCL21/CCR7 interaction on MDA-MB-231 cell adhesion on MSU1.1 PDPN cells in hypoxia. **(C)** Effect of CCL21/CCR7 interaction on MDA-MB-231 cell adhesion on MSU1.1 NC cells in normoxia. **(D)** Effect of CCL21/CCR7 interaction on MDA-MB-231 cell adhesion on MSU1.1 NC cells in hypoxia.

8.7. The effect of podoplanin expressed by fibroblasts on angiogenesis of endothelial cells under hypoxic and normoxic conditions

It has been shown that podoplanin expressed on CAFs affects the biological properties of tumor cells [20, 27]. However little is known about its effects on other cells present in tumor stroma, especially endothelial cells which are responsible for angiogenesis in the tumor. Thus, we co-cultured human MSU1.1 PDPN fibroblasts and human skin microvascular endothelial cells (HSkMEC) to analyze the effect of podoplanin on tube formation by assessing for the co-localization of fibroblasts with ECs. Using angiogenesis Matrigel™ assay, it was found that MSU.1.1.PDPN fibroblasts co-localized much more efficiently with HSkMEC cells than control MSU1.1.NC cells in normoxia **(Fig. 33A)**, as well as hypoxia **(Fig. 34A)**. Indeed the number of co-localized MSU.1.1.PDPN/ECs was 1.84 times higher than MSU1.1 NC/ECs in normoxia **(Fig. 33B)** and 1.5 times higher in hypoxia **(Fig. 34B)**.

Upon co-culture with control MSU1.1.NC fibroblasts, HSkMEC endothelial cells formed a structured network of pseudo-tubes **(Fig. 33A).** When co-cultured with podoplanin-expressing MSU1.1 PDPN fibroblasts, the pseudo-tubes formed by endothelial cells presented a disordered capillary-like network (**Fig. 33A and 34A)**. This observation was reflected by differences in numbers of nodes, meshes and segments as a measure of *in vitro* angiogenesis **(Fig. 33, 34)**.The number of nodes was decreased by 38% **(Fig. 33C)**, meshes by 64.2% **(Fig. 33D)** and segments by 33% **(Fig. 33E).**

The same angiogenic Matrigel™ assay was performed in hypoxic conditions and reported in figure 34. Similarly to normoxia, when HSkMEC cells were co-cultured with podoplanin-rich MSU1.1 PDPN fibroblasts, the EC capillary-like network presented lower numbers of nodes, meshes and segments than with MSU NC fibroblasts (**Fig. 34C, D and E**). The number of nodes was decreased by 33% **(Fig. 34C)**, meshes by 54% **(Fig. 34D)** and segments by 38% **(Fig. 34E)**. Taking these data together, podoplanin on the surface of fibroblasts affects tube formation by HSkMEC endothelial cells. This effect is evidenced by co-localisation experiments where direct interaction between podoplanin and putative ECs receptors can take place.

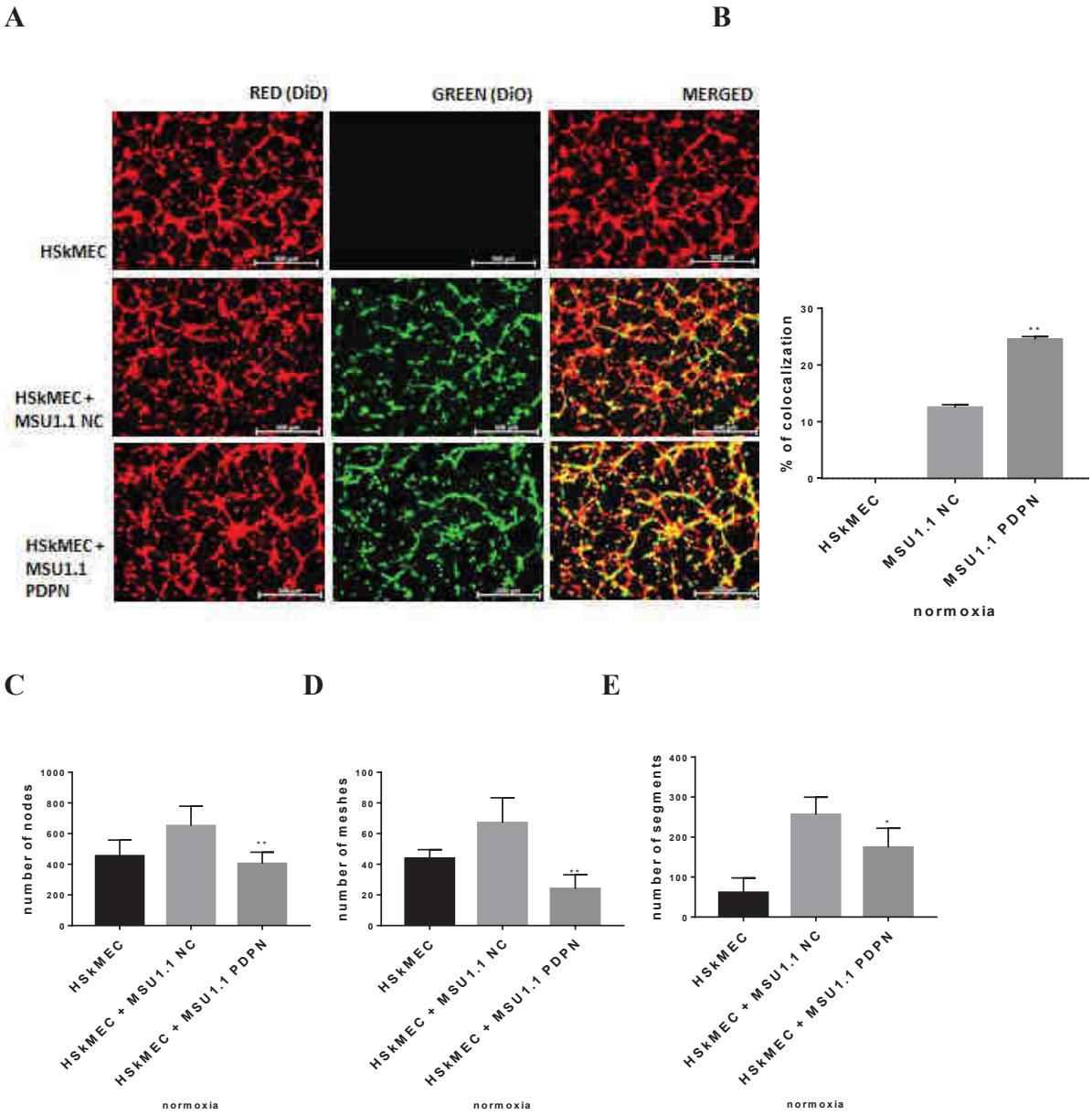

Figure 33. Angiogenic properties of endothelial HSkMEC cells co-cultured with fibroblastic MSU1.1. cells expressing different amounts of podoplanin in normoxic (18.75 % O2) conditions. (A) Angiogenic Matrigel™ assay in normoxia with fluorescently labeled (DiO) MSU.PDPN fibroblasts (green) overexpressing podoplanin and podoplanin-negative control MSU1.1 NC fibroblasts co-cultured with fluorescently labeled (DiD) endothelial HSkMEC cells (red). Images were analyzed after 12 h of assay duration**. (B)** Co-localization of MSU.PDPN and MSU1.1 NC fibroblastic cells with endothelial HSkMEC cells. **(C)** Number of nodes **(D)** number of meshes and **(E)** number of segments formed by HSkMEC endothelial cells co-cultured with MSU.PDPN fibroblasts overexpressing podoplanin and podoplanin-negative control MSU1.1 NC fibroblasts. The number of nodes, meshes, segments and percentage of fibroblasts co-localized with endothelial cells were estimated using ImageJ software. N = 3, * p <0.05, ** p <0.01.

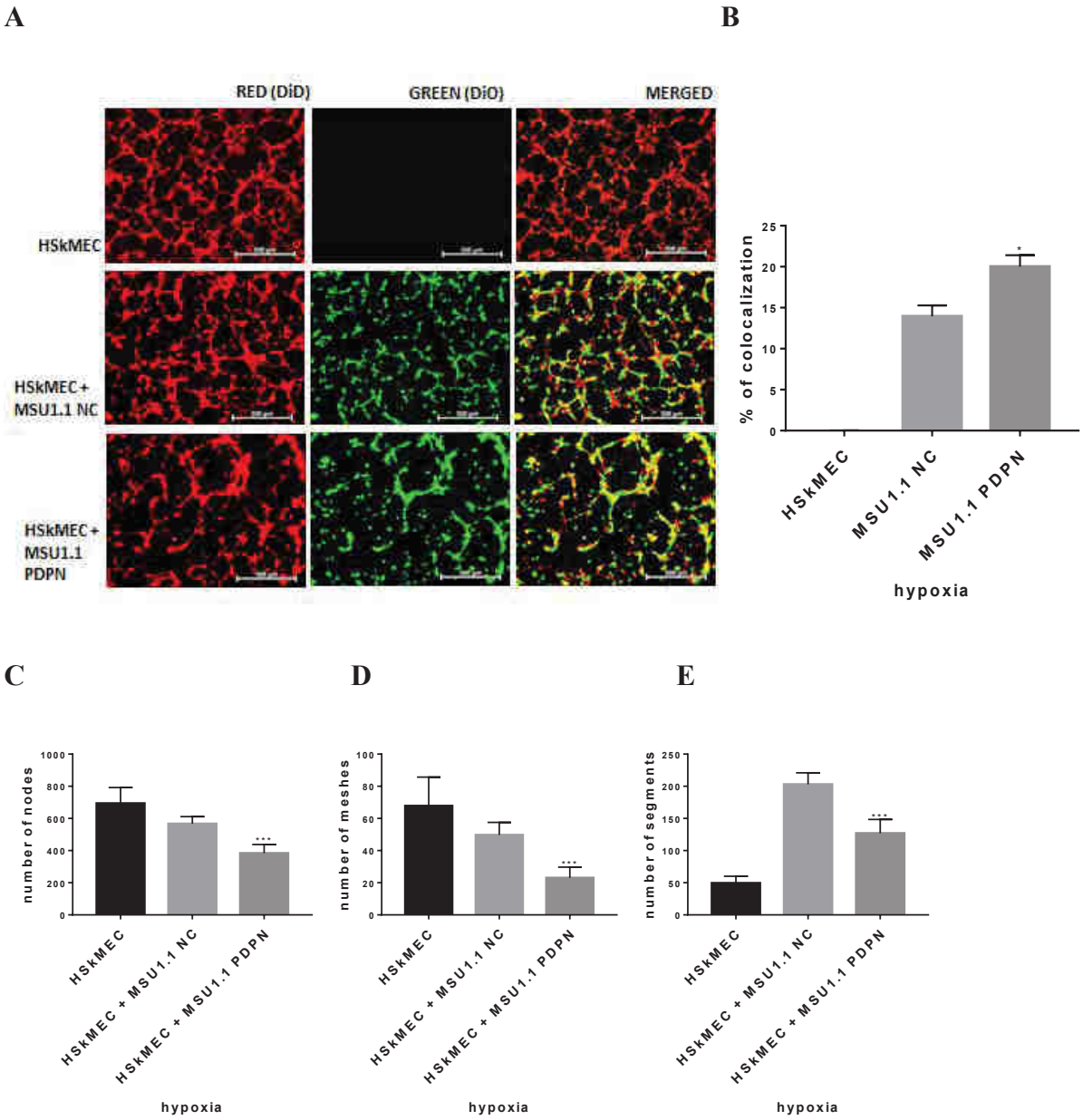

Figure 34. Angiogenic properties of endothelial HSkMEC cells co-cultured with fibroblastic MSU1.1 cells expressing different amounts of podoplanin in hypoxic conditions (1%O_2). (A) Angiogenic Matrigel™ assay in hypoxia with fluorescently labeled (DiO) MSU.PDPN fibroblasts (green) overexpressing podoplanin and podoplanin-negative control MSU1.1 NC fibroblasts co-cultured with fluorescently labeled (DiD) endothelial HSkMEC cells (red). Images were analyzed after 12 h of assay duration**. (B)** Co-localization of MSU.PDPN and MSU1.1 NC fibroblastic cells with endothelial HSkMEC cells. **(C)** Number of nodes **(D)** number of meshes and **(E)** number of segments formed by HSkMEC endothelial cells co-cultured with MSU.PDPN fibroblasts overexpressing podoplanin and podoplanin-negative control MSU1.1 NC fibroblasts. The number of nodes, meshes, segments and percentage of fibroblasts co-localized with endothelial cells were estimated using ImageJ software. N = 3, * p <0.05, ** p <0.01.. N = 3, * p <0.05***; p<0.001.

8.8. Effect of podoplanin and hypoxia on the expression of proangiogenic factors in human fibroblastic cells

Data obtained in angiogenesis experiments and co-localization assessment raised two possible suggestions: (1) Podoplanin can directly affect angiogenesis by interaction with a receptor on endothelial cells,

(2) In addition to direct cell-to-cell contact, podoplanin may affect the expression of angiogenic factors by fibroblasts.

To address this last question, expression of the following angiogenic factors: Vascular endothelial growth factor (VEGF-A), vascular endothelial cadherin (VE-cadh), angiopoietin 1 (ANGPT1), angiopoietin 2 (ANGPT2) and fibroblast growth factor 1 (FGF-1) in fibroblastic cell lines were analysed by real-time PCR. As hypoxia drives angiogenesis in tumor microenvironment [63] and induces production of proangiogenic factors by fibroblasts [161], their expression were studied in normoxic and hypoxic conditions.

In normoxia, figure 18 A shows that control MSU1.1 NC cells express 20% more VEGF-A mRNA than MSU1.1 PDPN cells **(Fig. 35A).** In hypoxia, this difference reaches 30% **(Fig. 35B)**. Hypoxia has a strong effect on VEGF-A mRNA expression as the relative amounts of VEGF-A mRNA in MSU1.1 NC cells and MSU1.1 PDPN cells were, respectively, 6 fold and 7 fold higher in hypoxia than in normoxia **(Fig. 35C and D)**.

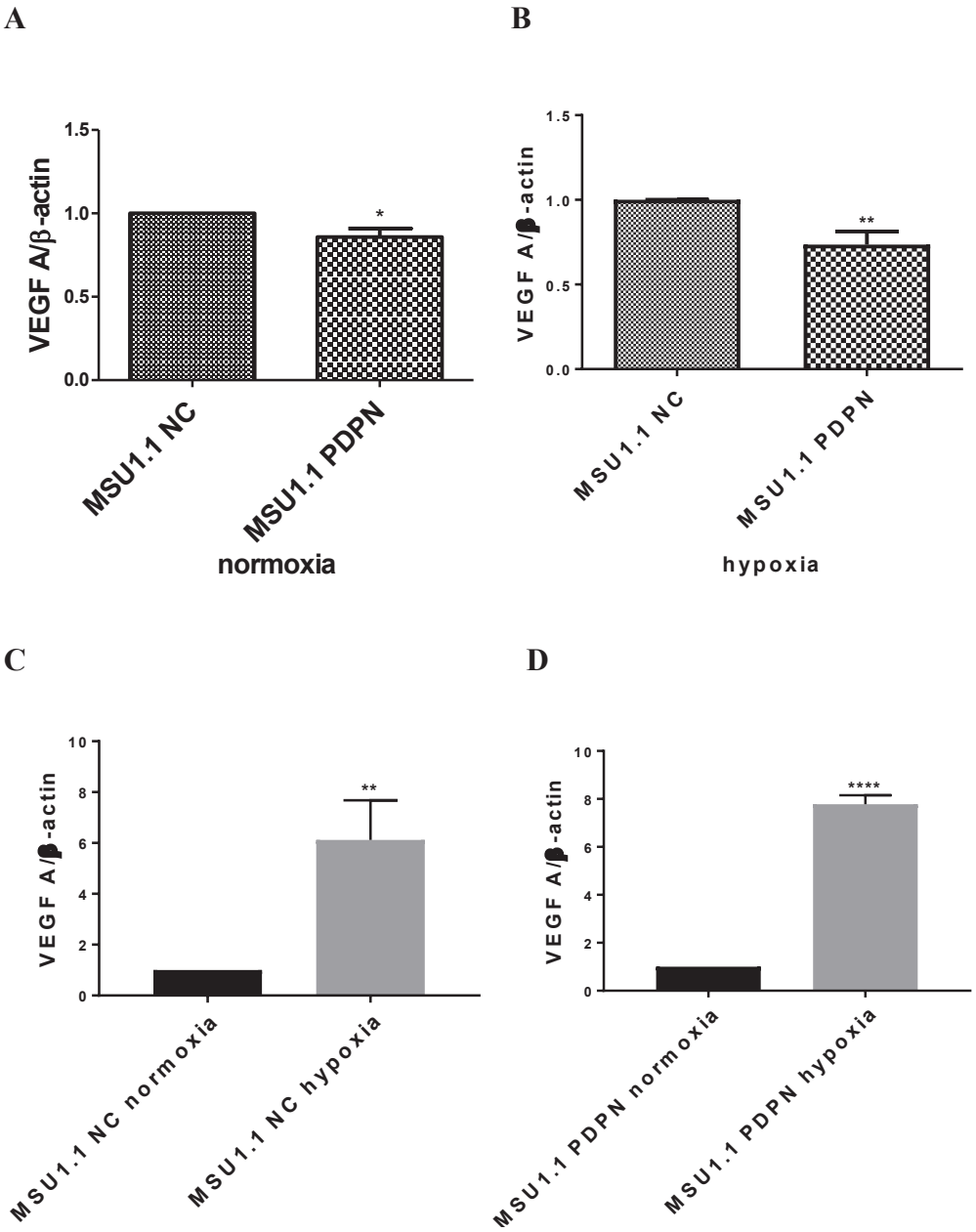

Figure 35. Expression of VEGF-A mRNA in fibroblastic cells lines: MSU1.1.PDPN overexpressing podoplanin and control MSU1.1 NC cells transduced with vector alone in (A) normoxia(18.75% O2) and **(B)** hypoxia (1% O2); expression of VEGF-A A on the level of mRNA in normoxia and hypoxia in **(C)** MSU1.1 NC and **(D)** MSU1.1 PDPN cells. Real-time RQ-PCR was used to analyze VEGF-A mRNA. VEGF-A levels were normalized against *ACTB* gene expression and cell line MSU1.1.NC or normoxia was assigned as a calibrator sample. Each bar represents mean ± SEM, RQ-PCR, ΔΔCt, N = (3-5), * $p < 0.05$, ** $p < 0.01$, **** $p< 0.0001$.

VE-cadh mRNA expression was reduced upon expression of podoplanin as it was70% lower in MSU1.1 PDPN cells than in MSU1.1 NC cells in normoxia **(Fig. 36A)** and 50% lower in hypoxia **(Fig. 36B)**. However hypoxia did not affect the expression of VE-cadh in MSU1.1 PDPN cells **(Fig. 36D),** while it inhibited its expression by 50% in MSU1.1 NC cells **(Fig. 36C)**.

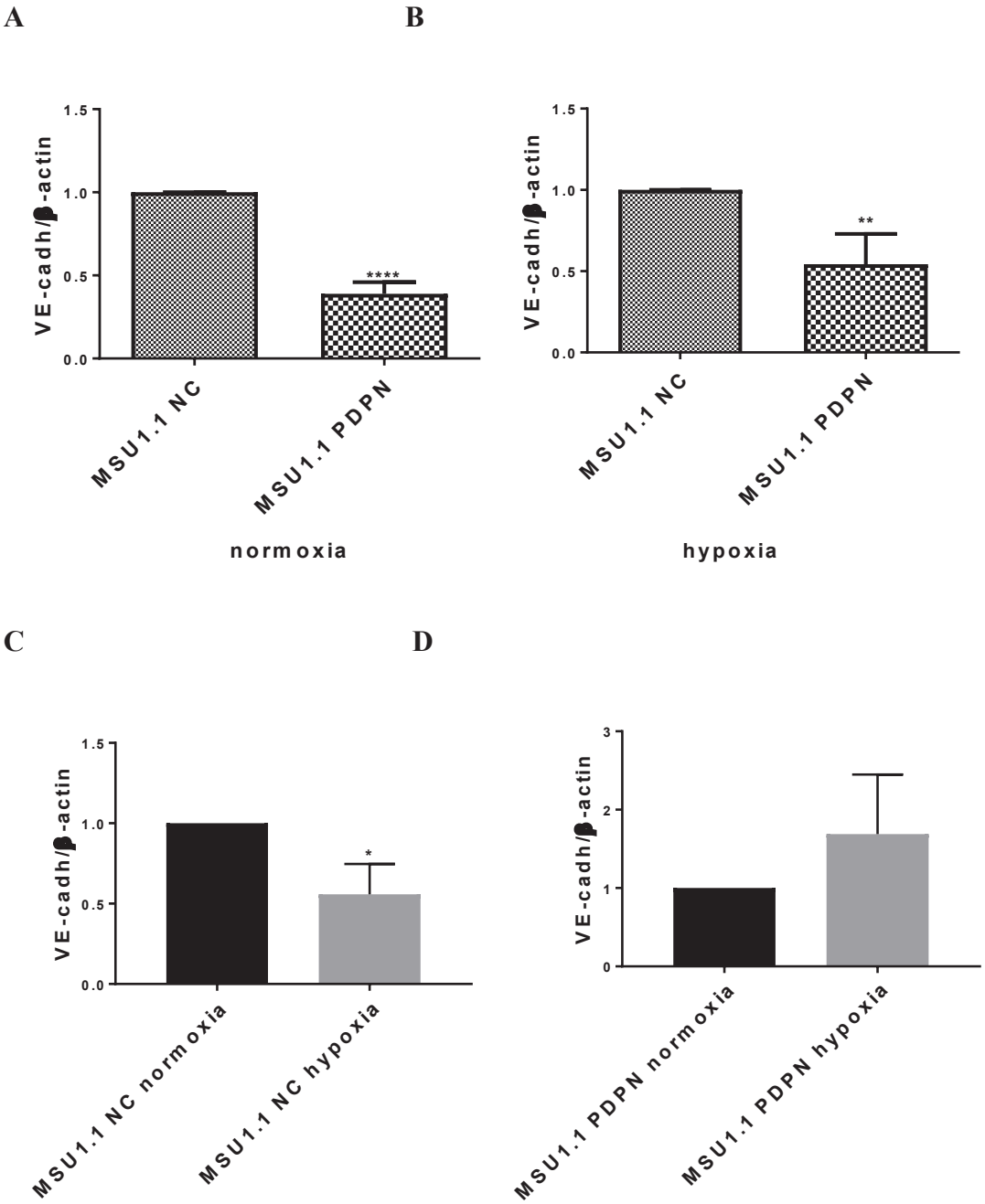

Figure 36. Expression of VE-cadh mRNA in fibroblastic cells lines: MSU1.1.PDPN overexpressing podoplanin and control MSU1.1 NC cells transduced with vector alone in (A) normoxia(18.75% O2) and **(B)** hypoxia (1% O2); expression of VE-cadh on the level of mRNA in normoxia and hypoxia in **(C)** MSU1.1 NC and **(D)** MSU1.1 PDPN cells. Real-time RQ-PCR was used to analyze VE-cadh mRNA. VE-cadh levels were normalized against *ACTB* gene expression and cell line MSU1.1.NC or normoxia was assigned as a calibrator sample. Each bar represents mean ± SEM, RQ-PCR, ΔΔCt, N = (3-5), * $p < 0.05$, ** $p < 0.01$**** $p < 0.0001$.

Similarly to above reported effects, MSU1.1 PDPN cells display 30% lower expression of ANGPT1 mRNA than MSU1.1 NC cells in normoxia **(Fig. 37A)** and 50% lower expression in hypoxia **(Fig. 37B)**. Hypoxia suppressed the expression of ANGPT1 in MSU1.1 PDPN cells and MSU1.1 NC cells by 60% in comparison to normoxia **(Fig. 37C and D)**.

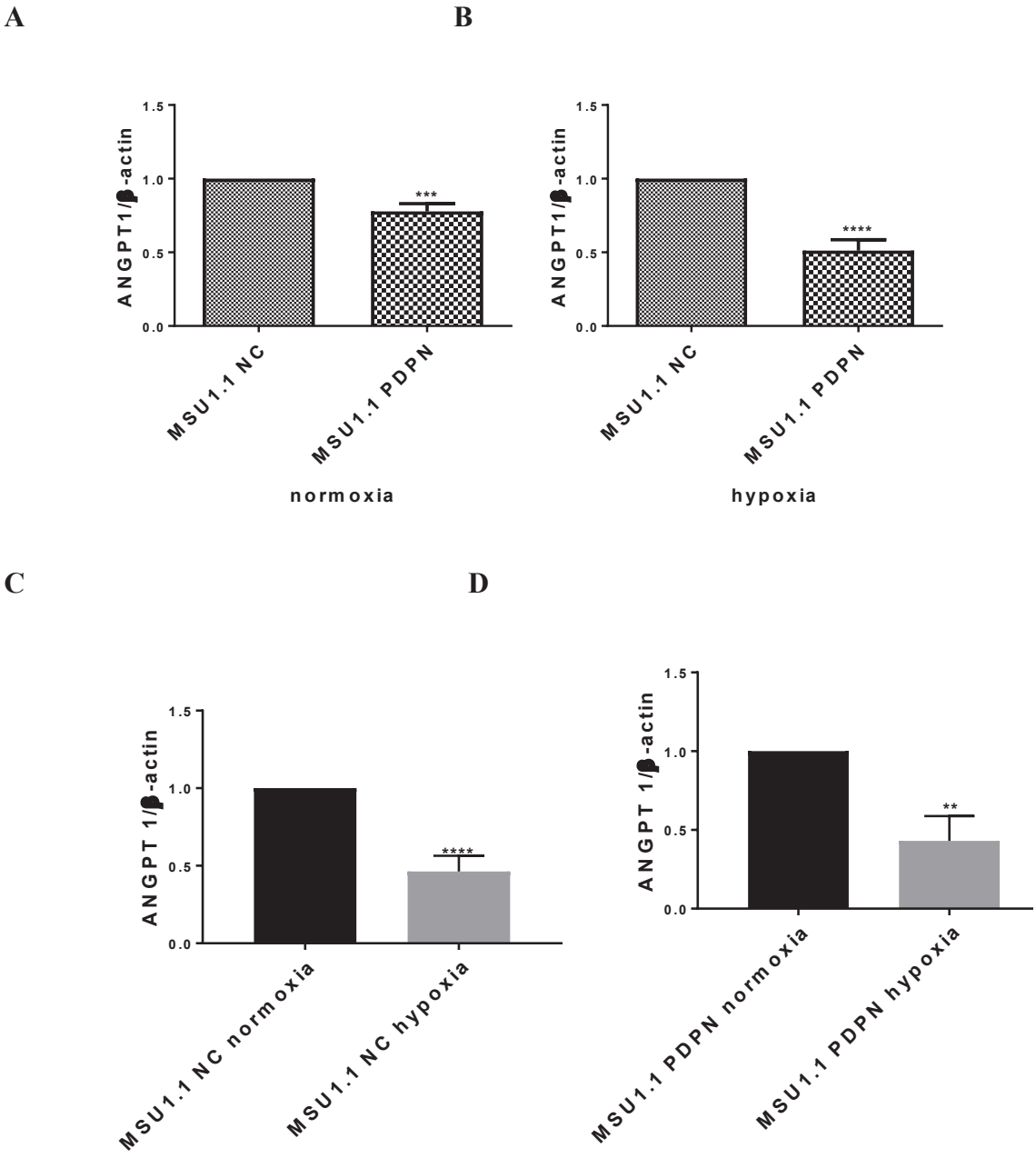

Figure 37. Expression of ANGPT1 on the level of mRNA in fibroblastic cells lines: MSU1.1.PDPN overexpressing podoplanin and control MSU1.1 NC cells transduced with vector alone in (A) normoxia(18.75% O2) and **(B)** hypoxia (1% O2); expression of ANGPT1 at the level of mRNA in normoxia and hypoxia in **(C)** MSU1.1 NC and **(D)** MSU1.1 PDPN cells. Real-time RQ-PCR was used to analyze ANGPT1 mRNA. ANGPT1 levels were normalized against *ACTB* gene expression and cell line MSU1.1.NC or normoxia was assigned as a calibrator sample. Each bar represents mean ± SEM, RQ-PCR, ΔΔCt, N = (3-5), ** $p < 0.01$, *** $p < 0.001$**** $p < 0.0001$.

On the contrary to the above observed effects for VEGF-A, VE-cadh and ANGPT1, ANGPT2 mRNA expression was increased in cells expressing podoplanin. In MSU1.1 PDPN cells its expression was 1.97 fold higher than in MSU1.1 NC in normoxic conditions **(Fig. 38A).** This increase reached 8.3 fold in

hypoxia **(Fig. 38B)**. In addition, this effect of podoplanin is underlined by the fact that in MSU1.1 NC cells, hypoxia strongly suppressed the expression of ANGPT2 (by 80%) **(Fig. 38C)**.

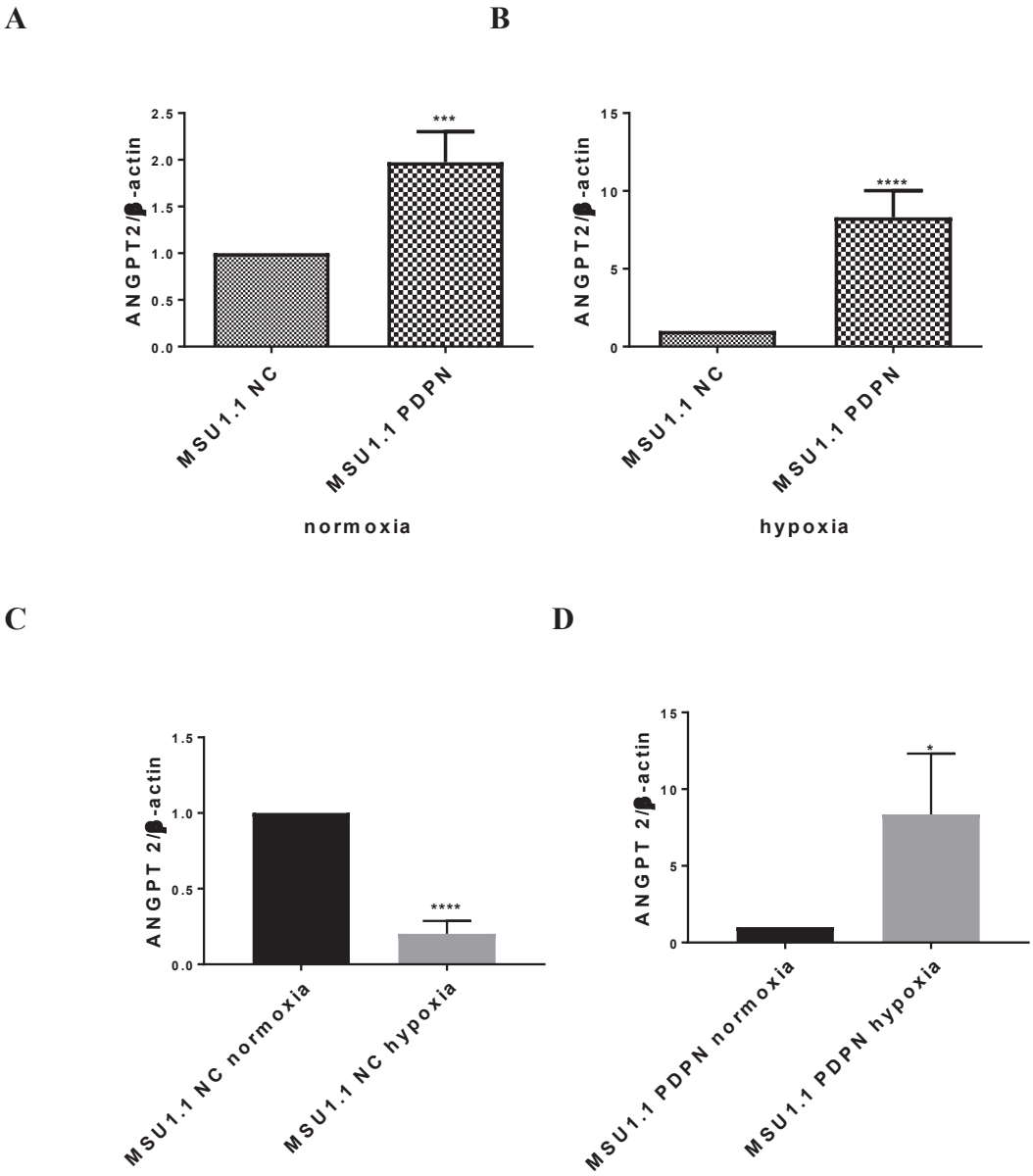

Figure 38. Expression of ANGPT2 at the level of mRNA in fibroblastic cells lines: MSU1.1.PDPN overexpressing podoplanin and control MSU1.1 NC cells transduced with vector alone in (A) normoxia (18.75% O2) and **(B)** hypoxia (1% O2); expression of ANGPT2 at the level of mRNA in normoxia and hypoxia in **(C)** MSU1.1 NC and **(D)** MSU1.1 PDPN cells. Real-time RQ-PCR was used to analyze ANGPT2 mRNA. ANGPT2 levels were normalized against *ACTB* gene expression and cell line MSU1.1 NC or normoxia was assigned as a calibrator sample. Each bar represents mean ± SEM, RQ-PCR, ΔΔCt, N = (3-5), ** $p < 0.01$, *** $p < 0.001$**** $p < 0.0001$.

FGF-1 expression in normoxia, in contrast to the above described proangiogenic factors was increased by 2.5 fold in MSU1.1 PDPN cells as compared to MSU1.1 NC **(Fig. 39A).** This effect was 2.13 fold higher in hypoxia **(Fig. 39B)**. Moreover, in hypoxic conditions FGF-1 mRNA expression was 3.8 fold increased inMSU1.1 PDPN cells and 4.3 fold increased in MSU1.1 NC cells **(Fig. 39C and D).**

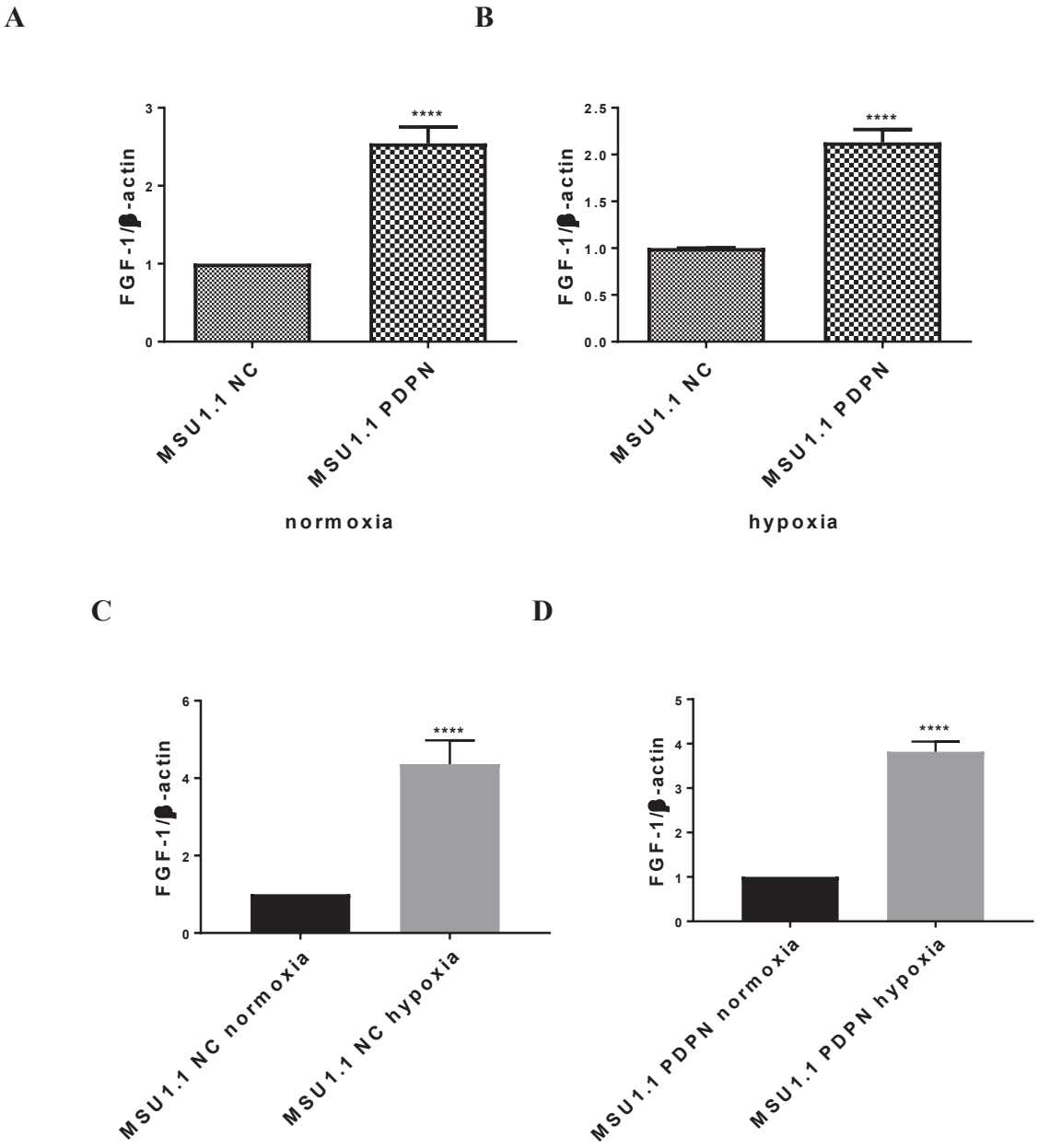

Figure 39. Expression of FGF-1 at the level of mRNA in fibroblastic cells lines: MSU1.1.PDPN overexpressing podoplanin and control MSU1.1 NC cells transduced with vector alone in (A) normoxia (18.75% O2) and **(B)** hypoxia (1% O2); expression of FGF-1 at the level of mRNA in normoxia and hypoxia in **(C)** MSU1.1 NC and **(D)** MSU1.1 PDPN cells. Real-time RQ-PCR was used to analyze FGF-1 mRNA. FGF-1 levels were normalized against *ACTB* gene expression and cell line MSU1.1.NC or normoxia was assigned as a calibrator sample. Each bar represents mean ± SEM, RQ-PCR, ΔΔCt, N = (3-5), **** $p < 0.0001$.

Taken together, these data suggest that (1) podoplanin affects the expression of proangiogenic factors in different ways; in normoxia it suppresses the expression of VEGF-A, ANGPT1 and VE-cadh. In hypoxia, PDPN increases VEGF-A but decreases VE-cadh and ANGPT1 mRNA expression. PDPN highly increases the expression of FGF-1 and ANGPT2 mRNA in normoxia and hypoxia, (2) similarly, hypoxia by itself affects the expression of various proangiogenic factors in different ways; it highly increases the expression

of VEGF-A, ANGPT2, and FGF-1 mRNA, in MSU1.1 PDPN cells. However, it suppresses ANGPT2 expression in MSU1.1 NC cells and, it has no effect on the expression of VE-cadh, in MSU1.1 PDPN and decreased it in MSU1.1 NC cells.

8.9. Effect of podoplanin in the context of hypoxia on the expression of miRNAs and their secretion via exosomes

In breast cancer, CAFs express podoplanin but little is known about its mechanism of expression [110][22] and modulation. This might be crucial for cancer cells movement and ability to escape the tumor site. In this view, a key control of tumor microenvironment is exerted by microRNAs (miRs) on gene expression. This is achieved post-transcriptionally, by degradation or blocking the translation of their target messenger RNA [162]. Among them, miR-21 is a regulator of the oncogenic process as it regulates cell proliferation, survival and migration in most cancer cells through its downstream target proteins among which stands the tumor suppressor PTEN (phosphatase and tensin homologue deleted on chromosome ten) [163][119]. As PTEN controls tumour growth and metastasis by regulating tumor angiogenesis [69] it rules the hypoxic status inside the tumor, thus, the possibility to alleviate hypoxia in tumors. MiR-29b is known as a tumor suppressor but its expression is also correlated with direct repression of PTEN expression resulting in cancer cell migration, invasion, and resistance to apoptosis [164].

Therefore to assess the role of miRNAs expressed by podoplanin positive fibroblasts in tumor stroma, miRNA profiling was performed (annex 5, 6, 7, 8) and specific miRNAs were chosen for further analysis. MSU1.1 NC and MSU1.1 PDPN cells were incubated in hypoxia and normoxia for 24h and miR-210, miR-21 and miR-29b expression level was evaluated using real-time qPCR method. In MSU1.1 NC cells, the level of miR-210 was 8.19 fold higher in hypoxia than in normoxia. In MSU1.1 PDPN cells level of miR-210 was 7.73 fold higher in hypoxia than in normoxia **(Fig. 40A)**. Expression level of miR-21 in MSU1.1 NC cells was increased upon hypoxia treatment by 1.66 fold as compared to normoxia and in MSU1.1 PDPN cells this increase was 4.7 fold **(Fig. 40B)**. As to MiR-29b a known regulator of PDPN and PTEN expression [165], its expression increased 3.06 fold in MSU1.1 PDPN expressing cells only while in MSU1.1 NC cells, no difference was observed for miR-29b expression in hypoxia vs normoxia **(Fig. 40C)**.

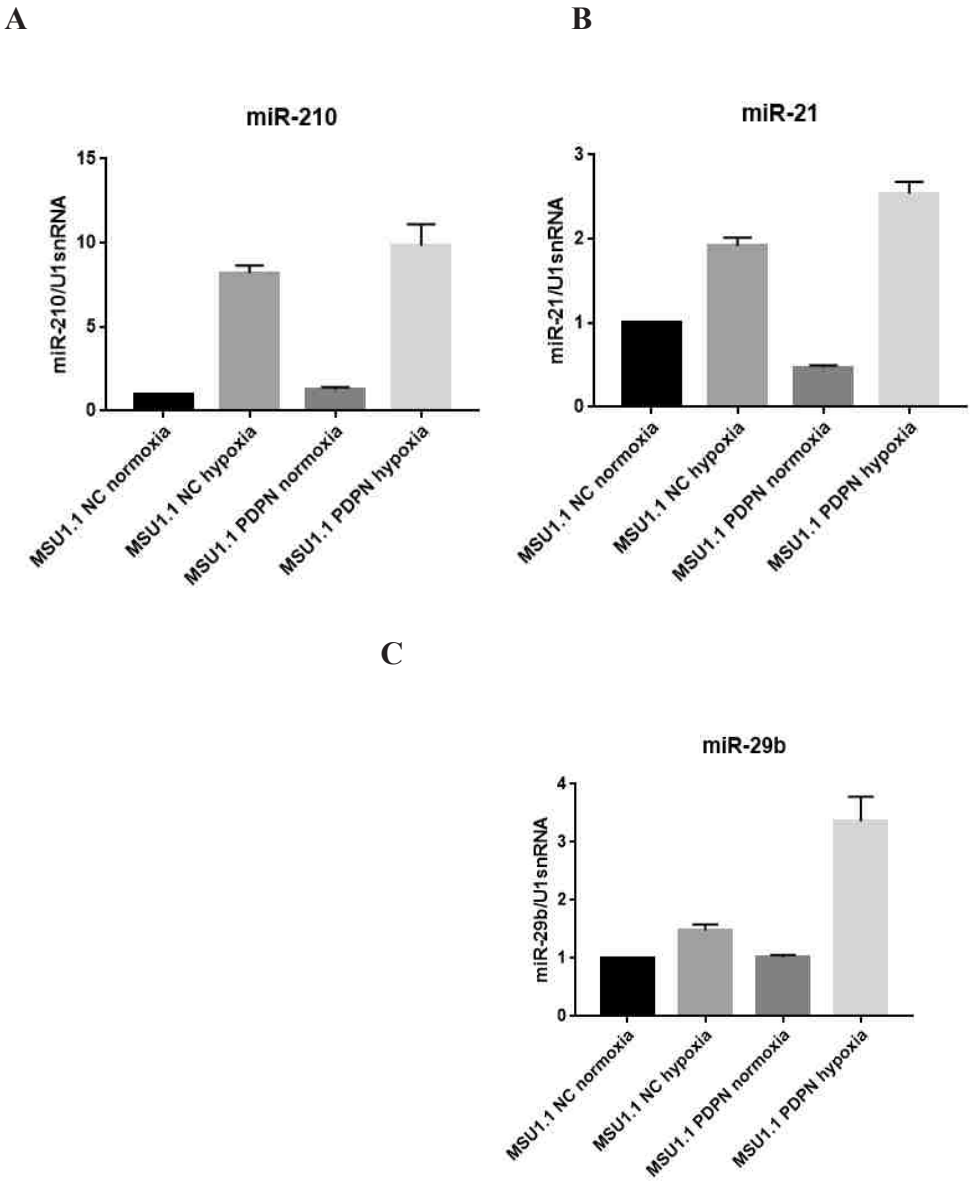

Figure 40. Expression of miRNAs in fibroblastic cells lines: MSU1.1.PDPN overexpressing podoplanin and control MSU1.1 NC cells transduced with vector alone in normoxia(18.75% O2) and hypoxia (1% O2). (A) miR-210; **(B)** miR-21; **(C)** miR-29b. Real-time RQ-PCR was used to analyze miRNA level which was normalized against *U1snRNA* gene expression and cell line MSU.1.NC was assigned as a calibrator sample. Each bar represents mean ± SEM, RQ-PCR, ΔΔCt, N = (3-5), **** $p < 0.0001$.

In order to verify the possible role of miR-21 in the regulation of podoplanin expression through downregulation of tumor suppressor gene PTEN (phosphatase and tensin homolog deleted on chromosome ten) PTEN mRNA expression in hypoxia was checked. The up-regulation of podoplanin mRNA expression correlated with PTEN mRNA down-regulation **(Fig. 41A, B)** Moreover addition of AKT inhibitor led to a decrease in podoplanin mRNA level as PTEN controls AKT pathway. This data suggests that miR-21 plays a role in podoplanin regulation through the PTEN mediated control of the AKT and hypoxia dependent pathway.

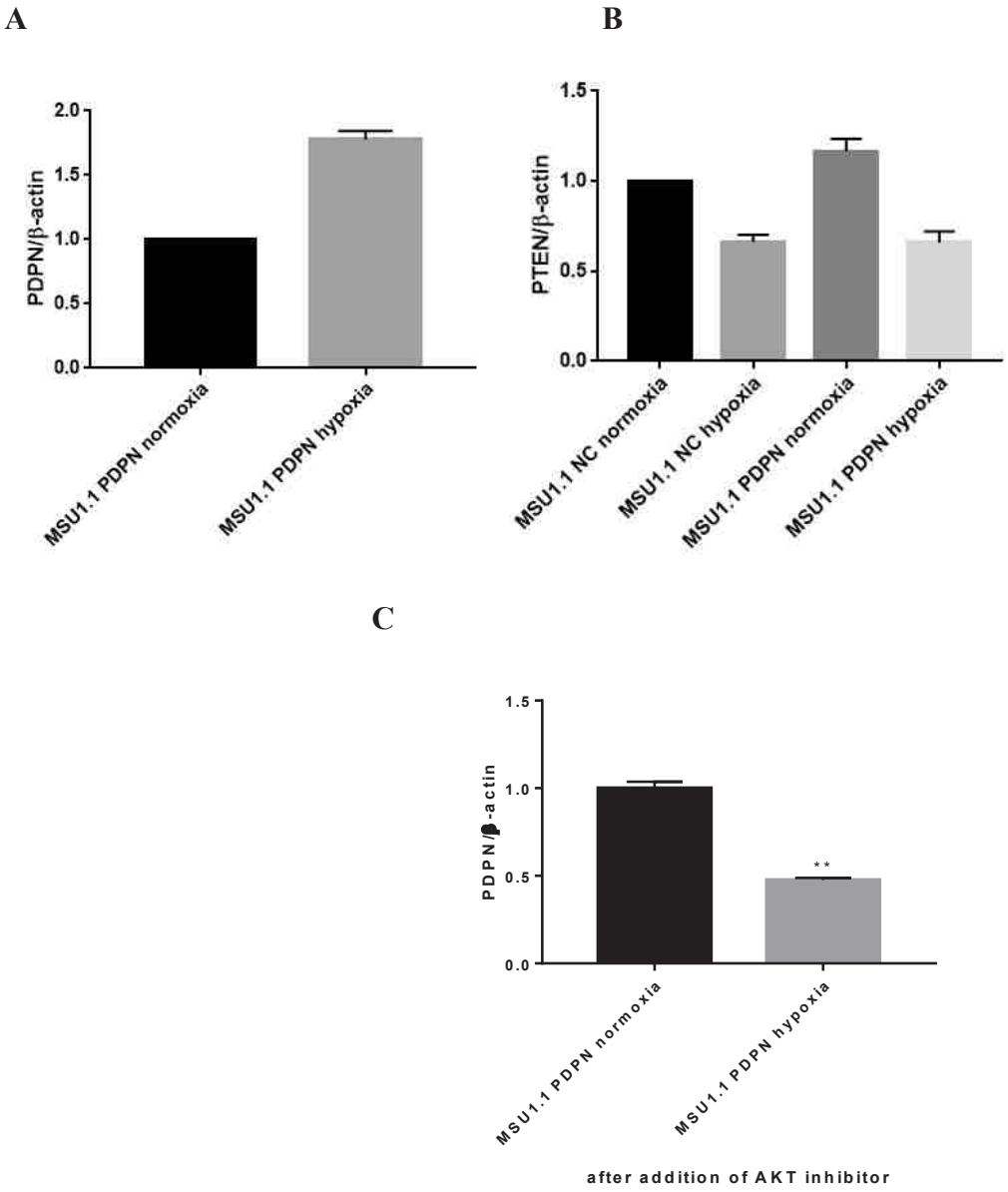

Figure 41. Modulation of expression of mRNA for PDPN and PTEN in fibroblastic cells lines: MSU1.1.PDPN overexpressing podoplanin and control MSU1.1 NC cells transduced with vector alone in normoxia (18.75% O2) and in hypoxia (1% O2) (A) expression of podoplanin mRNA **(B)** expression of PTEN mRNA **(C)** expression of podoplanin mRNA in MSU1.1 PDPN after addition of AKT inhibitor. Real-time RQ-PCR was used to analyze mRNA. Podoplanin and PTEN levels were normalized against *ACTB* gene expression and cell line MSU1.1 NC was assigned as a calibrator sample. Each bar represents mean ± SEM, RQ-PCR, ΔΔCt, N = (3-5), **** $p < 0.0001$.

The same experiment was performed with the exosomes secreted by MSU1.1 NC and MSU1.1 PDPN cells in normoxia and hypoxia. In exosomes secreted by MSU1.1 NC cells, the level of miR-210 was higher in hypoxia than in normoxia. In exosomes secreted by MSU1.1 PDPN cells level of miR-210 was higher in hypoxia than in normoxia **(Fig. 42A)**. Expression level of miR-21 in exosomes secreted by MSU1.1 NC cells was increased upon hypoxia treatment as compared to normoxia and in exosomes secreted by MSU1.1 PDPN cells an increase was observed **(Fig. 42B)**. Expression of MiR-29b

increased 6.4 fold in exosomes secreted by MSU1.1 PDPN expressing cells only while, in exosomes secreted by MSU1.1 NC cells, no difference was observed for miR-29b expression in hypoxia vs normoxia **(Fig. 42C)**.

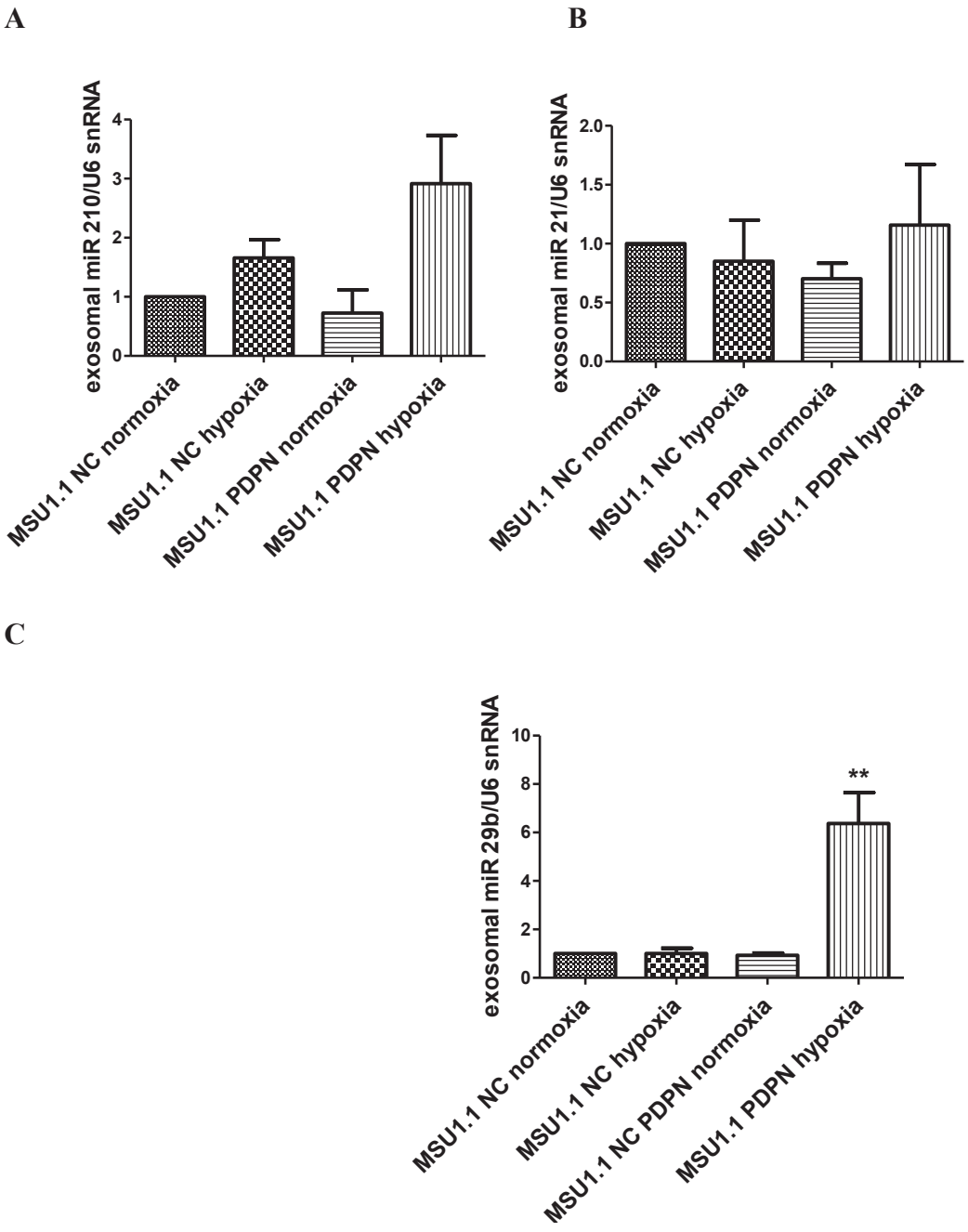

Figure 42. Expression of miRNAs in exosomes secreted by fibroblastic cells lines: MSU1.1.PDPN overexpressing podoplanin and control MSU1.1 NC cells transduced with vector alone in normoxia (18.75% O2) and hypoxia (1% O2). (A) miR-210; **(B)** miR-21; **(C)** miR-29b. Real-time RQ-PCR was used to analyze miRNA level which was normalized against *U6snRNA* gene expression and cell line MSU.1.NC was assigned as a calibrator sample. Each bar represents mean + SEM, RQ-PCR, ΔΔCt, N = (3-5), **** $p < 0.0001$.

Moreover to confirm and enrich obtained data the miRNA profiling was performed in cooperation with Tebu-Bio Company. The project was focused on understanding the interaction between podoplanin expression in cancer-associated fibroblasts (CAF) and breast cancer progression.

Anaxomics was the analytical program chosen to work on the following comparisons:

- Cell lysates: normoxia vs hypoxia (from MSU1.1 cells expressing and not expressing podoplanin)
- Exosomes: normoxia vs hypoxia (from MSU1.1 cells expressing – exoPDPN+ and not expressing podoplanin – exoPDPN-)

The table shows number of miRNAs which are differentially expressed in hypoxia compared in normoxia first globally then numbers of miRNAs which appears to be up-regulated and down-regulated. The table points to the number of mRNA targets the expression of which can be modified by these miRNAs **(Table 1)**. The table displays the differentially expressed miRNAs in the cell fraction and secreted via exosomes. In the cell fraction there is no clear difference in the total numbers of miRNAs differentially expressed. In MSU1.1 NC the number of up-regulated miRNAs (102) is close to the number of down-regulated miRNAs (110). When cells express podoplanin miRNAs differentially expressed are mainly down-regulated (180). In the Exosomal fraction from MSU1.1 NC the miRNA content is much lower than in the cell fraction. MiRNAs are mostly up-regulated by hypoxic conditions. When podoplanin is expressed, differentially expressed miRNAs are actively secreted and found into the exosomal fraction (540). They are mostly up-regulated (536) and very few were found to be down-regulated (4).

	Differential miRNAs	Up-regulated miRNAs	Down-regulated miRNAs	targets
MSU1.1 NC Hypoxia vs Normoxia	212	102	110	9588
MSU1.1 PDPN Hypoxia vs Normoxia	213	33	180	9558
Exosomes MSU1.1 NC Hypoxia vs Normoxia	63	62	1	4260
Exosomes MSU1.1 PDPN Hypoxia vs Normoxia	540	536	4	10149

Table 1. Summary of the differentially expressed miRNAs identified in each sample of interest.

The above table shows the deep effect of hypoxia on the miRNA mediated regulation and suggests that podoplanin may exert its biological activity through miRNA exported via exosomes in the tumor site.

Anaxomics has performed an enrichment analysis of the differentially expressed miRNA data obtained from each sample. The results are shown on heat maps (annex 5, 6, 7, 8). Main conclusions made by the company are presented below.

Among the processes linked to hypoxia: HIF-1α signalling pathway, cellular response to hypoxia; tissue invasion and metastasis such as positive regulation of chemotaxis, positive regulation of fibroblast migration, positive regulation of blood vessels endothelial cells migration; cancer microenvironment;pathways associated with PI3K-AKT, mTOR, and P53, chemokines signalling pathways

i. e. chemokine activity, chemokine biosynthetic process; angiogenesis i.e. cell migration involved in sprouting angiogenesis; extracellular matrix composition i.e. cell-matrix adhesion, ECM disassembly, remodeling and organization were analysed. MiRNAs appeared to be regulated by hypoxia. In cells that express podoplanin miRNAs associated were down-regulated while when cells did not express podoplanin were mainly up-regulated (annex 5, 6).

These processes were verified to be regulated by hypoxia in exosomes secreted by cells that express (exoPDPN+) and do not express podoplanin (exoPDPN-). MiRNAs targeting these hypoxia dependent processes were up-regulated and podoplanin expression enhanced considerably this effect (annex 7, 8).

Processes linked to glycosylation such as protein O-linked glycosylation, protein N-linked glycosylation via asparagine, glycosaminoglycan metabolic process, glycosaminoglycan biosynthetic process, glycan biosynthesis are regulated by hypoxia in cells that express podoplanin through the down-regulation of miRNAs. Processes linked to glycosylation are also regulated by hypoxia in exoPDPN+ through the up-regulation of miRNAs targeting these processes (annex 5, 6, 7, 8).

In exosomal fraction the miRNAs that are regulators of the pathways associated to PI3K-AKT, mTOR, and P53 i.e. phosphatidyloinosytol-3-kinase activity, phosphatidyloinosytol-4-phosphate binding, phosphatidyloinosytol-3-kinase signaling, phosphatidyloinosytol-3-phospate binding, negative regulation of TOR signaling, positive regulation of phosphatidyloinosytol-3-kinase activity, mTOR signaling pathway, phosphatidyloinosytol-3-kinase signaling, p53 signaling pathway were affected by hypoxia in both, exoPDPN+ and exoPDPN-. Furthermore, in cells these processes were strongly regulated by the presence of podoplanin in comparison with the cells that do not express this protein. In the absence of podoplanin the mTOR pathway is not regulated by hypoxia (annex 5, 6, 7, 8).

This analysis confirms the data obtained by RQ-PCR however further functional analyses are necessary to elucidate function of each miRNA.

9. DISCUSSION

Components of tumor microenvironment among which are cancer associated fibroblasts (CAFs) producing extracellular matrix (ECM), endothelial cells (ECs), macrophages, adipocytes, pericytes and immune cells controls progression of malignant tumors[21][166]. All these cells are working in hypoxic context in tumor stroma. Cancer associated fibroblasts and cancer cells express podoplanin among other mucin-type glycoproteins [22]. The role of podoplanin expression in tumor stroma of invasive ductal carcinoma of the breast remains to date to be fully elucidated. The presence of CAFs expressing podoplanin was positively correlated with tumor size, degree of malignancy, lymph node metastases, invasion into lymphatic and blood vessels, expression of Ki67 antigen, shorter patients' survival and VEGF-C expression [22][75]. The present study was undertaken to assess if fibroblasts expressing podoplanin can affect malignancy of breast cancer cells in context of hypoxia. Moreover, in order to reconstruct the tumor microenvironment the endothelial cells were included in the model as they are the cells which achieve angiogenesis.

CAFs present in tumor stroma act in various ways. They promote cancer progression by secretion of numerous chemokines, growth factors, enzymes and other proteins, which among other activities induce angiogenesis, recruit progenitor endothelial cells from bone marrow, or help in extracellular matrix remodeling [42]. CAFs apart from secreted proteins, release miRNAs mostly *via* exosomes [167]. MiRNAs are capable of controlling tumor microenvironment through targeting mRNAs of proteins and affect the tumor development [168]. Therefore, to define the specific role of podoplanin expressed by CAFs in cancer cell biology, a cellular model with overexpression of this protein was obtained using established *in vitro* fibroblastic cell line, MSU1.1 which represents normal, non-activated fibroblasts and does not express podoplanin.

Hypoxia occurs when the tumor mass reaches a critical volume, whichcauses insufficient oxygen partial pressure by lack of O_2 diffusion. Hypoxia plays a critical role during the evolution of the tumor microenvironment and is considered as determining cancer development, and formation of the cancer stem cell niches [169]. Podoplanin expression is induced byepithelial growth factor (EGF), fibroblast growth factor type 2 (FGF2) and tumor necrosis factor α (TNFα) in MCF-7 breast cancer cells as well as by bradykinin in 3T3 mouse fibroblasts [105][93], transforming growth factor β (TGFβ) in human fibrosarcoma cells [99]and interleukin-3 (IL-3) in lymphatic vessels of skin[107]. Endogenous factors, also activate the expression of podoplanin as shown in chemically-induced tumors of the skin like Fos protein belonging to the AP-1 transcription factor complex (Durchdewald et al., 2008), intracellular signalling pathway involving Src oncogene and the adapter protein Crk-associated substrate (Cas) in mouse embryonic fibroblasts

transformed with tumor-oncogene src[109]. Podoplanin expression being induced by various factors, suggests that expression in tumor cells may be affected by the overall tumor microenvironment which is shaped largely by hypoxia. It was thus necessary to check whether hypoxia may have such an effect.

Therefore, to determine if and how hypoxia affects podoplanin expression, human smooth muscle cells with fibroblastic morphology, namely T/G HA-VSMC cells naturally expressing podoplanin and human MSU1.1 fibroblasts, which do not express podoplanin, were analyzed for the expression of this glycoprotein under low pO2 level (1% of O_2). The expression of podoplanin was affected by hypoxia in T/G HA-VSMC cells that expressed podoplanin and an increase in podoplanin mRNA level was there observed, while podoplanin was not induced by hypoxia in case of MSU1.1 cells. Hence, while hypoxia is not sufficient to trigger podoplanin expression it increases its expression in cells expressing it as T/G HA-VSMC and where its expression is under the control of the CMV promoter sensitive to hypoxia as in the transduced cells [157].

Pathological hypoxic microenvironment, which is observed in many solid cancers, dramatically changes gene expression profiles, and confers various malignant characteristics to cancer cells as well as surrounding cells including fibroblasts. This may favour tumor progression. Therefore, taking into account that hypoxia affects podoplanin expression, experiments presented in this thesis were performed in normoxic as well as in hypoxic conditions.

It has been shown that podoplanin present on CAFs has an impact on cancer cells in invasive ductal carcinoma of pancreas [112]. Moreover podoplanin transduced breast cancer cell line: MCF-7 and keratinocyte cell line: HaCaT showed increased migratory and invasive properties [93]. Similarly increased invasive properties of pancreatic cancer cells were obtained after their co-culture with podoplanin positive CAFs [93]. However inhibition of podoplanin expression in CAF did not affect the invasive properties of pancreatic cancer cells suggesting that this effect was not significant[112]. In the present study the role of podoplanin expressed by CAFs on breast cancer cells migration was examined. Podoplanin present on the surface of fibroblasts has no impact on migration of MCF-7 and MDA-MB-231 cancer cells neither in normoxia nor in hypoxia as opposed to pancreatic cancer cells. However, in our modelectopic expression of podoplanin highly increases the migration of MSU1.1 PDPN fibroblasts in comparison to control MSU.1.NC cells. Nevertheless, in hypoxic environment the effect of podoplanin in CAF on migration was completely blocked and fibroblast migrated even slower than in normoxia. It has been shown that hypoxia deactivates CAFs, weakening their ability to remodel ECM and contraction. This leads to impairment of cancer cell invasion mediated by CAFs [170]. Thus fibroblasts may migrate into the tumor stroma and create microenvironment conditions that favor tumor progression through factors affecting survival, proliferation and invasion of cancer cells secreted by increased number of CAFs **(Fig. 43)**.

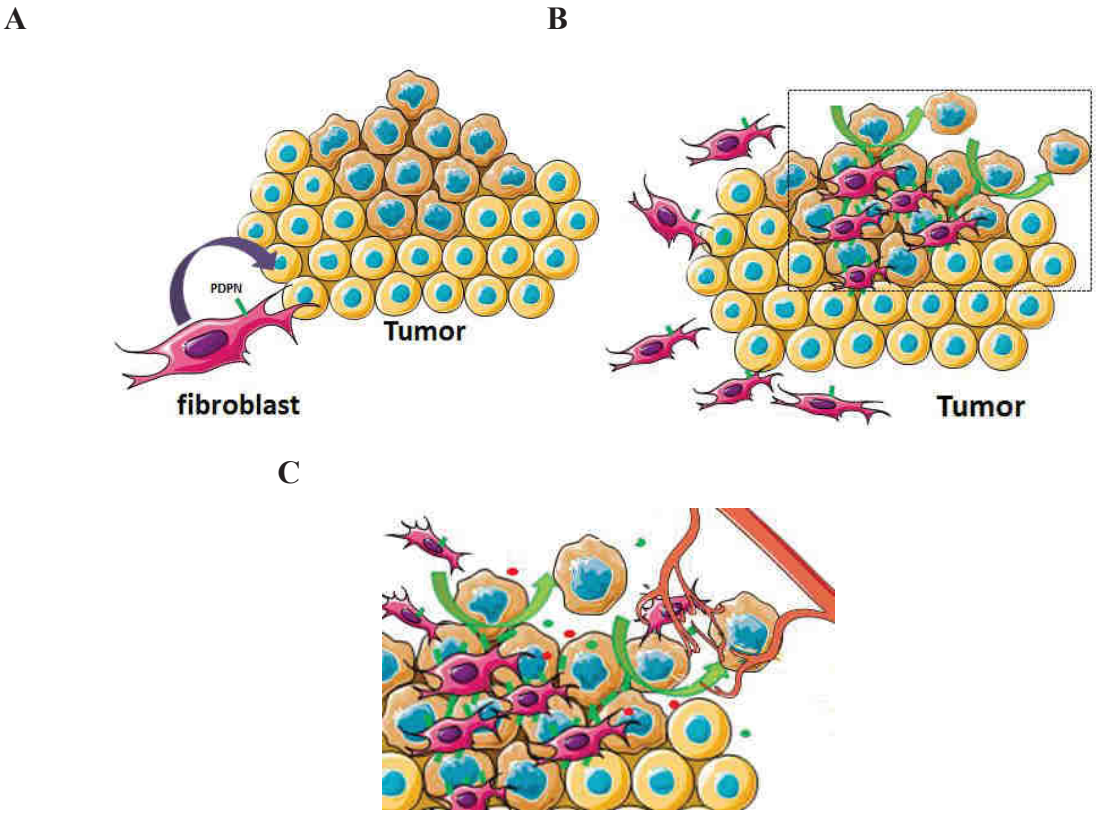

Figure 43. Schematic representation of the potential effect of podoplanin on fibroblasts in tumor microenvironment. **(A)** Expression of podoplanin in fibroblast close to the tumor site. **(B)** Podoplanin expression on fibroblast is increased in the tumor site. Itincreases CAF migration and incorporation into tumor. Podoplanin presented on fibroblasts act as an anti-adhesive molecule and dissolves cancer cell mass leading to metastasis.**(C)**Fibroblasts expressing podoplanin secrete proangiogenic factors (green) and chemokines (red) that stimulate cancer development.

In contrast, hypoxia increased the migration ability of MCF-7 cells, whereas migratory properties of MDA-MB-231 cells were not significantly affected. Recent studies have shown that hypoxia may promote migration and invasion of cancer cells [171–173]. Activated by oxygen deprivation hypoxia-inducible factor α (HIF1α) may activate genes responsible for motility as RHOA and ROCK1 (Rho kinase 1) **(Fig. 44)** [171]. During hypoxia-induced migration, cancer cells may access to the circulation through disordered, leaky and irregular tumor vasculature [171]. Therefore migration induced by hypoxia may help intravasation of cancer cells which is an early step of metastasis [171].

In contrast, hypoxia increased the migration ability of MCF-7 cells, whereas migratory properties of MDA-MB-231 cells were not significantly affected. Recent studies have shown that hypoxia may promote migration and invasion of cancer cells [171–173]. Activated by oxygen deprivation hypoxia-inducible factor α (HIF1α) may activate genes responsible for motility as RHOA and ROCK1 (Rho kinase 1) **(Fig. 44)** [171]. During hypoxia-induced migration, cancer cells may access to the circulation through disordered, leaky and

irregular tumor vasculature [171]. Therefore migration induced by hypoxia may help intravasation of cancer cells which is an early step of metastasis [171].

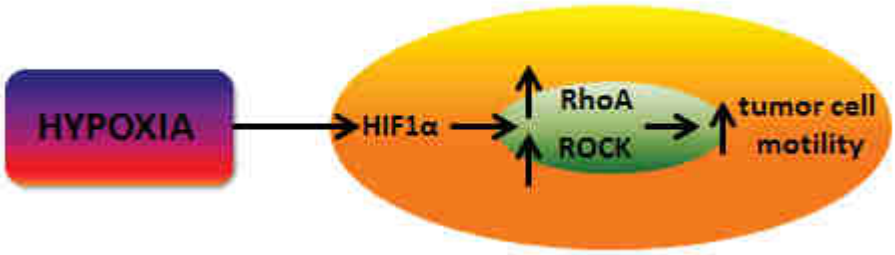

Figure 44. Effect of hypoxia which promotes migration of tumor cells. When hypoxia occurs HIF1-α is not degraded in the proteasome and activates RhoA and ROCK increasing the motility of tumor cells.Adapted from Hon S. Leong and Ann F. Chambers doi/10.1073/pnas.1322484111.

As other cancer cells, mammary carcinoma are able to metastasize into lymph nodes[174]what implies the mobilization from the tumor primary site in which they interact with CAFs which are overexpressing podoplanin[174]. Tumor cells may lose their adhesive properties and detach from the primary tumor foci, reach the vessels, intravasate into the lumen and this allow them to travel through the lymphatic system and bloodstream to other distant organs. Thus cancer cell-to-cell and cell-ECM adhesionplay a significant role in cancer progression and metastasis[175]. Metastasis is enabled by cell-cell interactions between endothelium and tumor cells in distant tissues. In circulation, tumor cells interact with platelets and leukocytes what leads to tumor cell adhesion, extravasation, and the creation of metastatic lesions. Cancer metastasis is a multistep cascade which starts with local invasion of tumor cells, survival in systemic circulation, extravasation in secondary sites, and ends with formation of metastatic lesions [176][175]. As mentioned in the introduction the organ-specific character of metastasis has been observed by S. Paget, and the "seed and soil" hypothesis assumes specific interactions of tumor cells with the environment of distant organs that permits the establishment of metastasis and later growth[11]. While vital steps in the metastatic cascade namely cancer cell-endothelial cell interactions enabling tumor cell adhesion in the vasculature of specific organs, cancer cell-ECM interactions in the primary tumor site are necessary for cancer cell escape to circulation. Up to now selectins and integrins, two major cell adhesion molecule families, have been identified among others to take part in metastasis[176]. The exact mechanism of cell-cell interactions involved in cancer progression remains to be fully elucidated. Integrin β1 facilitates local invasion within the primary site through cell–ECM adhesion and movement of tumor cells[176]. Overexpression of podoplanin results in a lower interaction of CAF-s with breast cancer cells within tumor

stroma contributing to further escape of tumor cells from the primary site and metastasizing toward the lymph nodes. Moreover, when overexpression of podoplanin occurs in hypoxic tumor microenvironment this movement effect is enhanced. This makes podoplanin an anti- adhesive molecule in this context.

As with other cancer cells, mammary carcinoma cells are able to metastasize into lymph nodes in a process involving the CCL21/CCR7 axis[174]. This implies mobilization from the tumor primary site in which they interact with CAFs overexpressing podoplanin. Since CCL21 was found to interact with PDPN[160], the regulation of both molecules may control the entry of CCR7+NK cells and cytotoxicity in the tumor. Furthermore, it may also modulate the movement and escape of CCR7+tumor cells achieving metastasis. Moreover, CCR7 was shown to promote mammary cell tumorigenesis through amplification of stem-like cells[177] which points to the key role played by the CCL21/CCR7 axis in the various steps of mammary tumor evolution.

Overexpression of podoplanin results in a lower interaction of CAFs with carcinoma cells. As shown here, higher expression is due to hypoxia under which condition, the addition of CCL21 is required to help the CAF/cancer cell interaction. In comparison to normoxia we showed that CCL21 production is not increased upon hypoxia in CAFs (annex 4). This confirms the anti-adhesive effect of podoplanin in the tumor microenvironment and its role in favoring CCR7+ carcinoma cell movement and mediating escape. CCR7+ carcinoma cells, while not retained in the primary tumor site, might thus be attracted to CCL21+ sites such as peripheral lymph nodes where the chemokine is presented on endothelial cells as shown in this work.

Fibroblasts stay in contact in tumor stroma next to cancer cells with endothelial cells[178]. Here we postulate that podoplanin presented on CAFs may impact ECs directly or through secretion of proangiogenic factors. Interestingly, in contrast to breast cancer cells, podoplanin positive CAFs cultured in separate compartments with endothelial cells increases endothelial cell migration however hypoxia blocks this effect.Endothelial migration is a key aspect of a range of physiologic and pathologic conditions. Recent studies on the role of podoplanin in endothelial cells migration were undertaken for the human lung microvascular lymphatic endothelial cells[179]. It has been shown that podoplanin present on lymphatic endothelial cells is a key regulator of their polarized migration and is required for tube formation[179]. This processes are controlled by podoplanin through regulation of Cdc42 and activation of RhoA[179].

Little is known about podoplanin effects on cells present in tumor stroma. The present study uncovered, that podoplanin can influence angiogenesis and participate to its pathologic properties in the tumor context. So far, podoplanin was described as a specific marker of lymphatic endothelium, absent in the blood vascular endothelial cells[74]. It was shown that this glycoprotein plays a key role in proper lymphatic vasculature formation and separation of lymphatic vasculature from blood vessels[82].

Present study shows also that podoplanin-rich CAFs co-localize more efficiently withhuman skin microvascular endothelial cells (HSkMEC) than control fibroblasts that do not express podoplanin in normoxia as well as in hypoxia. This increased co-localization of fibroblast over-expressing podoplanin with endothelial cells, results in much more disordered tube formation which is characteristic for vasculature in cancer as well as in corresponding angiogenesis induced by persistent hypoxia. Moreover podoplanin-expressing CAFs express less VE-cadherin than control fibroblasts. This may weaken the interactions between cells and leads to intravasation of immune cells into the tumor site. Stimuli within solid tumors, as hypoxia, induce the formation of new vessels to ensure a rich vascular supply for continuing tumor growth. However this fast angiogenesis results in a vascular network that is highly abnormal when compared to the organized structure of vessel networks in normal tissues[65]. This structurally abnormal network leads to aberrations in local blood flow, fluid dynamics, and oxygenation that in turn can augment tumor growth and metastatic potential while diminishing response to cytotoxic therapies[65]. Embryonic vessels fail to branch, expand and remodel, as endothelial junctional molecule VE-cadherin regulates survival function of VEGF[180]. Moreover secretion of MMP-2 and MMP-9 by CAFs lead to EMT through downregulation of E-cadherin in prostate carcinoma[21]. The transition from adenoma to carcinoma is strictly regulated by EMT process accompanied by down-regulation of E-cadherin[31]. Upon expression in transgenic mice and cancer cells podoplanin induces tumor formation without up-regulation of ezrin, radixin, moesin proteins (ERM) and without any need for EMT[181].In the present work we have shown that podoplanin present on the surface of fibroblasts affects the tube formation by HSkMEC endothelial cells in co-localisation experiments where direct interactions between fibroblastic cells and endothelium take place.

Data obtained in angiogenesis and co-localization experiments raised two possible suggestions: (1) PDPN can affect the angiogenesis directly by interaction with unknown receptor on ECs, (2) in addition to direct contact, podoplanin influences the production of angiogenic factors. To address these questions, the expression of angiogenic factors in fibroblastic cell lines with different expression of podoplanin was analysed. Proangiogenic factors induce weakening of VE-cadherin-mediated endothelial cell (EC) junctions and EC migration, altering vessel wall architecture[182]. Fibroblasts expressing as well as non-expressing podoplanin secrete pro-angiogenic factors as fibroblast growth factor (FGF-1) and angiopoietin 1 (Ang1) which have survival properties for endothelial cells[183][184].FGF modifies endothelial cell migration among other processes as cell growth, embryonic development, morphogenesis, invasion, angiogenesis[184]. However CAFs expressing podoplanin secrete less VEGF and VE-cadherin comparing to control. Moreover acceleration of endothelial cells migration was observed in normoxia but fibroblasts express more proangiogenic factors in hypoxia. This suggests that podoplanin positive CAFs secrete other factor(s) in normoxia, but not in hypoxia, able to accelerate movement of endothelial cells.

CAFs promote tumor angiogenesis by secretion of MMP-13 that accompanies the secretion of vascular endothelial growth factor (VEGF) what increases invasion in case of melanoma or squamous cell carcinoma[21]. PDGFRβ mediated adherence of pericytes to endothelial cells is blocked by formation of VEGFR-PDGFR complexes within pericytes induced by VEGF. Among other abnormalities accompanying tumor angiogenesis, one can cite the impaired structure of perivascular basement membrane (BM) which is thick in some regions and very thin in others[63]. VEGF is expressed by normal fibroblasts and its activity is regulated by MMP-7 secreted by cancer cells[185]. Present work indicates that CAFs expressing podoplanin express less VEGF than normal fibroblasts.

CAFs expressing podoplanin express more FGF-1, a heparin-binding polypeptide, than normal fibroblasts. FGF-1 regulates angiogenesis, differentiation and proliferation[184].

FGF-1 is mitogenic and chemotactic for fibroblasts, endothelial cells and smooth muscle cells[184].

The miRNAs are other regulators of podoplanin expression and cancer development[167][154]. The importance of podoplanin in the tumor microenvironment was confirmed by assessing the effect of its expression on micro RNAs (miR-21, miR-210, miR-29b) that are involved in tumor growth. Moreover results obtained in miRNA profiling shows the deep effect of hypoxia on the miRNA mediated regulation and suggest that podoplanin may exert its biological activity through miRNA exported via exosomes in the tumor site. MiR-21 is a known oncomiR which regulates tumor suppressors as PTEN **(Fig. 45)** and p53[69][119] while 210 is the most active hypoxa and angio - miR and miR-29b regulates several proangiogenic molecules. Podoplanin appears to be positively regulated by hypoxia and is coexpressed with miR-21 and miR-210. Since, miR-29b is a down regulator of podoplanin, its overexpression in hypoxia in cells and conditions which induces podoplanin expression, suggests a sequential and time-dependent or hypoxia level-dependent regulatory effect. This work points to the important part played by hypoxia-regulated podoplanin in tumors in increasing fibroblast migration into the tumor, impairing vessel formation and lowering tumor cells adhesiveness to tumor fibroblasts.

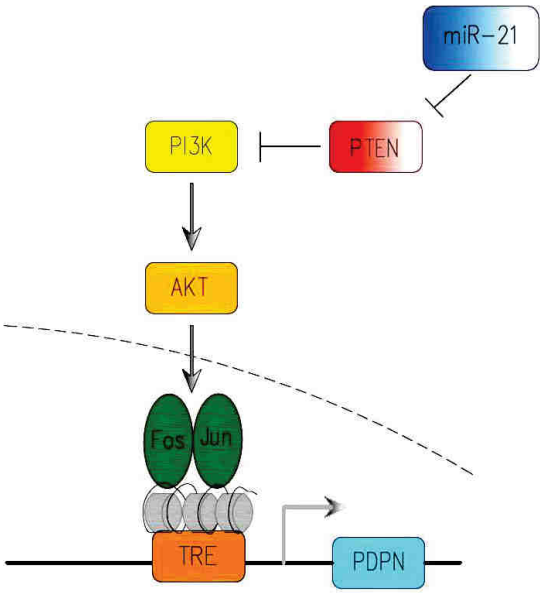

Figure 45. Schematic possible control of podoplanin through down-regulation of PTEN by miR-21 which allows activation of AKT.AP-1- activator protein 1,TRE-tetracycline response element, Fos-AP-1 transcription factor subunit, Jun-AP-1 transcription factor subunit.

In conclusion this work contributed to show that podoplanin:

- Acts as anti-adhesive molecule in the tumor site
- Expression is increased by hypoxia
- Mechanism of action is CAF-mediated
- Molecular mechanism is CCL21/CCR7 dependent
- Increases motility of tumor stromal fibroblasts and endothelial cells but not of tumor cells
- Regulation is dependent on miRNAs in hypoxia
- Expressed by CAFs induces hypoxia dependent secretion of exosomal miRNAs especially angiogenesis-related miRNAs

These data demonstrate the deep implication of podoplanin expression and activity in the tumor microenvironment.

This work offers perspectives for the design of new strategies of treatment based on the knowledge on tumor microenvironment. Podoplanin may serve as a good marker of the progression of breast cancer. Normalization of vessels decrease tumoral hypoxia what leads to the down-regulation of podoplanin expression in CAFs. Another possible treatment may be focused on miRNAs. Counteracting miRNAs secreted by podoplanin positive CAFs seems to be a good strategy. Furthermore, miRNAs targeting podoplanin may be considered as an approach for treatment of breast cancer.

10.Annexes

Annex 1

Fragment of DNA sequencing of pRRL-CPPT-CMV-PDPN-IRES-PURO-PRE-SIN construct with primersPovMLuI_R and PovEcoI_F containing the insert with cDNA for podoplanin showing a mutation of one nucleotide that does not alter the encoded amino acid.

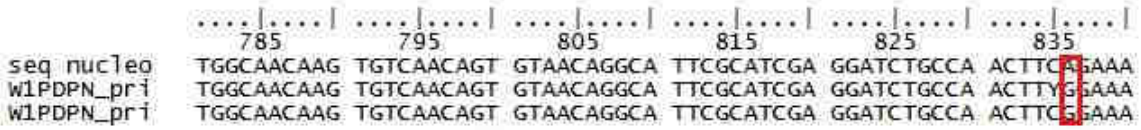

Annex 2

Expression of CCR7 on cancer cell lines at protein level.
Assessment by Flow Cytometry of thebinding of fluorescent mouse monoclonal anti-human CCR-7 antibody to MDA-MB-231 and MCF-7 cells.

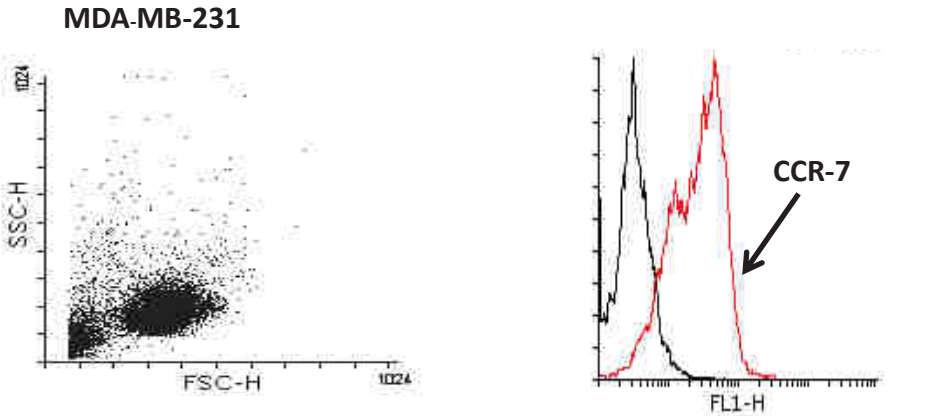

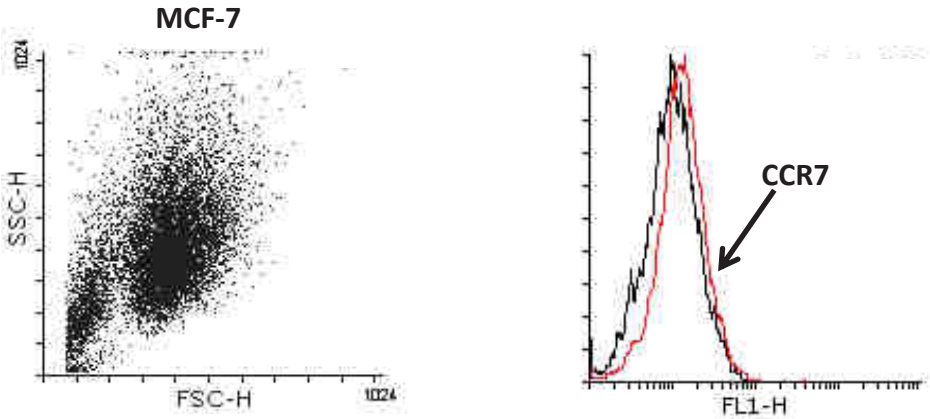

Annex 3

Reduction of adhesion of NKL3 cells to MSU1.1 PDPN vs MSU1.1 NC and MSU 1.1**.**

Quantification of the adhesion of NKL3 cells to MSU1.1 PDPN and MSU1.1 NC, effect of podoplanin. Each bar represents mean ± SEM, N = 3.

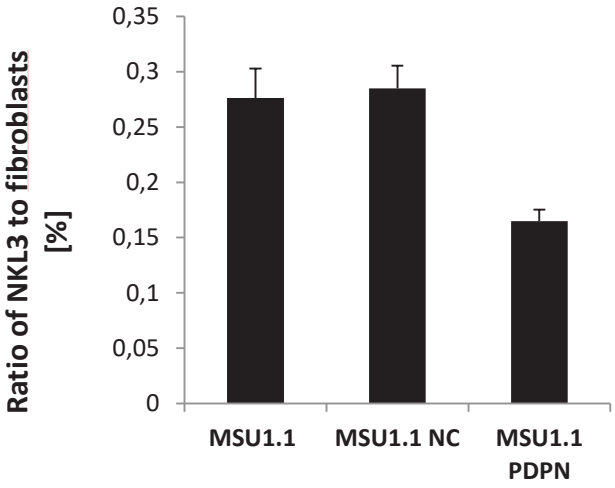

Annex 4

Expression of CCL21 mRNA in MSU1.1 PDPN fibroblasts after treatment with hypoxia.
Real-time RQ-PCR was used to analyze CCL21 mRNA. CCL21 levels were normalized against *ACTB* gene expression. Each bar represents mean ± SEM.

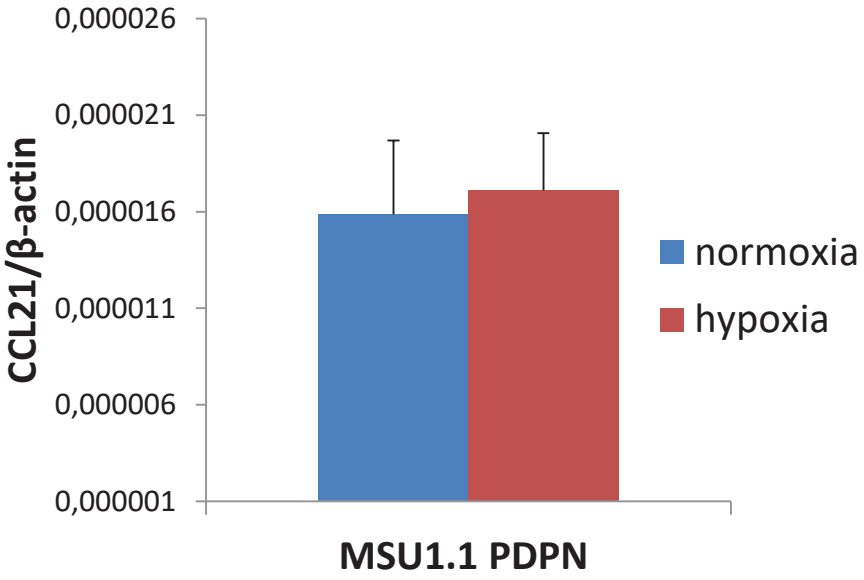

Annex 5

Heat map,gene set enrichment analysis (GSEA) for each differentially expressed miRNA in MSU1.1NC cells, non-cluster.

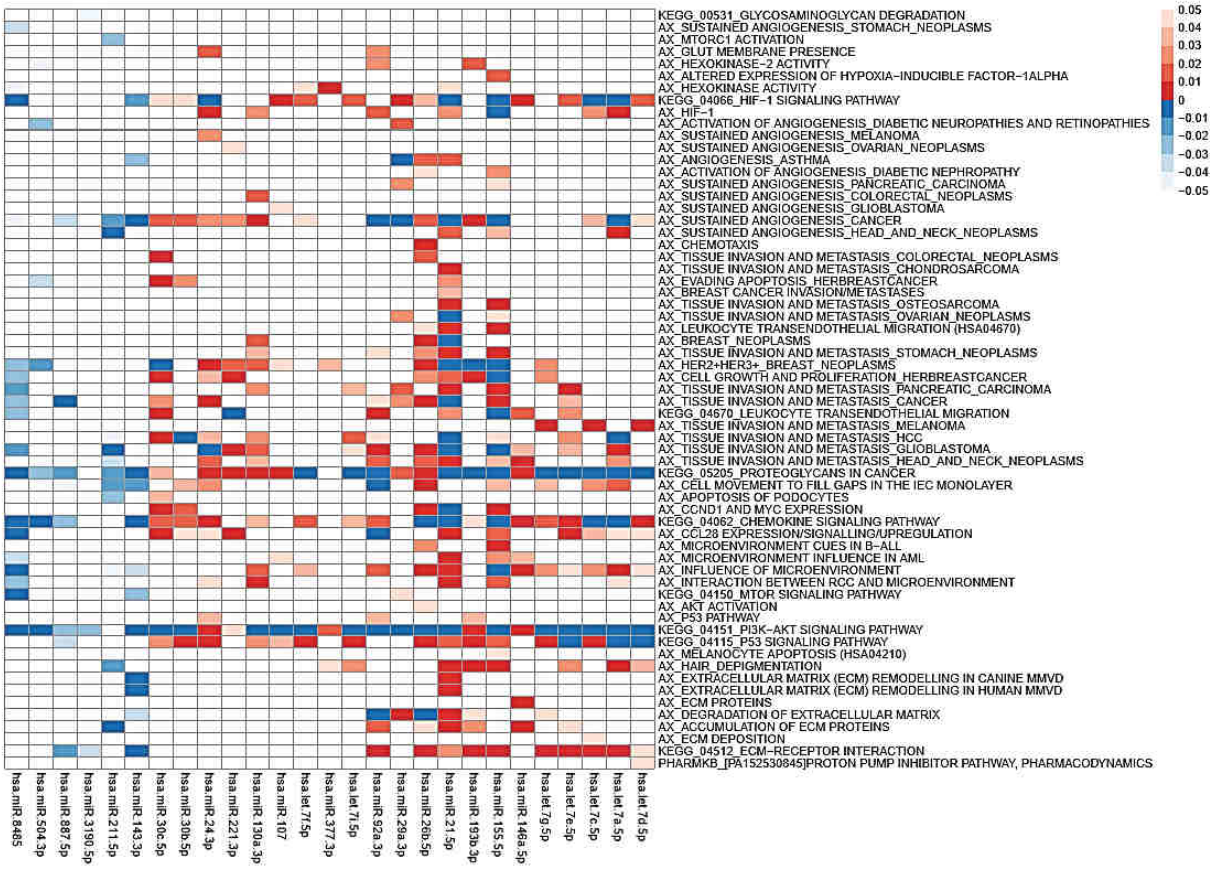

Annex 6.

Heat map, gene set enrichment analysis (GSEA) for each differentially expressed miRNA in MSU1.1 PDPN cells, non-cluster.

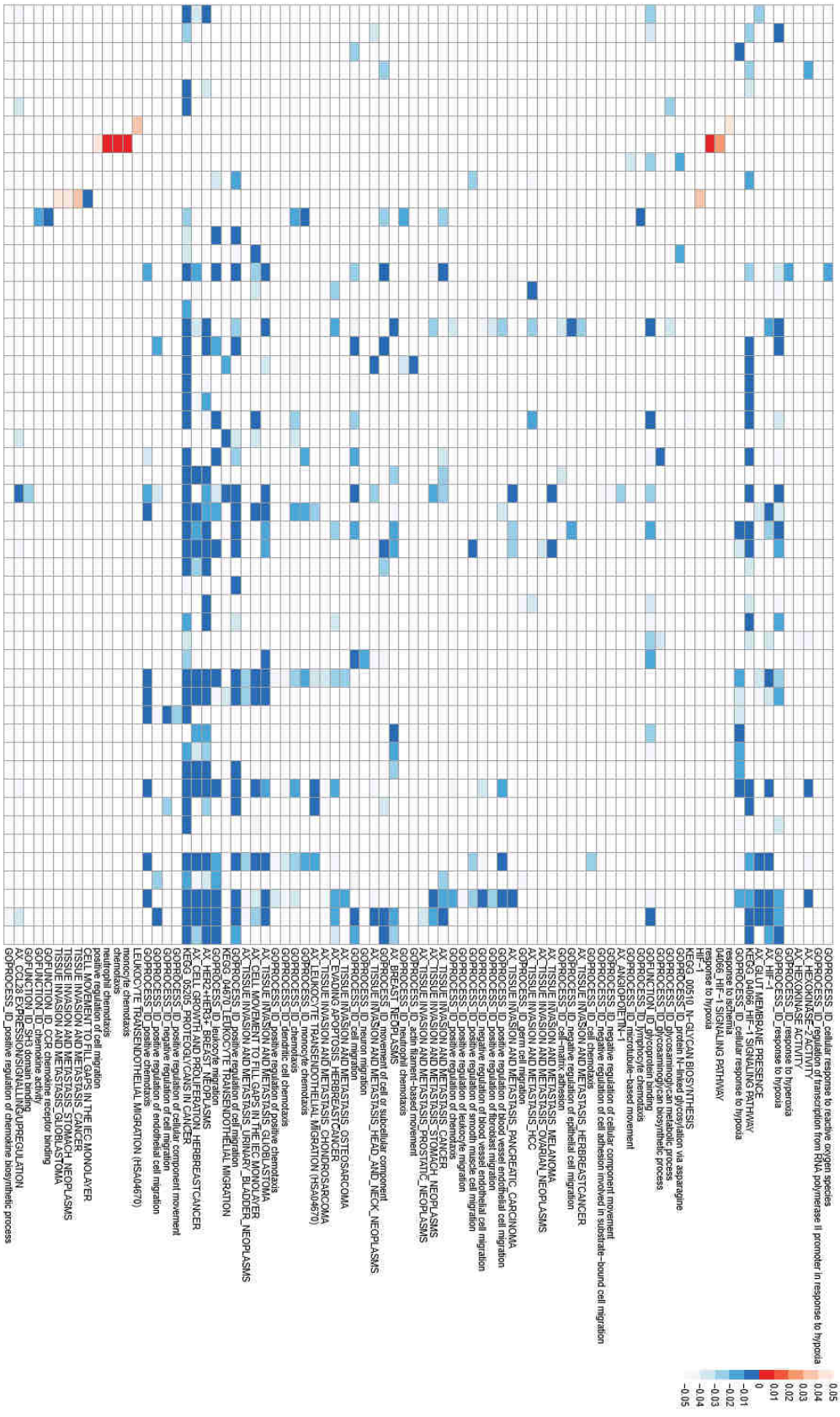

Annex 7

Heat map, gene set enrichment analysis (GSEA) for each differentially expressed miRNA in exosomes secreted by cells MSU1.1 NC, non-cluster.

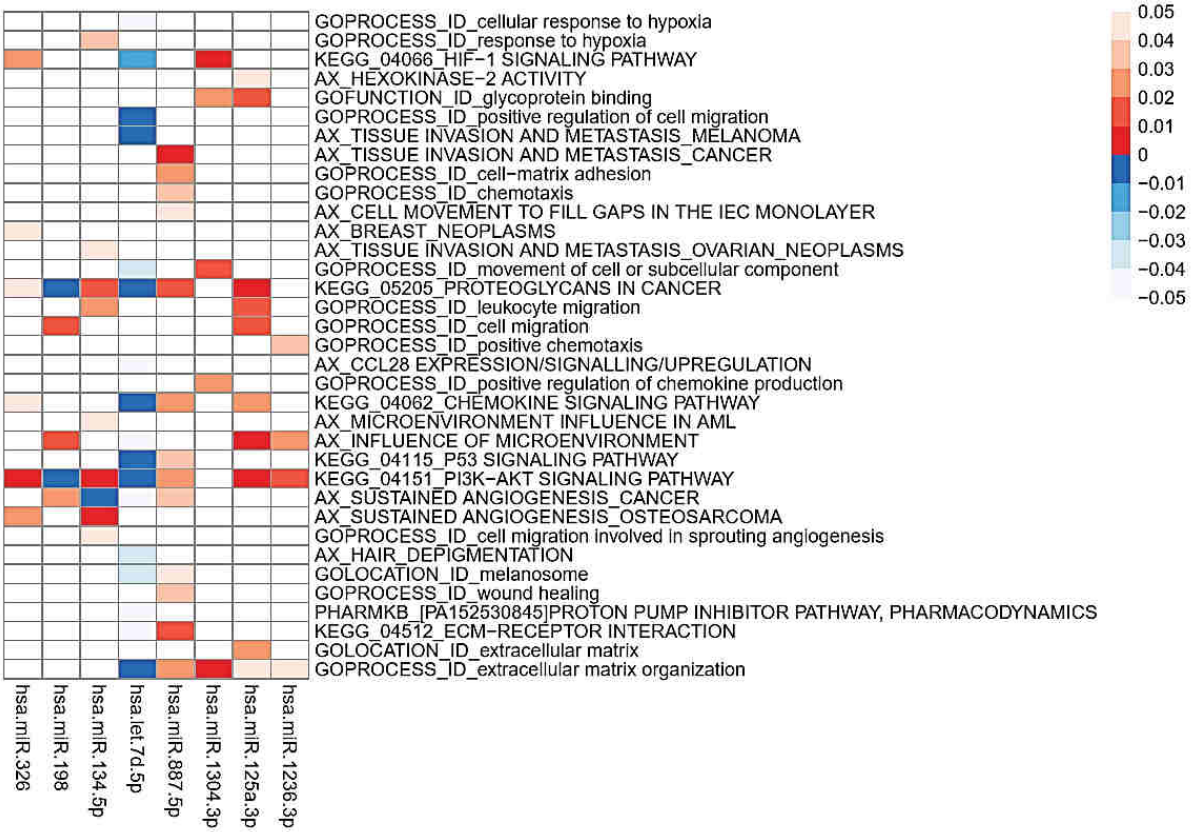

Annex 8

Heat map, gene set enrichment analysis (GSEA) for each differentially expressed miRNA in exosomes secreted by cells MSU1.1 PDPN, non-cluster.

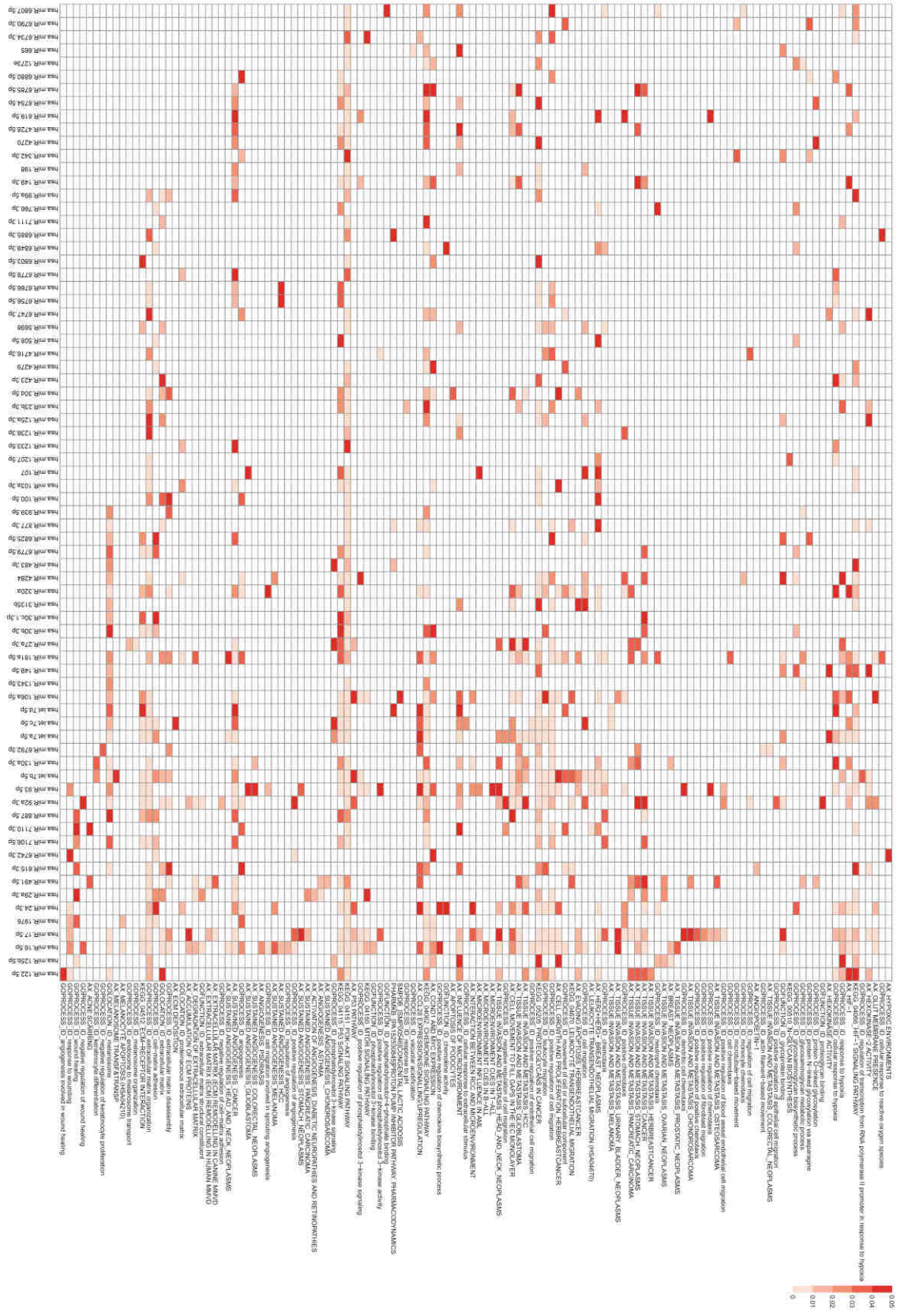

11.Bibliography

1. Sinna HP, Kreipeb H. A Brief Overview of the WHO Classification of Breast Tumors, 4th Edition, Focusing on Issues and Updates from the 3rd Edition.Breast Care (Basel). 2013; 8(2): 149–154.doi: 10.1159/000350774
2. Vincent TL, Gatenby RA. An evolutionary model for initiation, promotion and progression in carcinogenesis. Int J Oncol. 2008; 32: 729–37. doi: 10.3892/ijo.32.4.729
3. Slaga TJ. Overview of tumor promotion in animals. Environ Health Perspect. 1983; 50: 3–14. doi: 10.1289/ehp.83503
4. Friedewald WF, Rous P. the Initiating and Promoting Elements in Tumor Production : an Analysis of the Effects of Tar, Benzpyrene, and Methylcholanthrene on Rabbit Skin. J Exp Med. 1944; 80: 101–26.
5. Fallis A. The Part played by Injury and Repair in the Development of Cancer, with some Remarks on the Growth of Experimental Cancers. J Chem Inf Model. 2013; 53: 1689–99. doi: 10.1017/CBO9781107415324.004
6. Berenblum I. The Cocarcinogenic Action of Croton Resin The Cocarcinogenic Action of Croton Resin. Cancer Res. 1941; 1: 44–8.
7. Devi PU. Basics of carcinogenesis. 1989; 16–24.
8. Weigelt B, Bissell MJ. Mammary Gland and Breast Cancer. Semin Cancer Biol. 2008; 18: 311–21. doi: 10.1016/j.semcancer.2008.03.013.
9. The pathology of invasive breast cancer.Cancer. 1975 Jul;36(1):1-85.
10. Flier JS, Underhill LH, Dvorak HF. Tumors: Wounds That Do Not Heal. N Engl J Med. 1986; 315: 1650–9. doi: 10.1056/NEJM198612253152606
11. Paget S. The distribution of secondary growths in cancer of the breast. 1889. Cancer Metastasis Rev. 1989; 8: 98–101. doi: 10.1016/S0140-6736(00)49915-0
12. Berenblum I, Shubik P. An experimental study of the initiating state of carcinogenesis, and a re-examination of the somatic cell mutation theory of cancer. Br J Cancer. 1949; 3: 109–18.
13. Angelica MD, Fong Y.A Novel Function for the nm23-H1 Gene: Overexpression in Human Breast Carcinoma Cells Leads to the Formation of Basement Membrane and Growth Arrest.J Natl Cancer

Inst . 1994 December 21; 86(24): 1838–1844

14. Barcellos-hoff MH, Lyden D, Wang TC. The evolution of the cancer niche during multistage carcinogenesis. Nat Rev Cancer. 2013 Jul;13(7):511-8. doi:10.1038/nrc3536.

15. Kopelovich L. Genetic predisposition to cancer in man: in vitro studies. Int Rev Cytol. 1982; 77: 63–88.

16. Kalluri R, Zeisberg M. Fibroblasts in cancer. Nat Rev Cancer. 2006; 6: 392–401. doi: 10.1038/nrc1877

17. Chakroborty D, Sarkar C, Lu K, Bhat M, Dasgupta PS, Basu S. Activation of Dopamine D 1 Receptors in Dermal Fibroblasts Restores VEGF-A Production by These Cells and Subsequent Angiogenesis in Diabetic Cutaneous Wound Tissues. Am J Pathol. 2016; 186: 1–9. doi: 10.1016/j.ajpath.2016.05.008

18. Senger DR, Galli SJ, Dvorak AM, Perruzzi CA, Harvey VS, Dvorak HF. Tumor cells secrete a vascular permeability factor that promotes accumulation of ascites fluid. Science. 1983; 219: 983–5. doi: 6823562

19. Mueller MM, Fusenig NE. Friends or foes - bipolar effects of the tumour stroma in cancer. Nat Rev Cancer. 2004; 4: 839–49. doi: 10.1038/nrc1477

20. Barsky SH, Green WR, Grotendorst GR, Liotta LA. Desmoplastic breast carcinoma as a source of human myofibroblasts. Am J Pathol. 1984; 115: 329–33.

21. Cirri P, Chiarugi P. Cancer associated fibroblasts: the dark side of the coin. Am J Cancer Res. 2011; 1: 482–97.

22. Pula B, Jethon A, Piotrowska A, Gomulkiewicz A, Owczarek T, Calik J, Wojnar A, Witkiewicz W, Rys J, Ugorski M, Dziegiel P, Podhorska-Okolow M. Podoplanin expression by cancer-associated fibroblasts predicts poor outcome in invasive ductal breast carcinoma. Histopathology. 2011; 59: 1249–60. doi: 10.1111/j.1365-2559.2011.04060.x

23. Ohlund D, Elyada E, Tuveson D. Fibroblast heterogeneity in the cancer wound. J Exp Med. 2014; 211: 1503–23. doi: 10.1084/jem.20140692

24. Gallagher PG, Bao Y, Prorock A, Zigrino P, Nischt R, Politi V, Mauch C, Dragulev B, Fox JW. Gene expression profiling reveals cross-talk between melanoma and fibroblasts: Implications for host-tumor interactions in metastasis. Cancer Res. 2005; 65: 4134–46. doi: 10.1158/0008-5472.CAN-04-0415

25. Kojima Y, Acar A, Eaton EN, Mellody KT, Scheel C, Ben-Porath I, Onder TT, Wang ZC, Richardson AL, Weinberg RA, Orimo A. Autocrine TGF-beta and stromal cell-derived factor-1 (SDF-1) signaling

drives the evolution of tumor-promoting mammary stromal myofibroblasts. PNAS. 2010; 107: 20009–14. doi: 10.1073/pnas.1013805107

26. Dominici M, Le Blanc K, Mueller I, Slaper-Cortenbach I, Marini F, Krause D, Deans R, Keating A, Prockop D, Horwitz E. Minimal criteria for defining multipotent mesenchymal stromal cells. Cytotherapy. 2006; 8: 315–7. doi: 10.1080/14653240600855905

27. Kidd S, Spaeth E, Dembinski JL, Dietrich M, Watson K, Klopp A, Battula VL, Weil M, Andreeff M, Marini FC. Direct evidence of mesenchymal stem cell tropism for tumor and wounding microenvironments using in vivo bioluminescent imaging. Stem Cells. 2009; 27: 2614–23. doi: 10.1002/stem.187

28. Spaeth E, Klopp a, Dembinski J, Andreeff M, Marini F. Inflammation and tumor microenvironments: defining the migratory itinerary of mesenchymal stem cells. Gene Ther. 2008; 15: 730–8. doi: 10.1038/gt.2008.39

29. Spaeth EL, Dembinski JL, Sasser AK, Watson K, Klopp A, Hall B, Andreeff M, Marini F. Mesenchymal stem cell transition to tumor-associated fibroblasts contributes to fibrovascular network expansion and tumor progression. PLoS One. 2009; 4. doi: 10.1371/journal.pone.0004992

30. Radisky DC, Kenny PA, Bissell MJ. Fibrosis and cancer: Do myofibroblasts come also from epithelial cells via EMT? J Cell Biochem. 2007; 101: 830–9. doi: 10.1002/jcb.21186

31. Thiery JP. Epithelial – mesenchymal transitions in tumour progression.Nat Rev Cancer.2002; 2: 442–54. doi: 10.1038/nrc822

32. Radisky DC, Levy DD, Littlepage LE, Liu H, Nelson CM, Fata JE, Leake D, Godden EL, Albertson DG, Nieto MA, Werb Z, Bissell MJ. Rac1b and reactive oxygen species mediate MMP-3-induced EMT and genomic instability. Nature. 2005; 436: 123–7. doi: 10.1038/nature03688

33. Zeisberg EM, Potenta S, Xie L, Zeisberg M, Kalluri R. Discovery of endothelial to mesenchymal transition as a source for carcinoma-associated fibroblasts. Cancer Res. 2007; 67: 10123–8. doi: 10.1158/0008-5472.CAN-07-3127

34. Kalluri R. The biology and function of fibroblasts in cancer. Nature. 2016; 16: 582–98. doi: 10.1038/nrc.2016.73

35. Kurosaka H, Kurosaka D, Kato K, Mashima Y, Tanaka Y. Transforming growth factor-β1 promotes contraction of collagen gel by bovine corneal fibroblasts through differentiation of myofibroblasts. Investig Ophthalmol Vis Sci. 1998; 39: 699–704. doi: 10.1358/mf.2003.25.2.723680

36. Guo X, Oshima H, Kitmura T, Taketo MM, Oshima M. Stromal fibroblasts activated by tumor cells

promote angiogenesis in mouse gastric cancer. J Biol Chem. 2008; 283: 19864–71. doi: 10.1074/jbc.M800798200

37. Elenbaas B, Weinberg R a. Heterotypic signaling between epithelial tumor cells and fibroblasts in carcinoma formation. Exp Cell Res. 2001; 264: 169–84. doi: 10.1006/excr.2000.5133

38. Bhowmick NA. TGF-β Signaling in Fibroblasts Modulates the Oncogenic Potential of Adjacent Epithelia. Science. 2004; 303: 848–51. doi: 10.1126/science.1090922

39. Bhowmick NA, Neilson EG, Moses HL. Stromal fibroblasts in cancer initiation and progression. 2011; 432: 332–7. doi: 10.1038/nature03096

40. Kuperwasser C, Chavarria T, Wu M, Magrane G, Gray JW, Carey L, Richardson A, Weinberg RA. Reconstruction of functionally normal and malignant human breast tissues in mice. PNAS. 2004; 101: 4966–71. doi: 10.1073/pnas.0401064101

41. Olumi AF, Dazin P, Tlsty TD. A novel coculture technique demonstrates that normal human prostatic fibroblasts contribute to tumor formation of LNCaP cells by retarding cell death. Cancer Res. 1998; 58: 4525–30.

42. Orimo A, Gupta PB, Sgroi DC, Arenzana-Seisdedos F, Delaunay T, Naeem R, Carey VJ, Richardson AL, Weinberg RA. Stromal fibroblasts present in invasive human breast carcinomas promote tumor growth and angiogenesis through elevated SDF-1/CXCL12 secretion. Cell. 2005; 121: 335–48. doi: 10.1016/j.cell.2005.02.034

43. Olumi AF, Grossfeld GD, Hayward SW, Carroll PR, Tlsty TD, Cunha GR. Carcinoma-associated fibroblasts direct tumor progression of initiated human prostatic epithelium. Cancer Res. 1999; 59: 5002–11.

44. Funahashi H, Takeyama H, Tong Z, Guha S. CXCL8/IL-8 and CXCL12/SDF-1α Co-operatively Promote Invasiveness and Angiogenesis in Pancreatic Cancer. Int J Cancer. 2010; 124: 853–61. doi: 10.1002/ijc.24040

45. Augsten M, Hägglöf C, Olsson E, Stolz C, Tsagozis P, Levchenko T, Frederick MJ, Borg A, Micke P, Egevad L, Ostman A. CXCL14 is an autocrine growth factor for fibroblasts and acts as a multi-modal stimulator of prostate tumor growth. PNAS. 2009; 106: 3414–9. doi: 10.1073/pnas.0813144106

46. Erez N, Truitt M, Olson P, Hanahan D. Cancer-Associated Fibroblasts Are Activated in Incipient Neoplasia to Orchestrate Tumor-Promoting Inflammation in an NF-κB-Dependent Manner. Cancer Cell. 2010; 17: 135–47. doi: 10.1016/j.ccr.2009.12.041

47. Toullec A, Gerald D, Despouy G, Bourachot B, Cardon M, Lefort S, Richardson M, Rigaill G, Parrini

MC, Lucchesi C, Bellanger D, Stern MH, Dubois T, et al. Oxidative stress promotes myofibroblast differentiation and tumour spreading. EMBO Mol Med. 2010; 2: 211–30. doi: 10.1002/emmm.201000073

48. Insel PA. Location , location , location. Trends Endocrinol Metab.2003; 14: 100–2. doi: 10.1016/S1043-2760(03)00004-3

49. Roy R, Yang J, Moses MA. Matrix metalloproteinases as novel biomarkers and potential therapeutic targets in human cancer. J Clin Oncol. 2009; 27: 5287–97. doi: 10.1200/JCO.2009.23.5556

50. Blick T, Hugo H, Widodo E, Waltham M, Pinto C, Mani SA, Weinberg RA, Neve RM, Lenburg ME, Thompson EW. Epithelial mesenchymal transition traits in human breast cancer cell lines parallel the CD44HI/CD24lO/-stem cell phenotype in human breast cancer. J Mammary Gland Biol Neoplasia. 2010; 15: 235–52. doi: 10.1007/s10911-010-9175-z

51. Mani SA, Guo W, Liao MJ, Eaton EN, Ayyanan A, Zhou AY, Brooks M, Reinhard F, Zhang CC, Shipitsin M, Campbell LL, Polyak K, Brisken C, et al. The Epithelial-Mesenchymal Transition Generates Cells with Properties of Stem Cells. Cell. 2008; 133: 704–15. doi: 10.1016/j.cell.2008.03.027

52. Huijbers IJ, Iravani M, Popov S, Robertson D, Al-Sarraj S, Jones C, Isacke CM. A role for fibrillar collagen deposition and the collagen internalization receptor endo180 in glioma invasion. PLoS One. 2010; 5: 1–12. doi: 10.1371/journal.pone.0009808

53. Chun TH, Hotary KB, Sabeh F, Saltiel AR, Allen ED, Weiss SJ. A Pericellular Collagenase Directs the 3-Dimensional Development of White Adipose Tissue. Cell. 2006; 125: 577–91. doi: 10.1016/j.cell.2006.02.050

54. Paszek MJ, Zahir N, Johnson KR, Lakins JN, Rozenberg GI, Gefen A, Reinhart-King CA, Margulies SS, Dembo M, Boettiger D, Hammer DA, Weaver VM. Tensional homeostasis and the malignant phenotype. Cancer Cell. 2005; 8: 241–54. doi: 10.1016/j.ccr.2005.08.010

55. Santhanam AN, Baker AR, Hegamyer G, Kirschmann DA, Colburn NH. Pdcd4 repression of lysyl oxidase inhibits hypoxia-induced breast cancer cell invasion. Oncogene. 2010; 29: 3921–32. doi: 10.1038/onc.2010.158

56. Pankov R, Yamada KM. Fibronectin at a glance. J Cell Sci. 2002; 115: 3861–3. doi: 10.1242/jcs.00059

57. Zheng M, Jones DM, Horzempa C, Prasad A, Mckeown-longo PJ. The First Type III Domain of Fibronectin is Associated with the Expression of Cytokines within the Lung Tumor

Microenvironment. J Cancer. 2011;2:478-83

58. Kobayashi N, Miyoshi S, Mikami T, Koyama H, Kitazawa M, Takeoka M, Sano K, Amano J, Isogai Z, Niida S, Oguri K, Okayama M, McDonald JA, et al. Hyaluronan deficiency in tumor stroma impairs macrophage trafficking and tumor neovascularization. Cancer Res. 2010; 70: 7073–83. doi: 10.1158/0008-5472.CAN-09-4687

59. Hanahan D, Folkman J. Patterns and Emerging Mechanisms of the Angiogenic Switch during Tumorigenesis. 1996; 86: 353–64.

60. Bergers G, Benjamin LE.Tumorigenesis and the angiogenic switch. Nat Rev Cancer. 2003; 3: 1–10. doi: 10.1038/nrc1093

61. Ulahannan S V, Brahmer JR. Antiangiogenic agents in combination with chemotherapy in patients with advanced non-small cell lung cancer. Cancer Invest. 2011; 29: 325–37. doi: 10.3109/07357907.2011.554476

62. Kieda C, Greferath R, Crola da Silva C, Fylaktakidou KC, Lehn J-M, Nicolau C. Suppression of hypoxia-induced HIF-1alpha and of angiogenesis in endothelial cells by myo-inositol trispyrophosphate-treated erythrocytes. PNAS. 2006; 103: 15576–81. doi: 10.1073/pnas.0607109103

63. Goel S, Wong AH, Jain RK. Vascular Normalization as a Therapeutic Strategy. Cold Spring Harb Perspect Med. 2012; 2: 1–24. doi: 10.1101/cshperspect.a006486

64. Kamoun WS, Chae SS, Lacorre DA, Tyrrell JA, Mitre M, Gillissen MA, Fukumura D, Jain RK, Munn LL.Simultaneous measurement of RBC velocity, flux, hematocrit and shear rate in vascular networks.Nat Methods. 2011; 7: 655–60. doi: 10.1038/nmeth.1475.

65. Jain RK. Antiangiogenic therapy for cancer: current and emerging concepts. Oncology. 2005; 19: 7–16.

66. Goel S, Duda DG, Xu L, Munn LL, Boucher Y, Fukumura D, Jain RK.Normalization of the vasculature for treatment of cancer and other diseases.Physiol Rev. 2011; 91(3): 1071–1121. doi:10.1152/physrev.00038.2010.

67. Bock K De, Mazzone M, Carmeliet P. Antiangiogenic therapy , hypoxia , and metastasis : risky liaisons , or not ?. Nature. 2011; 8: 393–404. doi: 10.1038/nrclinonc.2011.83

68. Rivera LB, Bergers G. Tumor angiogenesis, from foe to friend. Science. 2015; 349: 694–5. doi: 10.1126/science.aad0862

69. Kieda C, El Hafny-Rahbi B, Collet G, Lamerant-Fayel N, Grillon C, Guichard A, Dulak J, Jozkowicz A, Kotlinowski J, Fylaktakidou KC, Vidal A, Auzeloux P, Miot-Noirault E, et al. Stable tumor vessel

normalization with pO2 increase and endothelial PTEN activation by inositol trispyrophosphate brings novel tumor treatment. J Mol Med. 2013; 91: 883–99. doi: 10.1007/s00109-013-0992-6

70. LaGory EL, Giaccia AJ.Nat Cell Biol.The ever-expanding role of HIF in tumour and stromal biology 2016; 18: 356–65. doi: 10.1038/ncb3330

71. Qin Y, Naito Y, Handa O, Hayashi N, Kuki A, Mizushima K, Omatsu T. Heat shock protein 70 dependent protective effect of polaprezinc on acetylsalicylic acid induced apoptosis of rat intestinal epithelial cells. J Clin Biochem Nutr. 2011; 49: 174–81. doi: 10.3164/jcbn.11

72. Papakonstantinou E, Roth M, Tamm M, Eickelberg O, Perruchoud AP, Karakiulakis G. Hypoxia differentially enhances the effects of transforming growth factor-beta isoforms on the synthesis and secretion of glycosaminoglycans by human lung fibroblasts. J Pharmacol Exp Ther. 2002; 301: 830–7. doi: 10.1124/jpet.301.3.830

73. Casazza A, Conza G Di, Wenes M, Finisguerra V, Deschoemaeker S, Mazzone M. Tumor stroma : a complexity dictated by the hypoxic tumor microenvironment. Nature. 2013; 1–12. doi: 10.1038/onc.2013.121

74. Breiteneder-Geleff S, Matsui K, Soleiman a, Meraner P, Poczewski H, Kalt R, Schaffner G, Kerjaschki D. Podoplanin, novel 43-kd membrane protein of glomerular epithelial cells, is down-regulated in puromycin nephrosis. Am J Pathol. 1997; 151: 1141–52.

75. Pula B, Witkiewicz W, Dziegiel P, Podhorska-Okolow M. Significance of podoplanin expression in cancer-associated fibroblasts: A comprehensive review. Int J Oncol. 2013; 42: 1849–57. doi: 10.3892/ijo.2013.1887

76. Astarita JL, Acton SE, Turley SJ. Podoplanin: Emerging functions in development, the immune system, and cancer. Front Immunol. 2012; 3: 1–11. doi: 10.3389/fimmu.2012.00283

77. Martín E, Gómez F, Gamallo C, Quintanilla M. a small mucin-like transmembrane glycoprotein associated with cell migration and cancer. Clin Transl Oncol. 2003; 5: 491–9.

78. Kunita A, Kashima TG, Morishita Y, Fukayama M, Kato Y, Tsuruo T, Fujita N. The platelet aggregation-inducing factor aggrus/podoplanin promotes pulmonary metastasis. Am J Pathol. 2007; 170: 1337–47. doi: 10.2353/ajpath.2007.060790

79. Farr a G, Berry ML, Kim a, Nelson a J, Welch MP, Aruffo a. Characterization and cloning of a novel glycoprotein expressed by stromal cells in T-dependent areas of peripheral lymphoid tissues. J Exp Med. 1992; 176: 1477–82. doi: 10.1084/jem.176.5.1477

80. Zimmer G, Oeffner F, Messling VV, Tschernig T, Gröne H, Klenk H, Herrler G. Cloning and

characterization of gp36, a human mucin-type glycoprotein preferentially expressed in vascular endothelium. Biochem J. 1999; 341: 277–84. doi: 10.1042/bj3410277

81. Ugorski M, Dziegiel P, Suchanski J. Podoplanin - a small glycoprotein with many faces. Am J Cancer Res. 2016; 15;6(2):370-86.

82. Schacht V, Ramirez MI, Hong YK, Hirakawa S, Feng D, Harvey N, Williams M, Dvorak AM, Dvorak HF, Oliver G, Detmar M. T1α/podoplanin deficiency disrupts normal lymphatic vasculature formation and causes lymphedema. EMBO J. 2003; 22: 3546–56. doi: 10.1093/emboj/cdg342

83. Ramirez MI, Millien G, Hinds A, Cao YX, Seldin DC, Williams MC. T1α, a lung type I cell differentiation gene, is required for normal lung cell proliferation and alveolus formation at birth. Dev Biol. 2003; 256: 61–72. doi: 10.1016/S0012-1606(02)00098-2

84. Matsui K, Breitender-Geleff S, Soleiman a, Kowalski H, Kerjaschki D. Podoplanin, a novel 43-kDa membrane protein, controls the shape of podocytes. Nephrol Dial Transplant. 1999; 14 Suppl 1: 9–11. doi: 10.1093/ndt/14.suppl_1.9

85. Gandarillas A, Scholl FG, Benito N, Gamallo C, Quintanilla M. Induction of PA2.26, a cell-surface antigen expressed by active fibroblasts, in mouse epidermal keratinocytes during carcinogenesis. Mol Carcinog. 1997; 20: 10–8. doi: 10.1002/(SICI)1098-2744(199709)20:1<10::AID-MC3>3.0.CO;2-M

86. Schmid H. Gene Expression Profiles of Podocyte-Associated Molecules as Diagnostic Markers in Acquired Proteinuric Diseases. J Am Soc Nephrol. 2003; 14: 2958–66. doi: 10.1097/01.ASN.0000090745.85482.06

87. Levidiotis V, Power DA. New insights into the molecular biology of the glomerular filtration barrier and associated disease. Nephrology. 2005; 10: 157–66. doi: 10.1111/j.1440-1797.2005.00385.x

88. Rahadiani N, Ikeda J, Makino T, Tian T, Qiu Y, Mamat S, Wang Y, Doki Y, Aozasa K, Morii E. Tumorigenic role of podoplanin in esophageal squamous-cell carcinoma. Ann Surg Oncol. 2010; 17: 1311–23. doi: 10.1245/s10434-009-0895-5

89. Dumoff KL, Chu CS, Harris EE, Holtz D, Xu X, Zhang PJ, Acs G. Low podoplanin expression in pretreatment biopsy material predicts poor prognosis in advanced-stage squamous cell carcinoma of the uterine cervix treated by primary radiation. Mod Pathol. 2006; 19: 708–16. doi: 10.1038/modpathol.3800580

90. Martín-Villar E, Megías D, Castel S, Yurrita MM, Vilaró S, Quintanilla M. Podoplanin binds ERM proteins to activate RhoA and promote epithelial-mesenchymal transition. J Cell Sci. 2006; 119: 4541–53. doi: 10.1242/jcs.03218

91. Cueni LN, Hegyi I, Shin JW, Albinger-Hegyi A, Gruber S, Kunstfeld R, Moch H, Detmar M. Tumor lymphangiogenesis and metastasis to lymph nodes induced by cancer cell expression of podoplanin. Am J Pathol. 2010; 177: 1004–16. doi: 10.2353/ajpath.2010.090703

92. Kaneko MK, Kato Y, Kameyama A, Ito H, Kuno A, Hirabayashi J, Kubota T, Amano K, Chiba Y, Hasegawa Y, Sasagawa I, Mishima K, Narimatsu H. Functional glycosylation of human podoplanin: Glycan structure of platelet aggregation-inducing factor. FEBS Lett. 2007; 581: 331–6. doi: 10.1016/j.febslet.2006.12.044

93. Wicki a, Christofori G. The potential role of podoplanin in tumour invasion. Br J Cancer. 2007; 96: 1–5. doi: 10.1038/sj.bjc.6603518

94. Kimura N, Kimura I. Podoplanin as a marker for mesothelioma. Pathol Int. 2005; 55: 83–6. doi: 10.1111/j.1440-1827.2005.01791.x

95. Naito Y, Ishii G, Kawai O, Hasebe T, Nishiwaki Y, Nagai K, Ochiai A. D2-40-positive solitary fibrous tumors of the pleura: Diagnostic pitfall of biopsy specimen. Pathol Int. 2007; 57: 618–21. doi: 10.1111/j.1440-1827.2007.02148.x

96. Kato Y, Fujita N, Kunita A, Sato S, Kaneko M, Osawa M, Tsuruo T. Molecular Identification of Aggrus/T1α as a Platelet Aggregation-inducing Factor Expressed in Colorectal Tumors. J Biol Chem. 2003; 278: 51599–605. doi: 10.1074/jbc.M309935200

97. Mishima K, Kato Y, Kaneko MK, Nishikawa R, Hirose T, Matsutani M. Increased expression of podoplanin in malignant astrocytic tumors as a novel molecular marker of malignant progression. Acta Neuropathol. 2006; 111: 483–8. doi: 10.1007/s00401-006-0063-y

98. Mahalingam M, Ugen KE, Kuo-Jang Kao, Klein PA. Functional role of platelets in experimental metastasis studied with cloned murine fibrosarcoma cell variants. Cancer Res. 1988; 48: 1460–4.

99. Suzuki H, Kato Y, Kaneko MK, Okita Y, Narimatsu H, Kato M. Induction of podoplanin by transforming growth factor-β in human fibrosarcoma. FEBS Lett. 2008; 582: 341–5. doi: 10.1016/j.febslet.2007.12.028

100. Suzuki-Inoue K, Kato Y, Inoue O, Mika KK, Mishima K, Yatomi Y, Yamazaki Y, Narimatsu H, Ozaki Y. Involvement of the snake toxin receptor CLEC-2, in podoplanin-mediated platelet activation, by cancer cells. J Biol Chem. 2007; 282: 25993–6001. doi: 10.1074/jbc.M702327200

101. Yuan P, Temam S, El-Naggar A, Zhou X, Liu DD, Lee JJ, Mao L. Overexpression of podoplanin in oral cancer and its association with poor clinical outcome. Cancer. 2006; 107: 563–9. doi: 10.1002/cncr.22061

102. Forsee WT, Cartee RT, Yother J.Biosynthesis of type 3 capsular polysaccharide in Streptococcus pneumoniae. Enzymatic chain release by an abortive translocation process. J Biol Chem. 2000. 25;275(34):25972-8.

103. Bretscher A, Edwards K, Fehon RG. ERM proteins and merlin: integrators at the cell cortex. Nat Rev Mol Cell Biol. 2002; 3: 586–99. doi: 10.1038/nrm882

104. Moustakas A, Heldin CH. Signaling networks guiding epithelial-mesenchymal transitions during embryogenesis and cancer progression. Cancer Sci. 2007; 98: 1512–20. doi: 10.1111/j.1349-7006.2007.00550.x

105. Scholl FG, Gamallo C, Vilaró S, Quintanilla M. Identification of PA2.26 antigen as a novel cell-surface mucin-type glycoprotein that induces plasma membrane extensions and increased motility in keratinocytes. J Cell Sci. 1999; 112: 4601–13.

106. Kłopocka W, Barańska J. Rola białek z rodziny Rho w kontroli migracji komórek pełzających. Postepy Biochem. 2005; 51: 36–43.

107. Gröger M, Loewe R, Holnthoner W, Embacher R, Pillinger M, Herron GS, Wolff K, Petzelbauer P. IL-3 induces expression of lymphatic markers Prox-1 and podoplanin in human endothelial cells. J Immunol. 2004; 173: 7161–9. doi: 173/12/7161

108. Durchdewald M, Guinea-Viniegra J, Haag D, Riehl A, Lichter P, Hahn M, Wagner EF, Angel P, Hess J.Podoplanin is a novel fos target gene in skin carcinogenesis. Cancer Res. 2008. 1;68(17):6877-83. doi: 10.1158/0008-5472.CAN-08-0299.

109. Shen Y, Chen CS, Ichikawa H, Goldberg GS. Src induces podoplanin expression to promote cell migration. J Biol Chem. 2010; 285: 9649–56. doi: 10.1074/jbc.M109.047696

110. Kawase A, Ishii G, Nagai K, Ito T, Nagano T, Murata Y, Hishida T, Nishimura M, Yoshida J, Suzuki K, Ochiai A. Podoplanin expression by cancer associated fibroblasts predicts poor prognosis of lung adenocarcinoma. Int J Cancer. 2008; 123: 1053–9. doi: 10.1002/ijc.23611

111. Shindo K, Aishima S, Ohuchida K, Fujiwara K, Fujino M, Mizuuchi Y, Hattori M, Mizumoto K, Tanaka M, Oda Y. Podoplanin expression in cancer-associated fibroblasts enhances tumor progression of invasive ductal carcinoma of the pancreas. Mol Cancer. 2013. 20;12(1):168. doi: 10.1186/1476-4598-12-168.

112. Shindo K, Aishima S, Ohuchida K, Fujiwara K, Fujino M, Mizuuchi Y, Hattori M, Mizumoto K, Tanaka M, Oda Y. Podoplanin expression in cancer-associated fibroblasts enhances tumor progression of invasive ductal carcinoma of the pancreas. Mol Cancer. 2013; 12: 168. doi: 1476-4598-

12-168 [pii]\r10.1186/1476-4598-12-168

113. Aishima S, Nishihara Y, Iguchi T, Taguchi K, Taketomi A, Maehara Y, Tsuneyoshi M. Lymphatic spread is related to VEGF-C expression and D2-40-positive myofibroblasts in intrahepatic cholangiocarcinoma. Mod Pathol. 2008; 21: 256–64. doi: 10.1038/modpathol.3800985

114. Yamanashi T, Nakanishi Y, Fujii G, Akishima-Fukasawa Y, Moriya Y, Kanai Y, Watanabe M, Hirohashi S. Podoplanin expression identified in stromal fibroblasts as a favorable prognostic marker in patients with colorectal carcinoma. Oncology. 2009; 77: 53–62. doi: 10.1159/000226112

115. Carvalho FM, Zaganelli FL, Almeida BGL, Goes JCS, Baracat EC, Carvalho JP. Prognostic value of podoplanin expression in intratumoral stroma and neoplastic cells of uterine cervical carcinomas. Clinics (Sao Paulo). 2010; 65: 1279–83. doi: 10.1590/S1807-59322010001200009

116. Yoshida T, Ishii G, Goto K, Neri S, Hashimoto H, Yoh K, Niho S, Umemura S, Matsumoto S, Ohmatsu H, Iida S, Niimi A, Nagai K, et al. Podoplanin-positive cancer-associated fibroblasts in the tumor microenvironment induce primary resistance to EGFR-TKIs in lung adenocarcinoma with EGFR mutation. Clin Cancer Res. 2015; 21: 642–51. doi: 10.1158/1078-0432.CCR-14-0846

117. Ito S, Ishii G, Hoshino A, Hashimoto H, Neri S, Kuwata T, Higashi M, Nagai K, Ochiai A. Tumor promoting effect of podoplanin-positive fibroblasts is mediated by enhanced RhoA activity. Biochem Biophys Res Commun. Elsevier Inc.; 2012; 422: 194–9. doi: 10.1016/j.bbrc.2012.04.158

118. Hoshino A, Ishii G, Ito T, Aoyagi K, Ohtaki Y, Nagai K, Sasaki H, Ochiai A. Podoplanin-positive fibroblasts enhance lung adenocarcinoma tumor formation: Podoplanin in fibroblast functions for tumor progression. Cancer Res. 2011; 71: 4769–79. doi: 10.1158/0008-5472.CAN-10-3228

119. Li Q, Zhang D, Wang Y, Sun P, Hou X, Larner J, Xiong W, Mi J. MiR-21/Smad 7 signaling determines TGF-β1-induced CAF formation. Sci Rep. 2013; 3: 2038. doi: 10.1038/srep02038

120. Shobha Vasudevan, Yingchun Tong JAS. Switching from Repression to Activation: MicroRNAs Can Up-Regulate Translation. Science. 2007; 318: 1931–4. doi: 10.1126/science.1149460

121. Jing Q, Huang S, Guth S, Zarubin T, Motoyama A, Chen J, Di Padova F, Lin SC, Gram H, Han J. Involvement of MicroRNA in AU-Rich Element-Mediated mRNA Instability. Cell. 2005; 120: 623–34. doi: 10.1016/j.cell.2004.12.038

122. Chalfie M, Horvitz HR, Sulston JE. Mutations that lead to reiterations in the cell lineages of C. elegans. Cell. 1981; 24: 59–69. doi: 10.1016/0092-8674(81)90501-8

123. Lagos-quintana M, Rauhut R, Lendeckel W, Tuschl T. Identification of novel genes Coding for RNAs of Small expressed RNAs. Science. 2001; 294: 853–8. doi: 10.1126/science.1064921

124. Lim LP, Lim LP, Lau NC, Lau NC, Weinstein EG, Weinstein EG, Abdelhakim A, Abdelhakim A, Yekta S, Yekta S, Rhoades MW, Rhoades MW, Burge CB, et al. The microRNAs of C. elegans. Genes Dev. 2003; : 991–1008. doi: 10.1101/gad.1074403.regulating

125. Grimson A, Farh KKH, Johnston WK, Garrett-Engele P, Lim LP, Bartel DP. MicroRNA Targeting Specificity in Mammals: Determinants beyond Seed Pairing. Mol Cell. 2007; 27: 91–105. doi: 10.1016/j.molcel.2007.06.017

126. Nielsen CB, Shomron N, Sandberg R, Hornstein E, Kitzman J, Burge CB. Determinants of targeting by endogenous and exogenous microRNAs and siRNAs. RNA. 2007; 13: 1894–910. doi: 10.1261/rna.768207

127. Doench JG, Petersen CP, Sharp PA. siRNAs can function as miRNAs. Genes Dev. 2003; 17: 438–42. doi: 10.1101/gad.1064703

128. Rodrigues ML, Nimrichter L, Oliveira DL, Nosanchuk JD, Casadevall A. Vesicular trans-cell wall Transport in fungi: A mechanism for the delivery of virulence-associated macromolecules? Lipid Insights. 2008; 2 1: 27–40. doi: 10.1038/ncb1596

129. Aravin A, Lagos-Quintana M, Yalcin A. The Small RNA Profile during *Drosophila melanogaster* Development. Dev Cell. 2003; 5: 337–50. doi: 10.1016/S1534-5807(03)00228-4

130. Lagos-Quintana M, Rauhut R, Yalcin A, Meyer J, Lendeckel W, Tuschl T. Identification of tissue-specific MicroRNAs from mouse. Curr Biol. 2002; 12: 735–9. doi: 10.1016/S0960-9822(02)00809-6

131. Lin SL, Miller JD, Ying SY. Intronic microRNA (miRNA). J Biomed Biotechnol. 2006; 2006: 1–13. doi: 10.1155/JBB/2006/26818

132. Baskerville S, Bartel DP. Microarray profiling of microRNAs reveals frequent coexpression with neighboring miRNAs and host genes. RNA. 2005; 11: 241–7. doi: 10.1261/rna.7240905

133. Lee Y, Kim M, Han J, Yeom K-H, Lee S, Baek SH, Kim VN. MicroRNA genes are transcribed by RNA polymerase II. Eur Mol Biol Organ J. 2004; 23: 4051–60. doi: 10.1038/sj.emboj.7600385

134. Altuvia Y, Landgraf P, Lithwick G, Elefant N, Pfeffer S, Aravin A, Brownstein MJ, Tuschl T, Margalit H. Clustering and conservation patterns of human microRNAs. Nucleic Acids Res. 2005; 33: 2697–706. doi: 10.1093/nar/gki567

135. Lee Y, Jeon K, Lee J-T, Kim S, Kim VN. MicroRNA maturation: stepwisee processing and subcellular localization. EMBO J. 2002; 21: 4663–70. doi: 10.1093/emboj/cdf476

136. Cullen BR. Transcription and processing of human microRNA precursors. Mol Cell. 2004; 16: 861–5. doi: 10.1016/j.molcel.2004.12.002

137. Berezikov E, Chung WJ, Willis J, Cuppen E, Lai EC. Mammalian Mirtron Genes. Mol Cell. 2007; 28: 328–36. doi: 10.1016/j.molcel.2007.09.028

138. Wheeler TJ, Clements J, Eddy SR, Hubley R, Jones TA, Jurka J, Smit AF, Finn RD.Dfam: a database of repetitive DNA based on profile hidden Markov models.Nucleic Acids Res. 2013;41:D70-82. doi: 10.1093/nar/gks1265

139. Calin GA, Dumitru CD, Shimizu M, Bichi R, Zupo S, Noch E, Aldler H, Rattan S, Keating M, Rai K, Rassenti L, Kipps T, Negrini M, et al. Frequent deletions and down-regulation of micro- RNA genes miR15 and miR16 at 13q14 in chronic lymphocytic leukemia. PNAS. 2002; 99: 15524–9. doi: 10.1073/pnas.242606799

140. Michael MZ, O' Connor SM, van Holst Pellekaan NG, Young GP, James RJ. Reduced accumulation of specific microRNAs in colorectal neoplasia. Mol Cancer Res. 2003; 1: 882–91.

141. Hayashita Y, Osada H, Tatematsu Y, Yamada H, Yanagisawa K, Tomida S, Yatabe Y, Kawahara K, Sekido Y, Takahashi T. A polycistronic MicroRNA cluster, miR-17-92, is overexpressed in human lung cancers and enhances cell proliferation. Cancer Res. 2005; 65: 9628–32. doi: 10.1158/0008-5472.CAN-05-2352

142. Ying Q, Liang L, Guo W, Zha R, Tian Q, Huang S, Yao J, Ding J, Bao M, Ge C, Yao M, Li J, He X. Hypoxia-inducible MicroRNA-210 augments the metastatic potential of tumor cells by targeting vacuole membrane protein 1 in hepatocellular carcinoma. Hepatology. 2011; 54: 2064–75. doi: 10.1002/hep.24614

143. Calvo-Garrido J, Carilla-Latorre S, Escalante R. Vacuole membrane protein 1, autophagy and much more. Autophagy. 2008; 4: 835–7. doi: 10.4161/auto.6574

144. Chen Y, Zhang J, Wang H, Zhao J, Xu C, Du Y, Luo X, Zheng F, Liu R, Zhang H, Ma D. miRNA-135a promotes breast cancer cell migration and invasion by targeting HOXA10. BMC Cancer; 2012; 12: 111. doi: 10.1186/1471-2407-12-111

145. Xu C, Liu S, Fu H, Li S, Tie Y, Zhu J, Xing R, Jin Y, Sun Z, Zheng X. MicroRNA-193b regulates proliferation, migration and invasion in human hepatocellular carcinoma cells. Eur J Cancer; 2010; 46: 2828–36. doi: 10.1016/j.ejca.2010.06.127

146. Wang S, Olson EN. AngiomiRs-Key regulators of angiogenesis. Curr Opin Genet Dev. 2009; 19: 205–11. doi: 10.1016/j.gde.2009.04.002

147. Wang S, Aurora AB, Johnson BA, Qi X, McAnally J, Hill JA, Richardson JA, Bassel-Duby R, Olson EN. The Endothelial-Specific MicroRNA miR-126 Governs Vascular Integrity and Angiogenesis.

Dev Cell. 2008; 15: 261–71. doi: 10.1016/j.devcel.2008.07.002

148. Ratajczak J, Wysoczynski M, Hayek F, Janowska-Wieczorek a, Ratajczak MZ. Membrane-derived microvesicles: important and underappreciated mediators of cell-to-cell communication. Leuk Off J Leuk Soc Am Leuk Res Fund, UK. 2006; 20: 1487–95. doi: 10.1038/sj.leu.2404296

149. Ciesla M, Skrzypek K, Kozakowska M, Loboda A, Jozkowicz A, Dulak J. MicroRNAs as biomarkers of disease onset. Anal Bioanal Chem. 2011; 401: 2051–61. doi: 10.1007/s00216-011-5001-8

150. Valadi H, Ekström H, Bossios A, Sjöstrand M, Lee J LJ. Exosome-mediated transfer of mRNAs and microRNAs is a novel mechanism of genetic exchange between cells.Nat Cell Biol. 2007;9(6):654-9

151. Bussolati B, Grange C, Camussi G. Tumor exploits alternative strategies to achieve vascularization. FASEB J. 2011; 25: 2874–82. doi: 10.1096/fj.10-180323

152. Janowska-Wieczorek A, Wysoczynski M, Kijowski J, Marquez-Curtis L, Machalinski B, Ratajczak J, Ratajczak MZ. Microvesicles derived from activated platelets induce metastasis and angiogenesis in lung cancer. Int J Cancer. 2005; 113: 752–60. doi: 10.1002/ijc.20657

153. Davis NM, Sokolosky M, Stadelman K, Abrams SL, Libra M, Candido S, Nicoletti F, Polesel J, Assoro AD, Drobot L, Rakus D. Deregulation of the EGFR / PI3K / PTEN / Akt / mTORC1 pathway in breast cancer : possibilities for therapeutic intervention. Oncotarget. 2014 Jul 15;5(13):4603-50.

154. Cortez MA, Nicoloso MS, Shimizu M, Rossi S, Gopisetty G, Molina JR, Carlotti C, Tirapelli D, Neder L, Brassesco MS, Scrideli CA, Tone LG, Georgescu M, et al. miR-29b and miR-125a Regulate Podoplanin and Suppress Invasion in Glioblastoma.Genes Chromosomes Cancer.2010; 990: 981–90. doi: 10.1002/gcc

155. Kieda, Claudine, Paprocka Maria, Krawczenko Agnieszka, Monsigny M. DP, Radzikowski C. DD. New human microvascular endothelial cell lines with specific adhesion molecules phenotype. Endothelium. 2002; 9: 242–61.

156. Song YR, You SJ, Lee YM, Chin HJ, Chae DW, Oh YK, Joo KW, Han JS, Na KY. Activation of hypoxia-inducible factor attenuates renal injury in rat remnant kidney. Nephrol Dial Transplant. 2010; 25: 77–85. doi: 10.1093/ndt/gfp454

157. Wendland K, Thielke M, Meisel A, Mergenthaler P. Intrinsic hypoxia sensitivity of the cytomegalovirus promoter. Cell Death Dis. Nature; 2015; 6: e1905. doi: 10.1038/cddis.2015.259

158. Neri S, Ishii G, Hashimoto H, Kuwata T, Nagai K, Date H, Ochiai A. Podoplanin-expressing cancer-associated fibroblasts lead and enhance the local invasion of cancer cells in lung adenocarcinoma. Int J Cancer. 2015; 137: 784–96. doi: 10.1002/ijc.29464

159. Tsuneki M, Yamazaki M, Maruyama S, Cheng J, Saku T. Podoplanin-mediated cell adhesion through extracellular matrix in oral squamous cell carcinoma. Lab Invest. Nature; 2013; 93: 921–32. doi: 10.1038/labinvest.2013.86

160. Kerjaschki D, Regele HM, Moosberger I, Nagy-Bojarski K, Watschinger B, Soleiman A, Birner P, Krieger S, Hovorka A, Silberhumer G, Laakkonen P, Petrova T, Langer B, et al. Lymphatic neoangiogenesis in human kidney transplants is associated with immunologically active lymphocytic infiltrates. J Am Soc Nephrol. 2004; 15: 603–12. doi: 10.1097/01.ASN.0000113316.52371.2E

161. Semenza G. Hypoxia-inducible factors in physiology and medicine. Cell. 2012; 148: 399–408. doi: 10.1016/j.cell.2012.01.021

162. Dalmay T, Edwards DR. MicroRNAs and the hallmarks of cancer. Oncogene. 2006; 25: 6170–5. doi: 10.1038/sj.onc.1209911

163. Loboda A, Sobczak M, Jozkowicz A, Dulak J. TGF- β 1 / Smads and miR-21 in Renal Fibrosis and Inflammation. Hindawi Publishing Corporation; 2016; 2016. doi: 10.1155/2016/8319283

164. Fu F. The role of miR-29b in cancer : regulation , function , and signaling.Onco Targets Ther. 2015; 8: 539–548

165. Saadi A, Shannon NB, Lao-Sirieix P, O'Donovan M, Walker E, Clemons NJ, Hardwick JS, Zhang C, Das M, Save V, Novelli M, Balkwill F, Fitzgerald RC. Stromal genes discriminate preinvasive from invasive disease, predict outcome, and highlight inflammatory pathways in digestive cancers. PNAS. 2010; 107: 2177–82. doi: 10.1073/pnas.0909797107

166. Augsten M. Cancer-associated fibroblasts as another polarized cell type of the tumor microenvironment.Front Oncol. 2014; 4: 62. doi: 10.3389/fonc.2014.00062

167. Zhao L, Sun Y, Hou Y, Peng Q, Wang L, Luo H, Tang X, Zeng Z, Liu M. MiRNA expression analysis of cancer-associated fibroblasts and normal fibroblasts in breast cancer. Int J Biochem Cell Biol. 2012; 44: 2051–9. doi: 10.1016/j.biocel.2012.08.005

168. Serpico D, Molino L, Di Cosimo S. MicroRNAs in breast cancer development and treatment. Cancer Treat Rev. 2014; 40: 595–604. doi: 10.1016/j.ctrv.2013.11.002

169. Collet G, El Hafny-Rahbi B, Nadim M, Tejchman A, Klimkiewicz K, Kieda C. Hypoxia-shaped vascular niche for cancer stem cells. Contemp Oncol (Poznań, Poland). 2015; 19: A39-43. doi: 10.5114/wo.2014.47130

170. Madsen CD, Pedersen JT, Venning FA, Singh LB, Charras G, Cox TR, Sahai E, Erler JT. Hypoxia and loss of PHD 2 inactivate stromal fibroblasts to decrease tumour stiffness and metastasis. EMBO

Rep. 2015;16(10):1394-408. doi: 10.15252/embr.201540107

171. Leong HS, Chambers AF. Hypoxia promotes tumor cell motility via RhoA and ROCK1 signaling pathways. PNAS. 2014; 111: 887–8. doi: 10.1073/pnas.1322484111

172. Cheng Y, Zhao K, Li G, Yao J, Dai Q, Hui H, Li Z, Guo Q, Lu N. Oroxylin A inhibits hypoxia-induced invasion and migration of MCF-7 cells by suppressing the Notch pathway. Anticancer Drugs. 2014; 25: 778–89. doi: 10.1097/CAD.0000000000000103

173. Nagelkerke A, Bussink J, Mujcic H, Wouters BG, Lehmann S, Sweep FCGJ, Span PN. Hypoxia stimulates migration of breast cancer cells via the PERK/ATF4/LAMP3-arm of the unfolded protein response. Breast Cancer Res. BioMed Central Ltd; 2013; 15: R2. doi: 10.1186/bcr3373

174. Tutunea-Fatan E, Majumder M, Lala PK. Abstract 5152: The role of CCL21/CCR7 chemokine axis in breast cancer induced lymphangiogenesis. Cancer Res. 2011; 71: 5152–5152. doi: 10.1158/1538-7445.AM2011-5152

175. Rizwan A, Cheng M, Bhujwalla ZM, Krishnamachary B, Jiang L, Glunde K. Breast cancer cell adhesome and degradome interact to drive metastasis. Nature. 2015; : 1–11. doi: 10.1038/npjbcancer.2015.17

176. Bendas G, Borsig L. Cancer cell adhesion and metastasis: Selectins, integrins, and the inhibitory potential of heparins. Int J Cell Biol. 2012; 2012. doi: 10.1155/2012/676731

177. Boyle ST, Ingman W V, Poltavets V, Faulkner JW, Whitfield RJ, McColl SR, Kochetkova M. The chemokine receptor CCR7 promotes mammary tumorigenesis through amplification of stem-like cells. Oncogene. 2016. 7;35(1):105-15. doi: 10.1038/onc.2015.66.

178. Brown LF, Guidi a J, Schnitt SJ, Van De Water L, Iruela-Arispe ML, Yeo TK, Tognazzi K, Dvorak HF. Vascular stroma formation in carcinoma in situ, invasive carcinoma, and metastatic carcinoma of the breast. Clin Cancer Res. 1999; 5: 1041–56.

179. Navarro A, Perez RE, Rezaiekhaligh MH, Mabry SM, Ekekezie II. Polarized migration of lymphatic endothelial cells is critically dependent on podoplanin regulation of Cdc42. Am J Physiol Lung Cell Mol Physiol. 2011. 300(1):L32-42. doi: 10.1152/ajplung.00171.2010.

180. Carmeliet P. Fibroblast Growth Factor-1 Stimulates Branching and Survival of Myocardial Arteries. Circ Res. 2000. 4;87(3):176-8.

181. Sawa Y. New trends in the study of podoplanin as a cell morphological regulator. Jpn Dent Sci Rev. 2010; 46: 165–72. doi: 10.1016/j.jdsr.2010.01.003

182. Hobbs SK, Monsky WL, Yuan F, Roberts WG, Griffith L, Torchilin VP, Jain RK. Regulation of

transport pathways in tumor vessels: role of tumor type and microenvironment. PNAS. 1998; 95: 4607–12. doi: 10.1073/pnas.95.8.4607

183. Newman a. C, Nakatsu MN, Chou W, Gershon PD, Hughes CCW. The requirement for fibroblasts in angiogenesis: fibroblast-derived matrix proteins are essential for endothelial cell lumen formation. Mol Biol Cell. 2011; 22: 3791–800. doi: 10.1091/mbc.E11-05-0393

184. Chaves RN, de Matos MH, Buratini J Jr, de Figueiredo JR.The fibroblast growth factor family : involvement in the regulation of folliculogenesis. Reprod Fertil Dev. 2012;24(7):905-15. doi: 10.1071/RD11318.

185. Ito T-K, Ishii G, Chiba H, Ochiai A. The VEGF angiogenic switch of fibroblasts is regulated by MMP-7 from cancer cells. Oncogene. 2007; 26: 7194–203. doi: 10.1038/sj.onc.1210535

Anna Tejchman

L'influence de l'hypoxie sur l'expression de podoplanine dans les fibroblastes associés au cancer (CAF) et son rôle dans la progression du cancer du sein

Le tissu tumoral comprend, outre les cellules cancéreuses, une matrice extra-cellulaire modifiée, les cellules endothéliales des vaisseaux sanguins et lymphatiques, immunes et inflammatoires et des fibroblastes activés associés au cancer (CAFs). La podoplanine (PDPN), glycoprotéine transmembranaire de type mucine, y est exprimée dans les cellules cancéreuses et les CAFs. Elleaideà la métastase commemontré dans le carcinome mammaire envahissant les ganglions lymphatiques. Ce travail montre que PDPN module l'interaction chimiokine/récepteur de l'axe CCL21/CCR7 et dépend de l'hypoxie. La progression tumoraleest aidée par le stroma où les CAFsont des propriétés particulières par rapport aux fibroblastes normaux. Ils promeuvent la croissance tumorale, le recrutement des précurseurs endothéliaux et l'angiogenèse. Dans le carcinome mammaire, 80% des fibroblastes ont un phénotype CAF. Un modèle de CAFs exprimant la PDPN a permis de démontrer l'implication de CCL21/CCR7 dans la reconnaissance entre cellules tumorales et CAFs via la liaison CCL21/PDPN. Les CAFsPDPN+ sécrètent des microARNs qui contrôlent des gènes des cellules cancéreuses. MiR-21 est un régulateur oncogène fondamental, par son action sur lesuppresseur de tumeurPTEN. Nous avons analysé l'effet de miR-21, ainsi que de miR-210 et miR-29b sur PDPN dans les fibroblastes en hypoxie pour mimer le microenvironnement intratumoral et mis en évidence les différences biologiques comparativement à la normoxie ainsi que l'effet de la podoplanine sur l'angiogenèse par les cellules endothélialesen colocalization avec lesCAFs exprimant la podoplanine et sur l'expression des facteurs proangiogéniques.
Carcinome mammaire, fibroblastes associés au cancer (CAFs), hypoxie, microenvironnement, podoplanine (PDPN).

The influence of hypoxia on podoplanin expression in cancer-associated fibroblasts (CAF) and its role in the progression of breast cancer

Tumor is a pathologic tissue including cancer cells, a modified extracellular matrix, endothelial cells, blood and lymphatic vessels, immune and inflammatory cells and activated fibroblasts called cancer-associated fibroblasts (CAFs). Podoplanin (PDPN), mucin-type transmembrane glycoprotein is expressed in tumor cells and CAFs, helps metastasis. Its role in metastaticprocess has been demonstrated for breast cancer cells into lymph nodes. Here we show that PDPN modulates the CCL21/CCR7 chemokine/receptor axis in a hypoxia-dependent manner. Cancer progression depends on the tumour stroma in which CAFs differ from normal fibroblasts. CAFs promote tumour growth, recruitment of endothelial progenitor cells and angiogenesis. In breast cancer up to 80% of fibroblasts display the CAF phenotype. Here a PDPN expressing model of CAFs made it possible to demonstrate the involvement of CCL21/CCR7 axis in the tumor cell-to-CAF recognition through podoplanin binding of CCL21. PDPN positive CAFs secrete microRNAs, which control gene expression at post-transcriptional level and influence cancer cells. MiR-21 is a key regulator of the oncogenic process, through its downstream target proteins among which the tumor suppressor, PTEN. We analyzed the effect of miR-21, but also oncogenic and hypoxia dependent miRs: miR-210 and miR-29b, on PDPN expression in fibroblasts in conditions mimicking the intra tumor microenvironment, i.e. in hypoxia. This points to crucial differences as compared to normoxia. Moreover we uncover the effect of podoplanin on angiogenesis by endothelial cells colocalizing with CAFs expressing podoplanin and on the expression of most prominent proangiogenic factors.
Cancer associated fibroblasts (CAFs), hypoxia, microenvironment, mammary carcinoma, podoplanin (PDPN)

Biologie cellulaire, Cibles moléculaires et Thérapies innovantes, Centre de Biophysique Moléculaire UPR CNRS 4301 Université d'Orléans, Orléans, France

Laboratory of Glycobiology and Intercellular Interactions, Institute of Immunology and Experimental Therapy, Polish Academy of Science, Ul. RudolfaWeigla 12, 53-114 Wrocław, Poland